Dissertation

Submitted to the

Combined Faculties of Mathematics,

Engineering and Natural Sciences

University of Heidelberg, Germany

for the degree of

Doctor of Natural Sciences (Dr. rer. Nat.)

presented by

M.Sc. Moritz Schroll

born in Ellwangen (Jagst), Germany

Oral examination: May 25th, 2022

Methane cycling in a eutrophic lake characterised by multiple stable isotope and flux measurements

Referees:

Prof. Dr. Frank Keppler

Prof. Dr. Hans-Peter Grossart

Abstract

Recent estimations demonstrate that methane (CH_4) emissions from aquatic systems are responsible for up to half of global CH_4 emissions. Lakes represent one of the largest CH_4 sources, and emissions are predicted to increase due to global warming. However, there is a large uncertainty associated with CH_4 emissions from freshwater environments to the atmosphere. Emissions result from the interplay between physical transport, CH_4 production and consumption processes, which remain poorly understood. Especially the recently discovered CH_4 production in oxic water layers (OMP) questions the traditional understanding of CH_4 formation processes and might constitute a major driver of limnic CH_4 emissions. However, the underlying mechanisms and pathways of OMP are largely unknown.

In the scope of this study, a combination of field measurements and laboratory incubation experiments as well as concentration measurements and stable isotope techniques were conducted to disentangle the complex processes involved in the CH_4 cycle of small, seasonally stratified, eutrophic Lake Willersinnweiher, which is situated in south-west Germany. Methane oversaturation in the water column of Lake Willersinnweiher was found throughout the whole year. However, seasonal and spatial variations of dissolved CH_4 depending on lake stratification were observed. Spatial disparities of epilimnic CH_4 concentrations indicated that lateral input of CH_4 originated mainly from a few selected shallow sites and not from the whole littoral area of the lake. Inflowing groundwater characterised by high CH_4 concentrations, which were unusually enriched in ^{13}C and deuterium (^{2}H), further contributed to CH_4 supersaturation in the water column. During the stratification period, accumulation of CH_4 just below the thermocline coincided with chlorophyll-a peaks, thus indicating the potential presence of OMP in connection with phytoplankton blooms at Lake Willersinnweiher. The potential occurrence of OMP was further validated by a mass-balance approach and by identifying methyl phosphonate, methylamine, and methionine as three potential precursor compounds of CH_4 in the oxic water column. In the sediment, the stable carbon ($\delta^{13}C$-CH_4) and stable hydrogen ($\delta^{2}H$-CH_4) isotope values of CH_4 revealed the contribution of different pathways of methanogenic CH_4 production depending on water depth. However, sulphate (SO_4^{2-})-dependent anaerobic methane oxidation (AOM), revealed by flux measurements, stable isotope evidence of CH_4 and dissolved inorganic carbon (DIC) acted as a sink of sedimentary CH_4 that substantially diminished CH_4 fluxes from the sediment into bottom waters. Furthermore, CH_4 from the anoxic CH_4-rich hypolimnion was largely depleted by aerobic methane oxidation (MOx) at the oxic-anoxic interface. Methane fluxes from the water column to the atmosphere as well as its stable isotopic values showed strong seasonal dependence and variations, with CH_4 being more enriched in ^{13}C and ^{2}H during the mixing period in winter compared to the stratification period in summer. While diffusive CH_4 fluxes dominated total CH_4 emissions during the mixing period, ebullition was the main contributor to CH_4 emissions during the stratification period. Furthermore, the recently introduced isotope indicator $\Delta(2,13)$ was applied to characterise CH_4 sources at Lake Willersinnweiher. $\Delta(2,13)$ values implied that littoral and

groundwater inputs of CH_4 mainly contributed to CH_4 supersaturation at Lake Willersinnweiher during the mixing period. However, lateral and vertical CH_4 inputs alone could not explain CH_4 supersaturation during the stratification period. Therefore, OMP might be another important CH_4 source. This study shows that all investigated sinks and sources of CH_4 are subject to strong variations based on lake stratification, physicochemical conditions, and lake depth. Hence, the results of this study suggest that a combination of dual isotope and concentration measurements of CH_4 is a promising tool in order to untangle seasonal and spatial dynamics of CH_4 sources and sinks in the complex CH_4 cycle of lakes.

Kurzfassung

Jüngste Schätzungen zeigen, dass Emissionen von Methan (CH_4) aus aquatischen Systemen bis zu 50 % der weltweiten Emissionen ausmachen. Dabei stellen Seen eine der größten CH_4-Quellen dar. Darüber hinaus wird prognostiziert, dass die Emissionen von CH_4 aufgrund der globalen Erwärmung noch weiter zunehmen werden. Die Emissionen von CH_4 aus Süßwassersystemen in die Atmosphäre sind jedoch mit großen Unsicherheiten behaftet. Sie ergeben sich aus dem Zusammenspiel von physikalischem Transport und den Prozessen von CH_4-Produktion und -Abbau, die nach wie vor nur unzureichend verstanden werden. Insbesondere die kürzlich entdeckte CH_4-Produktion in oxischen Wasserschichten (OMP) stellt das bisherige Verständnis der Bildungsprozesse von CH_4 in aquatischen Systemen in Frage. Die OMP könnte eine Hauptquelle für die CH_4-Emissionen aus Seen sein, sind bisher aber nur unzureichend verstanden. Im Rahmen dieser Studie wurde eine Kombination aus Feldmessungen und Inkubationsexperimenten im Labor, sowie Konzentrations- und stabile Isotopenuntersuchen durchgeführt, um die komplexen Vorgänge im CH_4-Kreislauf des kleinen eutrophen Sees Willersinnweiher mit saisonaler Schichtung zu entschlüsseln. Die Übersättigung von CH_4 in der Wassersäule des Willersinnweihers, der sich im Südwesten Deutschlands befindet, wurde das ganze Jahr über festgestellt. Es wurden jedoch jahreszeitliche und räumliche Schwankungen des gelösten CH_4 in Abhängigkeit von der Schichtung des Sees beobachtet. Die räumlichen Variationen der CH_4-Konzentrationen im Oberflächenwasser deuten darauf hin, dass der horizontale Eintrag von CH_4 eher von einigen ausgewählten flachen Stellen, als aus gesamten Litoralbereich des Sees stammt. Einströmendes Grundwasser, das sich durch hohe CH_4-Konzentrationen und ungewöhnlich hohe Anreicherung an ^{13}C-CH_4 und ^{2}H-CH_4 auszeichnet, trug außerdem zur CH_4-Übersättigung in der Wassersäule bei. Während der See eine Schichtung aufwies, bildeten sich Bereiche knapp unterhalb des Metalimnions aus, die durch erhöhte CH_4- und Chlorophyll-a-Konzentrationen charakterisiert waren. Diese Beobachtung weist möglicherweise auf eine Verbindung zwischen OMP und Phytoplanktonblüten im Willersinnweiher hin. Darüber hinaus wurde das Auftreten von OMP in der Wassersäule des Willersinnweiher durch ein Massenbilanzverfahren und durch die Identifizierung von Methylphosphonat, Methylamin und Methionin als drei potenzielle Vorläuferverbindungen von CH_4 bestätigt. Die stabile Isotopenzusammensetzung des Kohlenstoffs ($\delta^{13}C$-CH_4-Werte) und des Wasserstoffs ($\delta^{2}H$-CH_4-Werte) von CH_4 im Sediment zeigte den Beitrag verschiedener Arten der anaeroben Methanogenese je nach Wassertiefe auf. Im Sediment produziertes CH_4 wurde dort jedoch durch Sulfat (SO_4^{2-})-abhängige anaerobe Oxidation von CH_4 (AOM) teilweise wieder abgebaut. Das Auftreten von AOM, welches den Fluss von CH_4 aus dem Sediment in die Wassersäule erheblich verringerte, wurde durch eine Kombination von Flussmessungen und der Messungen der stabilen Isotopenzusammensetzung von CH_4 und gelöstem anorganischem Kohlenstoff (DIC) nachgewiesen.

Darüber hinaus wurde CH_4 aus dem anoxischen Hypolimnion durch aerobe Oxidation von CH_4 (MOx) an der oxisch-anoxischen Grenzfläche fast vollständig oxidiert. Die Flüsse von CH_4 aus der

Wassersäule in die Atmosphäre sowie deren stabile Isotopenzusammensetzung zeigten eine starke jahreszeitliche Abhängigkeit und Schwankungen, wobei CH_4 während der Durchmischung des Wasserkörpers im Winter stärker an ^{13}C-CH_4 und ^{2}H-CH_4 angereichert war als während der Schichtung im Sommer. Die Gesamt-Emissionen von CH_4 aus dem Willersinnweiher wurden im Winter durch diffusive CH_4-Flüsse dominiert, während im Sommer vor allem das Aufsteigen von Gasblasen zu den CH_4-Emissionen beitrug. Außerdem wurde der kürzlich eingeführte Isotopenindikator $\Delta(2,13)$ zur Charakterisierung der CH_4-Quellen im Willersinnweiher verwendet. Die $\Delta(2,13)$-Werte deuteten darauf hin, dass die Einträge von CH_4 aus dem Litoral und dem Grundwasser hauptsächlich zur Übersättigung von CH_4 während der Durchmischung der Wassersäule im Winter beigetragen haben. Wenn der See im Sommer geschichtet ist, zeigten die $\Delta(2,13)$-Werte, dass laterale und vertikale CH_4-Einträge allein die CH_4-Übersättigung nicht erklären können. Deshalb könnte OMP in dieser Zeit eine weitere wichtige Quelle von CH_4 darstellen.

Diese Studie zeigt, dass alle untersuchten Senken und Quellen von CH_4 im Willersinnweiher starken Schwankungen unterliegen, die auf der Schichtung des Sees, dessen physikalisch-chemischen Bedingungen und der Wassertiefe beruhen. Sie veranschaulicht außerdem, dass die Anwendung von Konzentrations- und $\delta^{13}C$-CH_4- und $\delta^{2}H$-CH_4-Werten ein vielversprechender Ansatz ist, um Senken und Quellen von CH_4 in Seen zu charakterisieren und weitere Informationen zu gewinnen, um die komplexe Dynamik des CH_4-Zyklus in Seen sowohl räumlich als auch saisonal zu entwirren.

Acknowledgments

First of all, I would like to thank the supervisor of my thesis, Frank Keppler, for all his endless support, encouragement and guidance throughout my PhD journey. With his ideas and enthusiasm about environmental sciences and analytics, he sparked my interest in these topics early in my bachelor studies and motivated me to follow this path. Moreover, I am especially very thankful for his advice and support during the preparation of publications and talks. Beyond that I would thank Frank for his openness and sincerity, while always being accessible for own ideas and support, whenever needed.

I would also like to thank my second supervisor Hans-Peter Grossart for his support, ideas and enjoyable collaboration during our meetings and field work at Lake Stechlin and Lake Willersinnweiher. I will fondly remember the time I spent at Neuglobsow during common field work. In this context, I would also like to thank Liu Liu for cooperativeness, especially concerning the applied methods during common field campaigns.

I am dearly obliged to Katharina Lenhart, who was especially present at the beginning of my PhD but also throughout the recent years. I could always count on her support, and learned a lot from her, especially during our first joint experiments. I am also grateful for the many helpful discussions that strongly extended my knowledge.

I would like to express my outmost gratitude to the Biogeochemistry group. Thank you for making the workspace a place with a familiar atmosphere, where sympathy, interest, humility, and helpfulness were always perceivable. This work atmosphere was very motivating and made me feel strongly supported throughout my PhD time. In particular I would like to thank: Markus Greule for technical support, help and guidance in the application of the stable isotope analytical systems. Christian Scholz, Silvia and Stefan Rheinberger for their relentless effort to measure the monthly reoccurring mountains of water samples from lake Willersinnweiher and assistance with all questions regarding the sampling campaigns at Lake Willersinnweiher. Bernd Knape, my roommate in the recent 4 years, for always knowing how to fix and improve any analytical system or item involved in the sampling campaigns, constantly constructing new (always working!) systems, patiently answering questions about technical issues, always thinking along and by always showing his gentle, helpful character in every situation.

Special thanks go out to Teresa Einzmann, for her extensive support throughout our numerous field campaigns and laboratory work. I am very grateful for your commitment and always positive mindset. I really enjoyed working together with you.

Furthermore, I would like to genuinely thank Teresa Einzmann, Bernd Knape, Frank Keppler, Jan Kleint, Iva Ralenekova, Kai Ernst, Martin Lienenlüke, Linda Jetter, Simon Ritter, Silvia and Stefan Rheinberger, Christian Scholz, Liu Liu, Markus Greule, Timo Schreiter, Yannic Wellach, Julian

Eschenröder, Hannah Geisinger, Anna Wieland, Christoph Hartmann, Marcus Schneider, Jonas Hädeler and Luna Nanasi (and all who I may have forgotten), who all supported me during the field campaigns at Lake Willersinnweiher and during the extensive analytical measurement sessions in the laboratory. Without you this thesis would not have been possible!

Beyond that, I do not want to forget to thank Heinz-Friedrich Schöler, Tobias Sattler and Margot Isenbeck-Schröter who all sparked my interest in Biogeochemistry from the start of my bachelor studies, supported me early on in my studies and kept me linked to their work groups.

I would like to express my special thanks and gratitude to Thomas Klintzsch, Jan Kleint, Teresa Einzmann, Tobias Sattler, Christoph Hartmann, Leonard Ernst for giving me valuable feedback and for the many earnest and fruitful discussions throughout the years.

Also, I would like to thank my family, who always supported me. Your constant understanding and support is much appreciated and of invaluable worth to me. Finally, I would like to express my deepest and earnest gratitude to Franziska Reiß for her patience, unconditional support and encouragement throughout my PhD.

Abbreviations

This list contains frequently used abbreviations throughout this study. Parameters and elements are described within the text.

Abbreviation	Description	Abbreviation	Description
$^{13}\alpha$	stable carbon isotope fractionation factor	ppbv	parts per billion by volume
		ppmv	parts per million by volume
$^{2}\alpha$	stable hydrogen isotope fractionation factor	SD	standard deviation
AOM	anaerobic methane oxidation	SMTZ	sulphate-methane transition zone
		SRB	sulphate reducing bacteria
BID	barrier discharge ionization detector	TMA	trimethyl amine
CRDS	cavity ring-down spectroscopy	$\Delta(2,13)$	novel isotope indicator for characterising methane sources using stable carbon and hydrogen isotopes
DIC	dissolved inorganic carbon		
FaRAGE	Fast Response Automated Gas Equilibrator	$\delta^{13}C\text{-}CH_4$	stable carbon isotope values of methane
FID	flame ionization detector		
GC	gas chromatograph	$\delta^{13}C\text{-}DIC$	stable carbon isotope values of dissolved inorganic carbon
ICP-OES	inductively coupled plasma optical emission spectrometer	$\delta^{2}H\text{-}CH_4$	stable hydrogen isotope values of methane
IRMS	isotope-ratio mass spectrometer		
MA	methyl amine	ε_C	stable carbon isotope fractionation
MET	L-methionine		
MOB	methane-oxidizing bacteria	ε_H	stable hydrogen isotope fractionation
MOx	aerobic methane oxidation	Λ	the ratio of stable hydrogen isotope fractionation vs. stable carbon isotope fractionation
MPn	methyl phosphonate		
OMP	oxic methane production		

Table of contents

List of Figures

List of Tables

List of Tables in Appendix

1 Introduction[1]

In this chapter firstly, methane (CH_4) in the atmosphere is discussed in context of global warming. Secondly, the global CH_4 budget is described. Thirdly, the CH_4 dynamics in limnic systems is outlined, especially concerning CH_4 sources, sinks, emission pathways and constraints of the stable isotope composition of CH_4. Finally, the research aims of this study are presented.

1.1 Methane in the atmosphere: a challenge for global warming

The radiative forcing and therefore the global climate is strongly regulated by the atmospheric gas composition, especially the mixing ratios of greenhouse gases. Methane constitutes the second most important anthropogenic greenhouse gas and contributes to ≈ 16 to 25 % of atmospheric global warming (Etminan et al., 2016; IPCC, 2013). The global warming potential of CH_4 (over a 100-year period) is about 32 times higher compared to carbon dioxide (CO_2) (Etminan et al., 2016; Myhre et al. 2013). Recently, atmospheric CH_4 concentrations reached 1893 ppbv (parts per billion by volume), thus accounting for 2.6 times higher CH_4 mixing ratios compared to pre-industrial times (Figure 1, Nisbet et al., 2021; Saunois et al., 2020). Hence, highlighting the importance of CH_4 emissions towards obtaining the climate goal of preventing the temperature increase from reaching 2 °C as stated in the Paris Agreement. Moreover, CH_4 plays a crucial role in atmospheric chemistry, as it is responsible for ≈ 33 % of tropospheric ozone production and the production of water vapour in the stratosphere (Crutzen, 1973; Dlugokencky et al., 2011; Kirschke et al., 2013; Nisbet et al., 2021).

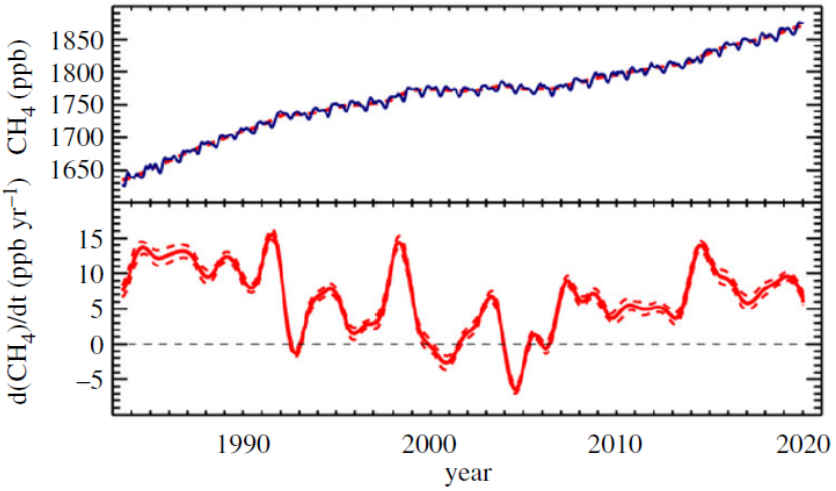

Figure 1. Change of global monthly mean atmospheric CH_4 mixing ratios from 1980 to 2020 (upper panel) and annual growth rates of global CH_4 (lower panel) (taken from Nisbet et al., 2021).

[1] Please note that parts of this section are taken from Einzmann et al. (2022) (Einzmann, T. and Schroll, M contributed euqally and share first authorship).

1.2 Global methane budget

The global CH_4 budget comprises CH_4 emissions of sources and CH_4 sinks from terrestrial and aquatic environments and is categorized into anthropogenic and natural (Figure 2). Two scenarios, namely the bottom-up and top-down estimates were applied in the most recent report on the global CH_4 budget by Saunois et al. (2020) and refer to the period between 2008 to 2017. Bottom-up estimates consist of anthropogenic inventories, land surface models and estimates of diverse natural sources. Top-down estimates on the other side derive from satellite observations and atmospheric inversion models (Kirschke et al., 2013; Saunois et al., 2020). They can accurately constrain the sinks and sources at an aggregate level, but insight into the underlying processes of CH_4 emissions is limited compared to bottom-up models (e.g., Nisbet and Weiss, 2010).

Anthropogenic CH_4 sources include agriculture and waste, production and use of fossil fuels, biomass/biofuel burning and comprise up to 60 % of total CH_4 emissions. Natural CH_4 sources include mainly wetlands, but also other natural CH_4 emissions from inland waters, oceans, permafrost, animals, geological sources and vegetation (Kirschke et al., 2013; Saunois et al., 2016, 2020). Anthropogenic and natural sources are balanced by chemical reactions in the atmosphere as the major sink of atmospheric CH_4. Thereby ≈ 90 % of CH_4 is oxidized in the troposphere by hydroxyl radicals (Ehhalt, 1974), while remaining degradation of atmospheric CH_4 occurs in the stratosphere via reactions with chlorine and oxygen atoms, in soils via oxidation (Curry, 2007; Dutaur and Verchot, 2007) and photochemically in the marine boundary layer (Allan et al., 2007). Saunois et al. (2020), reported that total CH_4 emissions account for 737 Tg (1 Tg = 10^{12} g) yr^{-1} for bottom-up estimates, while top-down estimates are smaller with 576 Tg yr^{-1}. This discrepancy is most probably based on large uncertainties of natural emission from inland water systems and/or the overestimation of individual reported CH_4 sources and highlights a lack of knowledge about the underlying processes of CH_4 formation (Saunois et al., 2020). Additionally, CH_4 sinks show different estimations for the bottom-up (625 Tg yr^{-1}) and top-down (556 Tg yr^{-1}) approach. Nevertheless, estimations for CH_4 sinks are smaller compared to CH_4 sources in both scenarios, which explains the observed increase in atmospheric CH_4 emissions. According to Saunois et al. (2020), CH_4 emissions from inland water systems (rivers, ponds, reservoirs and lakes) account for up to 159 Tg yr^{-1} and lakes constitute the largest part of up to 70 % of these aquatic (limnic and marine) sources (Bastviken et al., 2011; DelSontro et al., 2018). However, in a recent study by Rosentreter et al. (2021), CH_4 emissions from aquatic systems were estimated to be even higher (253 to 455 Tg yr^{-1}), thus accounting for up to 53 % of total global CH_4 emissions (bottom-up approach). According to this study, lakes alone supply about 17 % of total global CH_4 emissions (151 ± 73 Tg CH_4 yr^{-1}).

These high contributions of CH_4 from aquatic freshwater systems, especially from lakes, highlight its importance for the global CH_4 budget but also show that aquatic CH_4 emissions are highly variable. Furthermore, the processes and mechanisms underlying CH_4 supersaturation of dissolved CH_4 in

oxygenated water column of lakes and basins, the so called “Methane-Paradox”, are not fully resolved, and were highly debated within the last decade (Bižić et al., 2020b; DelSontro et al., 2018; Encinas Fernández et al., 2016; Grossart et al., 2011; Günthel et al., 2019, 2020; Peeters et al., 2019; Peeters and Hofmann, 2021). Thus, a better understanding of the processes underlying the CH_4 emissions from lakes and other aquatic systems are strongly needed, especially as eutrophication and positive climate feedbacks are predicted to increase aquatic CH_4 emissions (Aben et al., 2017; Beaulieu et al., 2019; Rosentreter et al., 2021; Saunois et al., 2020).

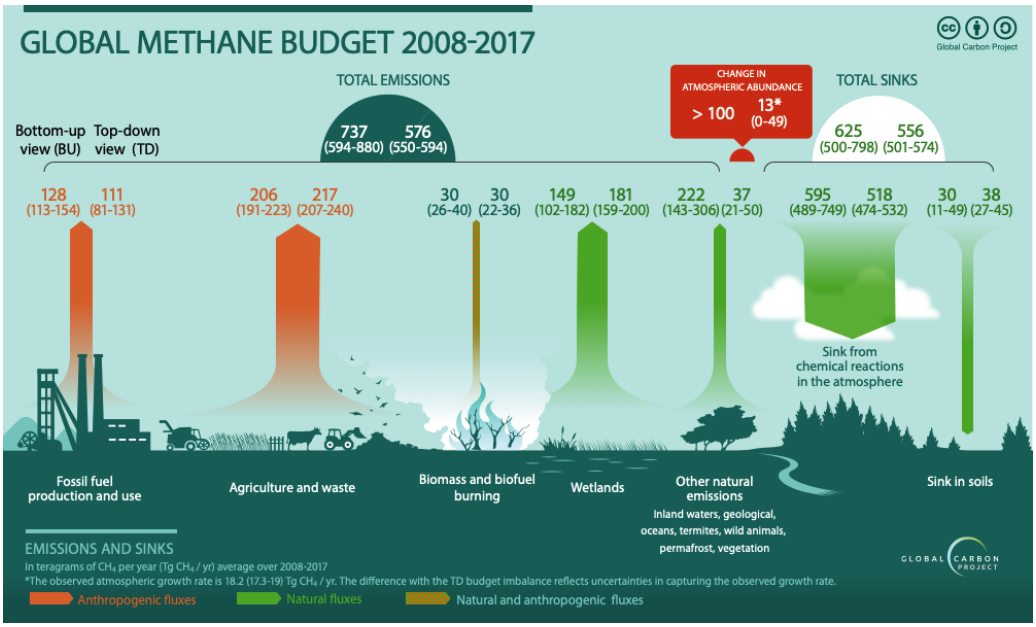

Figure 2. Global CH_4 budget for the decade from 2008 to 2017. For each category a bottom-up estimation (left number) and top-down estimation (right number) for CH_4 fluxes is given. The ranges of the CH_4 flux estimations are shown below. The colour of each category represents its anthropogenic (orange), natural (green) or a mix of both origins (orange-green striped) (taken from Saunois et al., 2020).

1.3 Methane formation processes

Methane formation processes underlying natural and anthropogenic sources are further categorised as thermogenic, pyrogenic, and biotic (Kirschke et al., 2013; Saunois et al., 2016, 2020). Methane of thermogenic origin is produced as a result of geologic processes, which include the conversion of organic matter in the earth’s crust under high temperature and pressure conditions. Thermogenic CH_4 is then released to the atmosphere either anthropogenically via fossil fuel exploitation or naturally via gas-exchange processes regarding volcanoes or terrestrial and marine seeps (Etiope and Sherwood Lollar, 2013; Kirschke et al., 2013; Saunois et al., 2016, 2020; Wegener et al., 2008). Similarly, pyrogenic CH_4, which is generated during incomplete combustion of biomass, enters the atmosphere either via anthropogenic processes such as biofuel or fossil fuel combustion or naturally during wildfires (Kirschke et al., 2013; Saunois et al., 2016, 2020). Biogenic CH_4 constitutes a major part (70 %) of global CH_4 formation. Traditionally biogenic CH_4 is produced under strictly anaerobic

conditions by methanogenic archaea e.g., in the anoxic sediment of lakes, wetlands, rice paddies, landfills and ruminant livestock (Bižić et al., 2020b; Kirschke et al., 2013; Saunois et al., 2020). Methanogenic archaea produce CH_4 in the process of anoxic methanogenesis for the remineralization of organic matter but only if other terminal electron acceptors which would yield a greater energy gain are depleted (e.g., Whiticar, 1999; Conrad, 2005). Consequently, anoxic methanogenesis is only the final step of a redox sequence involved in the degradation of organic matter (Froelich et al., 1979). The succession of the redox sequence is determined by the highest energy gains for the microorganisms starting with oxygen (O_2), followed by nitrate (NO_3^-), nitrite (NO_2^-), manganese ions (Mn^{4+}), iron ions (Fe^{3+}), sulphate (SO_4^{2-}), and lastly methanogenesis. Methanogenesis is dependent on the availability of a few substrates and limited to only a small number of pathways. Substrates for anoxic methanogenesis constitute CO_2 (hydrogenotrophic pathway), acetate (acetoclastic pathway) and methylated compounds (Conrad, 2005, 2009; Deppenmeier et al., 1996; Gruca-Rokosz et al., 2020; Lessner, 2009; Thauer et al., 2008).

Opposed to the long-standing paradigm that CH_4 is only produced in anoxic environments by methanogenic archaea, an increasing number of studies have demonstrated that many organisms produce CH_4 in the presence of O_2. The first evidence for these new sources of CH_4 was presented by Keppler et al. (2006), and showed CH_4 formation by plants. In the following many other organisms such as animals, saprotrophic fungi, lichens, marine and freshwater algae, aquatic and terrestrial cyanobacteria, bacteria, archaea and human cell lines were identified to belong to the group of novel sources of CH_4 (Bižić et al., 2020a; Ernst et al., 2022; Ghyczy et al., 2008; Klintzsch et al., 2019; Lenhart et al., 2012, 2015, 2016).

Just recently, CH_4 formation under oxic conditions was proposed to occur in all three domains of life (Ernst et al., 2022). The authors demonstrated a universal mechanism for CH_4 formation on a cellular level in organisms. Thereby, CH_4 formation is triggered by the interaction of reactive oxygen species (ROS) with free Fe^{2+} and methylated compounds in cells. The complex interplay of methylated compounds and oxidative stress in cells could explain the large variations in CH_4 emission rates between different organisms. However, the large uncertainties in the estimated CH_4 emissions from these novel CH_4 sources of up to 2 magnitudes have prevented it from being considered in the global CH_4 budget yet (Boros and Keppler, 2018; Li et al., 2020; Liu et al., 2015, 2021; Saunois et al., 2020; Wang et al., 2013, 2020).

1.4 Methane dynamics in limnic systems

As described in the section above, CH_4 emissions from aquatic freshwater systems and especially lakes are responsible for up to a third of global CH_4 emissions (Rosentreter et al., 2021; Saunois et al., 2020). However, CH_4 dynamics in limnic systems are very complex, as they are subject to many different processes and mechanisms (Figure 3). Recently, the observation of peaks in CH_4

concentrations in the O_2-saturated water layers of aquatic environments also called the "Methane Paradox", has attained a lot of attention and has been intensively discussed, as it contradicts the traditional conception that CH_4 is formed strictly under anoxic conditions by methanogenic archaea (e.g., Bižić et al., 2020b). This phenomenon was first described for oceans (Scranton and Brewer, 1977), but more recently has also been reported for a large number of lakes (e.g., Bogard et al., 2014; Blees et al., 2015; Tang et al., 2016; Grossart et al., 2011; Günthel et al., 2019; Hartmann et al., 2020). The origin of the occurrence of the "Methane Paradox", however, is still unclear, but there are two opposing hypotheses that are suggested to explain it. The first proposes that CH_4 is produced in the anoxic sediment of aquatic systems and then physical transport processes lead to the development of CH_4 peaks in the oxygenated water column (e.g., Encinas Fernández et al., 2016; Hofmann et al., 2010; Peeters et al., 2019; Peeters and Hofmann, 2021). The second hypothesis on the other hand suggests that the CH_4 peak in the oxic water column is produced locally via oxic CH_4 production (OMP), e.g., by phytoplankton, cyanobacteria, or bacteria and that the contribution of OMP to CH_4 emissions from lakes increases with lake size (Bižić-Ionescu et al., 2018; Bižić et al., 2020a; Grossart et al., 2011; Günthel et al., 2019, 2020; Hartmann et al., 2020). Nevertheless, a combination of the occurrence of both suggested pathways is the most probable scenario (Bižić et al., 2020b). In the following three chapters sources, sinks and emission pathways of CH_4 in lakes are described.

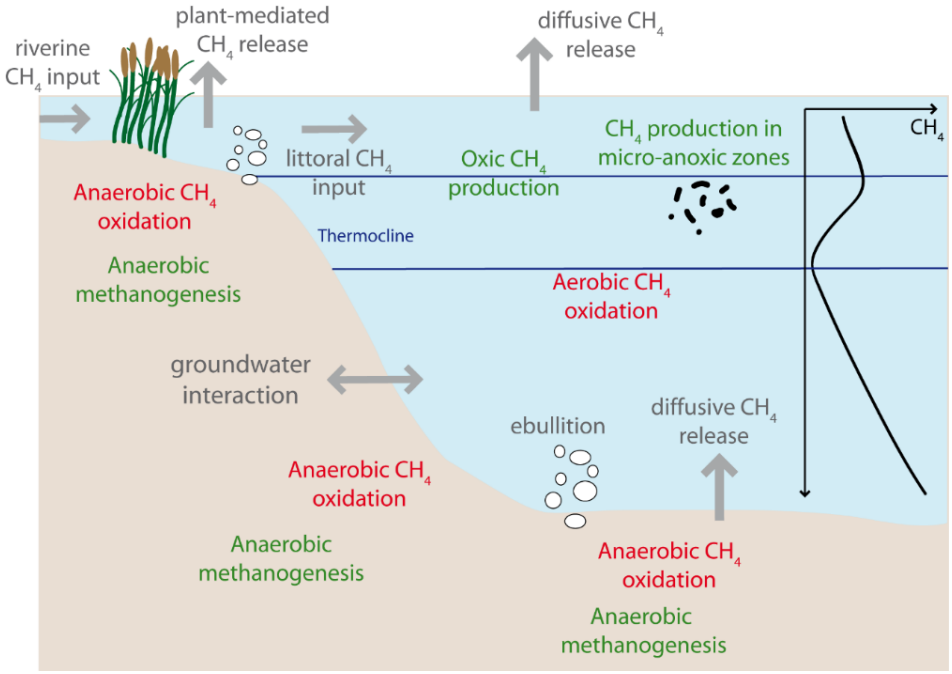

Figure 3. Overview of sources (green) and sinks (red) of CH_4 in the limnic environment. Transport processes (grey) and its transport direction are indicated by grey arrows. A typical concentration profile of CH_4 (black) during thermal stratification is shown in the right part of the figure (taken from Einzmann et al., 2022).

1.4.1 Sources of methane in lakes

In limnic environments, similar to the traditional views on CH_4 formation processes, biogenic CH_4 was believed to exclusively stem from anoxic methanogenesis in the sediment and consequent transport processes into the water column, e.g., via vertical or lateral input or ebullition (Encinas Fernández et al., 2016; Hofmann et al., 2010; Peeters et al., 2019; Peeters and Hofmann, 2021). Currently there is a lively debate about whether a non-traditional source of CH_4 (in this case OMP) in the surface water layer is needed to explain vertical and spatial CH_4 concentrations in the water column of lakes and to compensate for diffusive CH_4 losses to the atmosphere. Supporters of this hypothesis argue that no additional CH_4 source is needed and thus CH_4 production and its transport from the anoxic sediments and transport of CH_4 rich water masses from shallow areas of the lake is sufficient to explain CH_4 supersaturation in lakes (e.g., Peeters and Hofmann, 2021; Peeters et al., 2019). These processes were previously used to explain the "Methane Paradox", the occurrence of CH_4 peaks and supersaturation in the oxygenated water column.

However, a large number of studies reported the in-situ production of CH_4 in the O_2-rich water layers of lakes (e.g., Bižić et al., 2020b; Bižić-Ionescu et al., 2018; Bogard et al., 2014; DelSontro et al., 2018; Donis et al., 2017; Grossart et al., 2011; Günthel et al., 2019, 2020; Hartmann et al., 2020; Khatun et al., 2020, 2019; León-Palmero et al., 2020; Perez-Coronel et al., 2021; Yao et al., 2016). Nevertheless, OMP is complex to detect, as to date it cannot be measured directly and all occurring CH_4 fluxes into and out of the water column of the lake, as well as CH_4 production and consumption processes have to be considered. Thus, mass balance approaches are frequently used to estimate OMP rates (Donis et al., 2017; Günthel et al., 2019; Hartmann et al., 2020). Large uncertainties in the estimations of OMP and its contribution to surface water CH_4 supersaturations prevail and highlight that there is a lack of understanding about the underlying processes and pathways, as well as their temporal and spatial variations.

So far, several pathways of OMP have been identified, including (1) methanogenesis by methanogens in anoxic micro-niches (e.g., de Angelis and Lee, 1994; Schmale et al., 2018), (2) direct production of CH_4 by algae associated with oxidative stress and/or photosynthesis (Klintzsch et al., 2019; Lenhart et al., 2016; Liu et al., 2022) or the conversion of dimethyl sulphoniopropionate (DMSP) by nitrogen-limited microorganisms (Damm et al., 2010, 2015), (3) demethylation of methyl phosphonates (MPn) by cyanobacteria (e.g., Karl et al., 2008; Repeta et al., 2016) or release of CH_4 by cyanobacteria associated with photosynthesis (Bižić et al., 2020a), (4) CH_4 formation as a by-product in the metabolism of N_2-fixing microorganisms from the reduction of CO_2 (Zheng et al., 2018) and (5) the microbiological conversion of methyl amine (MA), trimethyl amine (TMA) and methionine (MET) to CH_4 in oxygenated water layers (Bižić-Ionescu et al., 2018; Lenhart et al., 2016; Wang et al., 2021).

For atmospheric CH_4 emissions, OMP is of particular importance as the production of CH_4 takes place closer to the water-atmosphere interface. Thus, OMP was proposed to strongly contribute to

subsequent CH_4 emissions from aquatic freshwater systems, especially in large lakes (> 1 km^2), where the transport and influence of CH_4 produced in shallow lake sediments is little (Günthel et al., 2019; Tang et al., 2016).

However, evaluating the contribution of OMP to CH_4 supersaturation and distinguishing it from CH_4 produced via anoxic methanogenesis is very challenging due to the complex interactions and transport processes in limnic systems (Figure 3). Therefore, the application of stable carbon ($\delta^{13}C$-CH_4) and stable hydrogen ($\delta^{2}H$-CH_4) isotopes might be helpful to distinguish between formation and degradation processes in the environment (Figure 4; e.g., Schenk et al., 2021; Whiticar, 2020). The great advantage of stable isotope investigations is that CH_4 formed from different processes can be distinguished based on its $\delta^{13}C$-CH_4 and $\delta^{2}H$-CH_4 values. These differences in the stable isotope values for instance allow for a distinction between different types of methanogenesis since different enzyme systems fractionate differently against ^{13}C and ^{2}H (e.g., Conrad, 2005).

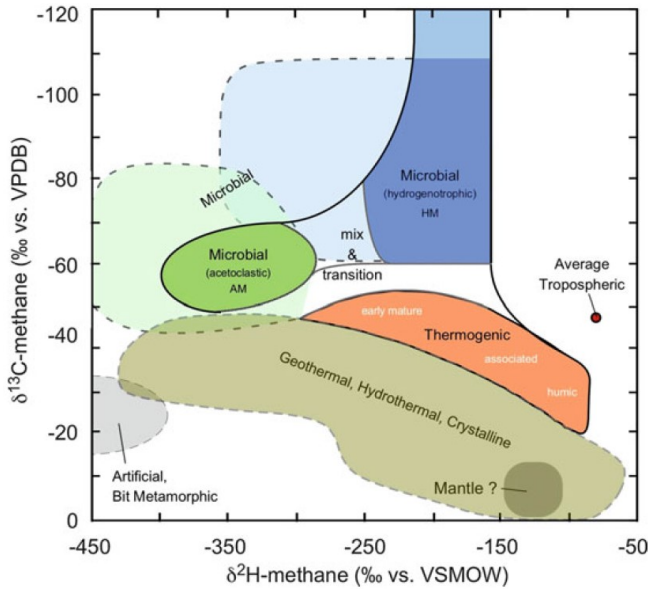

Figure 4. Classification of stable carbon and stable hydrogen isotope values of various CH_4 formation pathways (taken from Whiticar, 2020).

Hence, CH_4 produced via the acetoclastic pathway shows $\delta^{2}H$-CH_4 values (-250 to -150 ‰) that are more positive and $\delta^{13}C$-CH_4 values (-110 to -60 ‰) that are more negative compared to CH_4 produced via the hydrogenotrophic pathway ($\delta^{2}H$-CH_4 values between -400 to -250 ‰ and $\delta^{13}C$-CH_4 values between -60 to -40 ‰; Whiticar, 2020). If the stable isotope composition of methanogenic CH_4 is different compared to CH_4 originating from OMP, isotopic signatures might be useful to distinguish between traditional anoxic CH_4 formation and OMP. However, only limited data for $\delta^{13}C$-CH_4 and $\delta^{2}H$-CH_4 values of CH_4 from OMP are available to date. Klintzsch (2021) reported $\delta^{13}C$-CH_4 values of CH_4 produced by three widespread marine algae ranging from -49 to -23 ‰, while Luxem et al. (2020) reported $\delta^{13}C$-CH_4 ranging from -100 to -70 ‰ and $\delta^{2}H$-CH_4 values ranging from -550 to -450 ‰ for nitrogenase derived CH_4. Both studies report $\delta^{13}C$-CH_4 and $\delta^{2}H$-CH_4 values that can be distinguished

from traditional CH_4 sources from the anoxic environment. Especially the relatively positive $\delta^{13}C\text{-}CH_4$ values (compared to atmospheric $\delta^{13}C\text{-}CH_4$ values) reported for marine algae species are of great interest, as such positive $\delta^{13}C\text{-}CH_4$ values could at least partially explain the observed $\delta^{13}C\text{-}CH_4$ values in the surface water layer, which were more enriched in $^{13}C\text{-}CH_4$ and $^{2}H\text{-}CH_4$ compared to CH_4 originating from anoxic methanogenesis (e.g., Hartmann et al., 2020; Klintzsch, 2021).

1.4.2 Sinks of methane in lakes

In aquatic environments oxidation of CH_4 takes place in both oxic and anoxic habitats, removing CH_4 from the water column and sediment and thus mitigating CH_4 emissions from these systems to the atmosphere (e.g., Reeburgh, 1996; King, 1992; Whiticar, 2020). Aerobic methane oxidation (MOx) consumes between 30 to 99 % of limnically produced CH_4 (Bastviken et al., 2008). Aerobic methane oxidation occurs in the oxygenated water column by CH_4-oxidizing bacteria (MOB) that use CH_4 or other single-carbon compounds (C_1) as their carbon and energy source in the presence of O_2. Thereby, CH_4 is converted to CO_2 via intermediate compounds such as methanol, formaldehyde, and formate (Dedysh and Dunfield, 2011; McDonald et al., 2008; Roslev and King, 1995) according to Eq. (1). Nevertheless, the parameters and mechanisms underlying MOx are complex and depend on, e.g., the diversity of methanotrophs and occurrence in different habitats (Trotsenko and Khmelenina, 2002; Utsumi et al., 1998).

$$CH_4 + O_2 \rightarrow CO_2 + 2H_2O \quad (1)$$

In contrast to MOx, anaerobic methane oxidation (AOM) is an important sink of CH_4 in the anoxic water bodies or the sediment of aquatic systems. Anaerobic methane oxidation requires the presence of other terminal electron acceptors than O_2 and has been associated with the reduction of NO_3^-, NO_2^- (Deutzmann et al., 2014; Ettwig et al., 2008; Norði and Thamdrup, 2014; Raghoebarsing et al., 2006), Mn^{4+} (Beal et al., 2009), Fe^{3+} (Crowe et al., 2011; He et al., 2018; Norði et al., 2013) and SO_4^{2-} (Martens and Berner, 1974; Reeburgh, 1976). While SO_4^{2-}-dependent AOM is most prevalent in marine environments in the so-called sulphate-methane-transition zones (SMTZ) due to high prevailing SO_4^{2-} concentrations, SO_4^{2-}-dependent AOM has also been reported for a few limnic environments (Eq. (2); Aben et al., 2017; Knittel and Boetius, 2009; Kleint et al., 2021; Whiticar, 2020; Schubert et al., 2011; Timmers et al., 2016).

$$CH_4 + SO_4^{2-} \rightarrow HCO_3^- + HS^- + 2H_2O \quad (2)$$

Limnic freshwater systems are usually characterised by low SO_4^{2-} concentrations thus preventing the occurrence of SO_4^{2-}-dependent AOM. However, in recent years AOM related to the reduction of SO_4^{2-} and the presence of SMTZs in the sediment were reported for an increasing number of freshwater systems (Kleint et al., 2021; Schubert et al., 2011; Timmers et al., 2016).

In SMTZs CH_4 is oxidized via SO_4^{2-} by a syntrophic coexistence of sulphate-reducing bacteria (SRB) and methane-oxidizing archaea (e.g., Orcutt and Meile, 2008; Boetius et al., 2000; Alperin and

Reeburgh, 1985). Thus, CH_4 fluxes of CH_4 from the sediment into the water column are strongly reduced in these systems and were reported to account for up to 90 % of sedimentary produced CH_4 (Hartmann, 2018).

Microbial oxidation of CH_4 leads to an enrichment of ^{13}C-CH_4 and ^{2}H-CH_4, as the consumption of CH_4 by microorganisms is linked to kinetic isotope effects (Barker and Fritz, 1981). Furthermore, hydrogen isotope fractionation of CH_4 was reported to be 5 to 10 times higher when compared with carbon isotope fractionation. Hence, MOx and AOM consume the heavier ^{13}C-CH_4 more slowly than the lighter ^{2}H-CH_4. Hence, the relation between $\delta^{13}C$-CH_4 and $\delta^{2}H$-CH_4 values are good indicators for the zones of aquatic systems where MOx or AOM occur (Cadieux et al., 2016; Norði et al., 2013; Riedinger et al., 2010; Schubert et al., 2011; Tsunogai et al., 2020).

1.4.3 Methane emissions from lakes

As introduced in section 1.2, CH_4 emissions from aquatic freshwater environments are estimated to be a major source of the global CH_4 cycle (Rosentreter et al., 2021; Saunois et al., 2020). This is especially noteworthy, as about 30 to 99 % of produced CH_4 is estimated to be oxidized before reaching the atmosphere, indicating that without this CH_4 sink in the water column of lakes CH_4 emissions from aquatic freshwater systems would be substantially higher (Bastviken et al., 2008). Thus, many studies have covered the CH_4 emissions from limnic systems in the recent decades and several pathways of limnic CH_4 emissions have been described (e.g., Bastviken et al., 2002, 2011). The three major pathways of CH_4 emissions constitute plant-mediated CH_4 release, diffusion, and ebullition (Figure 3, e.g., Bastviken et al., 2004).

Even though the plant-mediated release of CH_4 is of particular importance for wetlands and flooded rice fields, this process is also important in limnic systems containing emergent plant coverage (Cicerone and Shetter, 1981; Sebacher et al., 1985; Whiting and Chanton, 1993). Thereby, CH_4 from anoxic sediments is transported through the roots and aerenchyma (air channels) of plants to the atmosphere. Thus, CH_4 emissions circumvent potential oxidation in the water column (Bridgham et al., 2013; Sebacher et al., 1985). Methane emissions from plant-mediated release are, on the one hand, dependent on plant characteristics such as plant surface area and plant density, but, on the other hand, also on plant coverage and lake size, as in bigger lakes, proportionally, a smaller part of the lake is covered by emerged plants (Bastviken et al., 2002; Bridgham et al., 2013).

Diffusive CH_4 fluxes at the water-atmosphere interface constitute another important pathway for CH_4 emission from aquatic systems. The understanding of the underlying factors of this emission pathway is fundamental for the biogeochemical cycle of CH_4 in aquatic systems (Klaus and Vachon, 2020). Diffusive CH_4 fluxes are dependent on lake area, and their importance enhances with increasing lake size (Bastviken et al., 2002). Subsequently, diffusive CH_4 fluxes account for ≈ 50 % of CH_4 emissions in large lakes. The magnitude of diffusive CH_4 emissions is associated with complex interactions in

the near-surface water column and depend on dissolved CH_4 concentrations and turbulences. Turbulences in the uppermost water layer are mostly generated by wind. Nevertheless, they are also controlled by surface heat fluxes and lake characteristics such as size and shape, as well as the surroundings of the lake (e.g., trees or mountains). These factors then influence wind speed and its spatial distribution across the lake (Klaus and Vachon, 2020; Kwan and Taylor, 1994; Markfort et al., 2010; Prairie and del Giorgio, 2013). Beyond these parameters, the occurrence of microbubbles can also substantially contribute to diffusive CH_4 emissions (Prairie and del Giorgio, 2013). For a more detailed discussion of diffusive CH_4 emissions and applied methods, please refer to the articles by Cole et al. (2010), Prairie and del Giorgio (2013) and Klaus and Vachon (2020).

Finally, CH_4 release from aquatic systems via ebullition (uprising of gas bubbles rich in CH_4 from the sediment) comprises presumably the most important contributor to total limnic CH_4 emissions, especially in eutrophic systems (Aben et al., 2017; Bastviken et al., 2004; Wik et al., 2016). Gas bubbles migrating upwards in the water column are subject to gas exchange with the surrounding water column, especially when they originate from greater depths (McGinnis et al., 2006). However, ebullitive CH_4 fluxes from shallow areas of the lake are only subject to short interactions with the water column and thus mostly reach the atmosphere directly (Ostrovsky et al., 2008). Environmental factors controlling ebullitive fluxes are highly episodic, show strong spatial variations and are therefore hard to evaluate and predict (e.g., West et al., 2016; Thottathil and Prairie, 2021; DelSontro et al., 2016). Parameters that control ebullition include the productivity of CH_4 in the sediment (e.g., controlled by temperature; DelSontro et al., 2016; Aben et al., 2017), change of hydrostatic pressure (Mattson and Likens, 1990; Wik et al., 2013) and disturbance of sediments by wind-induced turbulences (Joyce and Jewell, 2003). However, the contribution of ebullitive fluxes to total CH_4 emission decreases with increasing water depth (Bastviken et al., 2004).

The described emission pathways of CH_4 from limnic systems lead to the strong contribution of limnic CH_4 emissions to total atmospheric CH_4 emissions. However, allocating and distinguishing between different CH_4 sources is very challenging but necessary in order to create accurate budgets of atmospheric CH_4. The stable isotope signatures of CH_4 provide strong assistance in assessing global and regional CH_4 budgets, as often different CH_4 sources are characterised by a distinct source signature of $\delta^{13}C\text{-}CH_4$ and $\delta^{2}H\text{-}CH_4$ values and therefore allow to differentiate between different atmospheric sources of CH_4, e.g., lakes and wetlands (Mikaloff Fletcher et al., 2004; Nisbet et al., 2021; Thottathil and Prairie, 2021).

1.5 Motivation and research aims of this study

As discussed above, CH_4 emissions from aquatic systems constitute up to 50 % of global CH_4 emissions, and lakes are estimated to be the major contributor (Rosentreter et al., 2021; Saunois et al., 2020). Furthermore, CH_4 emissions from lakes are predicted to increase in the scope of climate change due to increasing temperatures and eutrophication (Aben et al., 2017; Beaulieu et al., 2019; Sepulveda-Jauregui et al., 2018). Even though the CH_4 cycle of lakes and subsequent CH_4 emissions have been the subject to extensive investigations and debate, many key parameters and factors are still unclear. Beyond that, the limnic CH_4 cycle is very complex, as many different mechanisms and pathways are involved in CH_4 production and consumption.

Therefore, the overall aim of this study was **to obtain an overall understanding of the CH_4 cycle in lake Willersinnweiher via the temporal and spatial analysis of CH_4 production, oxidation and emission processes in the sediment and water column**.

The overall aim is subclassified into the following more specified aims:

1) characterising the CH_4 production in the sediment and diffusion fluxes from the sediment into the water column both temporally and spatially

2) delivering isotopic evidence for the occurrence of AOM in the sediment of Lake Willersinnweiher

3) characterising the temporal and spatial patterns of CH_4 concentrations, $\delta^{13}C\text{-}CH_4$ and $\delta^{2}H\text{-}CH_4$ values over a period of 2.5 years and analysing the distribution of epilimnic CH_4 concentrations of Lake Willersinnweiher at a high resolution

4) investigating the potential contribution of CH_4 input from groundwater as well as its stable isotope composition and its temporal variations over the course of 2.5 years

5) identifying zones of occurring MOx in the water column of Lake Willersinnweiher and determining potential MOx rates and their temporal variation between the stratification period in summer and the mixing period during winter

6) estimating OMP rates at Lake Willersinnweiher during stratification and mixing period using a mass balance approach and investigating the potential precursor compounds MPn, MA, TMA and MET for their potential to be converted to CH_4 in the oxygenated water layers of Lake Willersinnweiher

7) quantifying and determinating the temporal variations of CH_4 emissions (diffusion and ebullition) from Lake Willersinnweiher as well as their $\delta^{13}C\text{-}CH_4$ and $\delta^{2}H\text{-}CH_4$ values

8) disentangling the contribution of different CH_4 sources to CH_4 supersaturation during periods of stratification and mixing of the water column at Lake Willersinnweiher using the novel $\Delta(2,13)$ isotope indicator.

2 Materials and Methods[2]

2.1 Study site and its geochemical characterisation

Lake Willersinnweiher is a eutrophic monomictic lake in the south-west of Germany near Ludwigshafen in the Upper Rhine Valley (Figure 5A). It used to be a gravel pit and comprises an area of ca. 0.17 km^{-2}, a width of 325 m and a length 825 m. (Figure 5A, B; Sandler, 2000). Lake Willersinnweiher, has no in- or outflows at the surface and is therefore fed solely by groundwater and precipitation (Wollschläger et al., 2007). Its average depth is ≈ 8 m. However, the lake is divided into a south-western basin that is characterised by a maximum depth of ≈ 20 m and a shallower north-western basin with a maximum depth of ≈ 14 m. A swell, which is situated in a depth of about 8 m, divides the two basins and restrains the exchange of water masses between the two basins (Figure 5C; Sandler, 2000; Schmid, 2002; Schröder, 2004).

Groundwater enters the lake from the south-west towards north-east, according to its flow direction and passes at least one other lake prior to reaching Lake Willersinnweiher (Figure 5C, Kluge et al., 2007; Wollschläger et al., 2007). As groundwater is the main source of solutes at Lake Willersinnweiher, it highly influences its water chemistry. The water column of Lake Willersinnweiher is characterised by high concentrations of SO_4^{2-} (≈ 2 mmol l^{-1}), which are rarely found in freshwater systems (Kleint et al., 2021). The high SO_4^{2-} concentrations in lake water originate from pyrite oxidation in the Quaternary river sediments of the Rhine and are transported to the lake via inflowing groundwater (Isenbeck-Schröter et al., 2016; Schröder, 2004). Furthermore, eutrophic conditions in the water column of Lake Willersinnweiher originate from nutrient input from agricultural land in close proximity to the lake (Laukenmann, 2002).

The water column of Lake Willersinnweiher was characterised by seasonal stratification during the summer months and a period of complete mixing of the water column between November/December to March/April (Kleint et al., 2021; Wollschläger et al., 2007). During the stratification period the water column is vertically divided in three layers: 1) The uppermost water layer is the epilimnion in which water masses are fully mixed and oxygenated due to wind-induced turbulences at the water surface. In this layer, gases dissolved in the water are in exchange with the atmosphere. Below follows 2) the metalimnion, in which the water temperature decreases sharply with depth. This temperature gradient, referred to as thermocline, prevents the water bodies from mixing due to differences in their respective density. In the metalimnion, O_2 concentrations decline with increasing depth until O_2 is completely consumed leading to the development of a chemocline at the bottom of the metalimnion.

[2] Please note that parts of this section are taken from Einzmann et al. (2022).

The top and the bottom of the metalimnion are furthermore characterised by chlorophyll-a (Chl-a) peaks, thus indicating phytoplankton activity. 3) The anoxic hypolimnion follows below the metalimnion. It is anoxic due to organic matter turnover from bioproduction in the overlying water layers. High SO_4^{2-} concentrations in the sediment originating from groundwater input make SO_4^{2-} reduction the main process of organic matter turnover at Lake Willersinnweiher (Kleint et al., 2021). Thus, production and release of S^{2-} from the sediment into the hypolimnion via SO_4^{2-} reduction lead to the development of euxinic conditions during stratification (Schröder, 2004). In autumn decreasing temperatures lead to a weakening of the stratification until complete circulation of the water column is established. Hence, the whole water column is characterized by fully oxic conditions during mixing period that can reach up to a few millimetres into the uppermost sediment layers (Schröder, 2004).

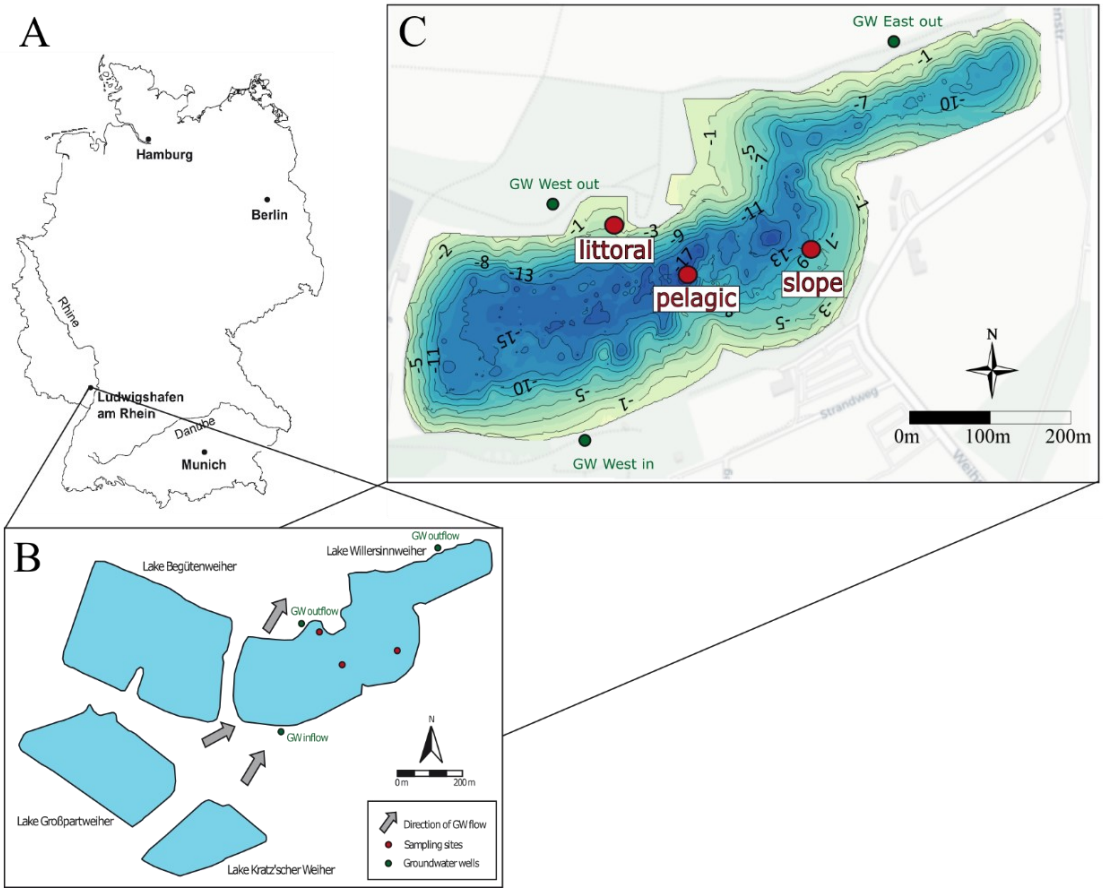

Figure 5. Location of (A, B) Lake Willersinnweiher and three circumjacent lakes in Germany modified after Kleint et al. (2021) and Einzmann et al. (2022). (C) Sampling sites (pelagic, slope and littoral) at the lake as well as groundwater sampling sites (GW West in, GW West out, GW East out) are represented by red and green points, respectively. The flow direction of groundwater is indicated after Wollschläger et al. (2007).

2.2 Field sampling and preparation of samples for laboratory analysis

Sampling of the water column and sediment at Lake Willersinnweiher was carried out in the scope of 19 field campaigns between May 2019 and September 2021. A detailed outline of the field campaigns and the investigated parameters are shown in the appendix according to Table A 1. Field sampling was performed at three different sites with different water depths: the pelagic site with a depth of 20 m and located in the deepest part of the southwestern basin of Lake Willersinnweiher, the slope site, which is located in the south-eastern part of the lake and about 9 m deep, and the littoral site, which is situated in the littoral zone close to the north-western shore and therefore only 1.5 m deep. Additionally, three groundwater wells (GW West In, GW West Out, GW East Out) upstream and downstream of the lake were sampled (location, sampling sites and groundwater wells are shown in Figure 5C). Data for the wind speed and direction derive from a close-by weather station.

2.2.1 Bathymetric map

Profiles of water depths to the bottom of Lake Willersinnweiher were measured using a split-beam echo sounder (120 kHz, *Simrad EY60*, USA) similar to Liu et al. (2021). The software Sonar 5-Pro was used to process the acquired data. The bathymetric map (Figure 5C) was generated using the software Surfer (Surfer 22, *Golden Software*, USA). The same software was furthermore used to calculate the water volume, planar and sediment areas of Lake Willersinnweiher.

2.2.2 Sediment

The sediment of Lake Willersinnweiher was sampled in the period between May 2019 and March 2021. During sediment sampling, two sediment cores with a length of up to 35 cm were obtained with a manually operated gravity corer at each of the three sites. The first core was used to analyse pore water and the second core to analyse the dissolved CH_4. The cores were prepared for laboratory analyses immediately after sampling.

In the first core pore water was extracted in 1, 2 and 3 cm intervals for core depths between 0 to 10 cm, 10 to 20 cm and 20 to 35 cm, respectively, using rhizons with a pore-size of 0.15 µm (*Rhizosphere Research Products*, Netherlands). The obtained pore water samples were analysed for their dissolved ion composition during all sediment samplings and for its $\delta^{13}C$ values of dissolved inorganic carbon (DIC) during field campaigns from May 2020 to March 2021. Samples for the analysis of stable isotope values of DIC ($\delta^{13}C$-DIC) were prepared by transferring 1 ml of the filtered water sample into a 3 ml glass vial and acidifying it with a few drops of hydrochloric acid (25 %) in order to convert all DIC to CO_2. After shaking vigorously, the headspace was extracted, transferred into evacuated 1.5 ml glass vials and stored until analysis.

The second core was subsampled in the same intervals as the pore water by transferring 3 ml of sediment with a cut-off plastic syringe into 20 ml glass vials for the analysis of dissolved CH_4

concentrations, $\delta^{13}C\text{-}CH_4$ and $\delta^{2}H\text{-}CH_4$ values in the laboratory (sections 2.4.1 and 2.4.2). Furthermore, sediment samples in the glass vials were treated with 3 to 5 ml of a 1 M sodium hydroxide solution, crimped with a lid containing a septum and shaken vigorously for ≈ 10 min, in order to prevent any alterations by microbial activity and establish an equilibrium between the gases dissolved in the water and the headspace. Afterwards, the headspace was extracted for laboratory analysis, and the remaining sediment samples in the glass vials were dried in an oven at 105 °C for at least 48 h and weighed before and after drying to determine water content and porosity.

2.2.3 Water column

The water parameters temperature, pH, dissolved O_2, and Chl-a concentrations were recorded at high temporal resolution (1 Hz) within the water column of each site using a Exo1 multiparameter probe (*Xylem Analytics*, Norway). Prior to each field campaign, the probe was calibrated for the different parameters in the laboratory. Samples at different water depths were taken using a submersible pump (*COMET-Pumpen Systemtechnik GmbH &Co. KG*, Germany). Water samples used for the determination of dissolved CH_4 concentrations, $\delta^{13}C\text{-}CH_4$ and $\delta^{2}H\text{-}CH_4$ values were taken using the headspace technique (Wilson et al., 1989). For this purpose, 100 ml of water was transferred to a 140 ml syringe, and 40 ml of Helium (He) gas was added via a three-port valve to create a headspace. The sample was shaken vigorously for 1.5 min to equilibrate the water and gas headspace. Subsequently, the headspace was extracted with another syringe and transferred into an evacuated 12 ml Exetainer® (*Labco*, UK). Water samples used to measure dissolved ion composition as well as DIC concentrations in the laboratory were filtered through a 0.2 µm filter into 15 ml falcon tubes (*Corning*, USA). Samples for cation analysis were furthermore acidified with 150 µl of 6M HNO_3 and stored at a temperature of 4 °C until analysis. Water samples for the analysis of $\delta^{13}C\text{-}DIC$ were prepared by transferring 1 ml of the filtered water sample into a 3 ml glass vial and acidifying it with a few drops of hydrochloric acid (25 %) in order to convert all DIC to CO_2. After shaking vigorously, the headspace was extracted, transferred into evacuated 1.5 ml glass vials and stored until analysis.

2.2.4 Spatial distribution of methane in the epilimnion

The spatial distribution of CH_4 in the surface water of Lake Willersinnweiher was analysed using a Fast-Response Automated Gas Equilibrator (FaRAGE) coupled to a cavity-ring down spectroscope (CRDS; Picarro G431, *Picarro*, USA). The FaRAGE system was built in-house after the setup described by Xiao et al. (2020) (Figure 6). In combination with the CRDS, it allows continuous in-situ measurements of CH_4 almost in real time. While driving across the lake by boat, water samples were pumped into the FaRAGE system using a peristaltic pump coupled to a flow meter with a flow rate of 350 ml min^{-1}. At the same time, compressed atmospheric air entered the system via a mass-flow controller (MFC) with a flow rate of 1050 ml min^{-1}. Sampled water and added gas met in a gas-water mixing unit, that consisted of a modified 10 ml syringe (Plastipak®, *BD*, USA) in which a bubble

diffusor was placed. A 0.2 µm teflon membrane filter was placed between the gas-water mixing unit and the MFC in order to avoid high water vapor content damaging the MFC. In the gas-water mixing unit the inflowing water and gas mixed and the thereby generated turbulent mixing leading to degassing of dissolved CH_4 from the water sample. The gas-water mixture was then transferred to a gas-water separation unit via a 2 m long tube with a diameter of 0.32 mm (Tygon, *Saint Gobain*, France). The gas-water separation unit consisted of a modified 30 ml syringe (Plastipak®, *BD*, USA). In the lower part of the syringe the water was discharged from the system using another peristaltic pump with a flow rate of 500 ml min^{-1}. The gas phase that accumulated in the top of the syringe was transferred to the CRDS (sample rate: 1000 ml min^{-1}) while excess gas was released from the system via a vent consisting of a tube (length: 1 m, i.d.: 0.32 mm) in order to prevent pressure building up in the system. Water vapor in the sample gas was removed prior to the analysis with the CRDS using a water desiccant consisting of a 30 ml syringe filled with Drierite®. Concentrations of dissolved CH_4 in the samples water were then calculated according to the method described in section 2.6.2.

In order to identify the exact location of the spatial and continuous CH_4 measurement spots, a GPS-kit connected to the CRDS recorded the coordinates during the sampling with the boat. The driving speed, distance between the individual measurement points, distance from the shore, and water depth at the given coordinate were calculated from the GPS-locations. Due to the driving speed of ≈ 1 km h^{-1} and a response time of ≈ 40 s between introduction of the water sample into the FaRAGE and analysis with the CRDS, a spatial resolution of ≈ 10 m was achieved (Eq. (3)).

$$SpRes = v_{boat} * t_{response} \quad (3)$$

where SpRes is the spatial resolution in [m], v_{boat} the driving speed of the boat in [m s^{-1}] and $t_{response}$ the response time of the FaRAGE-CRDS system in [s].

The FaRAGE system was calibrated in the laboratory using in-house standard mixtures of water with different dissolved CH_4 concentrations. Measurements of different standard mixtures with the FaRAGE-CRDS system were compared to samples that were collected from the same water using the headspace-method (section 2.2.3) and analysed at the gas chromatograph coupled to a flame ionization detector (GC-FID; section 2.4.1). For the calibration, the calculated dissolved CH_4 concentration of the manually gathered samples in [nmol l^{-1}] and the CH_4 concentration from samples measured by the FaRAGE-CRDS system in [ppmv] (parts per million by volume) were used. Two different calibrations were conducted at 6 °C and 19 °C to account for differences in temperature dependent solubility of CH_4 in water (Table A 2).

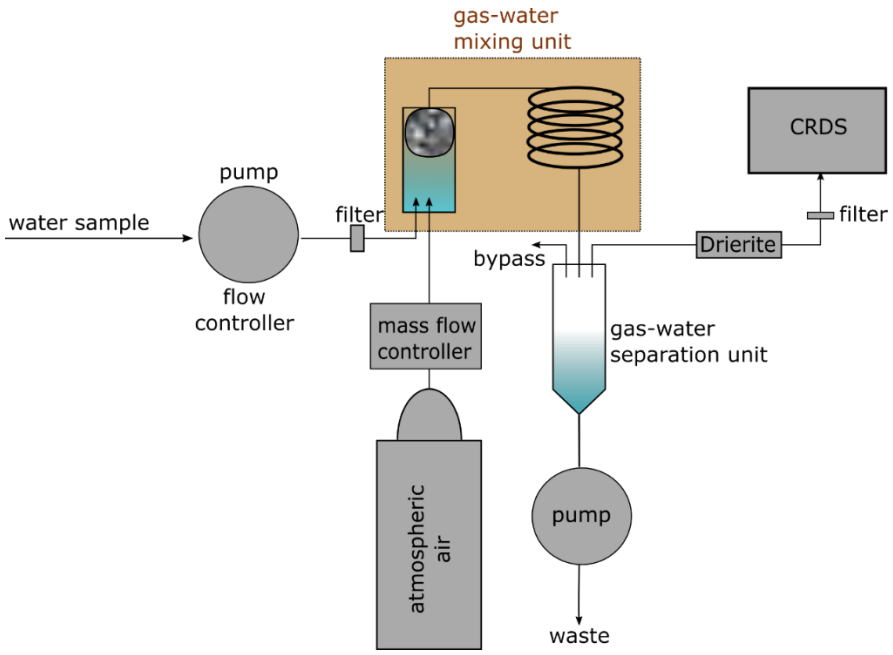

Figure 6. Schematic setup of the Fast-Response Automated Gas Equilibrator (FaRAGE) (modified after Xiao et al. (2020)). The FaRAGE consisted of two peristaltic pumps with integrated flow controllers, one for taking and one for discharging water samples. A tank of atmospheric air was coupled to a mass flow controller to generate a constant air flow. Several teflon membrane filters were installed throughout the setup to protect the system from being flooded. The tank of atmospheric air and the water pump tanking samples were linked to a gas-water mixing unit and a gas-water separation unit, where dissolved gases from the water were equilibrated with the air. The gas-water separation unit was coupled to a cavity ring-down gas analyser (CRDS), via a water desiccant to dry the sample gas before entering the CRDS.

2.2.5 Groundwater

At the three groundwater wells, groundwater parameters were recorded after ≈ 30 min of pumping with a submersible pump (MP1, *Grundfos GMBH*, Germany) and on-site parameters temperature, pH, dissolved O_2 and conductivity, which were measured in a side stream, were stable. Groundwater samples were prepared for CH_4 concentration, $\delta^{13}C\text{-}CH_4$, $\delta^{2}H\text{-}CH_4$ and $\delta^{13}C\text{-}DIC$ analysis as well as dissolved ion composition in the same way as lake water samples (section 2.2.3).

2.2.6 Diffusion

Diffusive CH_4 fluxes were determined between October 2019 and September 2021 at the three sampling sites (pelagic, slope and littoral; Figure 5C) using a floating chamber (Figure 7). The floating chamber consisted of a plastic body with a volume of 8.6 l and two tubes equipped with three-way valves to take samples. A floatable ring made from polyethylene maintained the chamber afloat and kept the edges of the chamber in a water depth between 2 and 3 cm. Before sampling, the floating chamber was fixed to the boat but care was taken to leave the chamber room for movement to prevent the generation of artificial turbulences under the chamber that might influence the measured CH_4

concentrations. To flush the tubes and prevent sampling air that was present in the tubes prior to sampling, a gas tight syringe was connected to one three-way valve and 80 ml of air were withdrawn. For the analysis of CH_4 concentrations, $\delta^{13}C$-CH_4 and $\delta^{2}H$-CH_4 values in the laboratory, samples were collected after 0, 15 and 30 min, and 40 ml of headspace gas was transferred into an Exetainer® (*Labco*, UK).

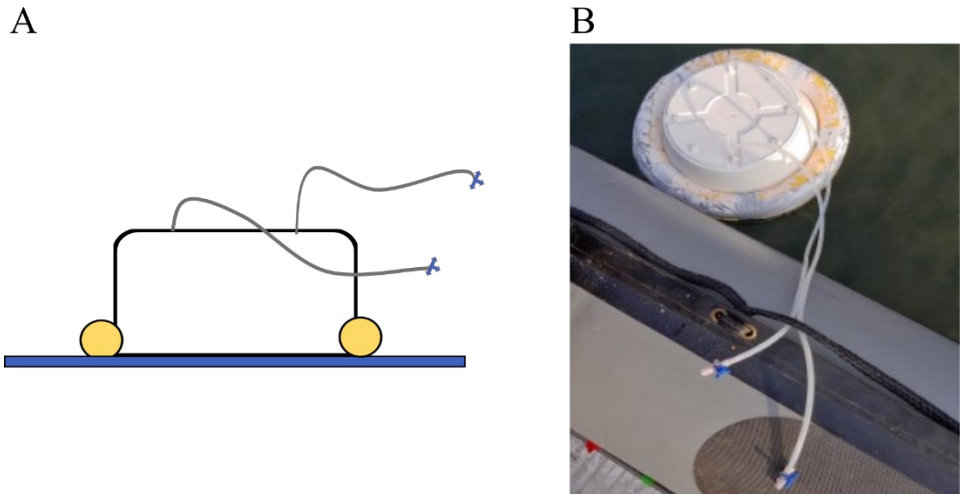

Figure 7. (A) Schematic setup of the diffusion flux chamber and (B) application of the diffusion flux chamber in the field. The flux chamber consisted of a plastic body and a ring of polyethylene keeps the chamber afloat. Two tubes were attached to the top of the chamber to allow sampling.

2.2.7 Ebullition

Ebullition flux rates of CH_4 were determined in field campaigns between November 2020 and August 2021. For the measurement of ebullition fluxes, bubble traps modified after Huttunen et al. (2001) were employed (Figure 8A-C). They were composed of an inverted funnel, with a 15 cm diameter, that was connected to a syringe equipped with a three-way valve (140 ml, Monoject™) via a tube and sealed airtight with a plug. Additionally, a weight was installed on top of the inverted funnel to keep the bubble trap in a vertical position when placed in water. The length of the tube was chosen to position the inverted funnel in a depth of ≈ 1 m at the pelagic and slope sites. At the littoral site, the tube length was shorter (Figure 8B) as the water depth at this site is only 1.5 m. In November 2020, the bubble traps at the pelagic and slope sites were complemented with a metal frame with a diameter of 50 cm to create a bigger area in which gas bubbles could be collected in order to account for potential smaller ebullition fluxes during the mixing period compared to the stratification period. The frame was fitted to the bubble trap with plastic foil that was adjusted to the inverted funnel. During the stratification period, the metal frames were removed, and measurements took place with the initial setup without the metal frame.

For the determination of the ebullition flux rates, the bubble traps were installed at the pelagic, slope and littoral sites. When placing the traps into the water the three-way valves were open to let the air within the bubble trap and syringe escape. Once the trap was completely filled with water, the three-

way valve was closed under water and left in place to collect gas bubbles ascending from the sediment. The bubble traps were always sampled at the next field campaign accounting for sampling durations between 13 to 36 days. The sampling was conducted via a gas tight syringe that was connected to the three-way valve of the bubble trap. Accumulated gas bubbles that replaced water within the trap were extracted while the volume was measured by using the scale of the employed sampling syringe. The ebullitive flux rates were then calculated as described in section 2.6.11. Methane concentrations, $\delta^{13}C\text{-}CH_4$ and $\delta^{2}H\text{-}CH_4$ values of ebullitive CH_4 were determined in November 2020 and September 2021. Therefore, samples of gas bubbles were acquired by dropping a gravity corer into the sediment to release gas bubbles from the sediment (Figure 8D-E). Released gas bubbles were then collected at the surface using a bubble trap. Collected samples in the bubble trap were then transferred into 12 ml Exetainers® (*Labco*, UK) and analysed in the laboratory. This method was only used at the littoral and slope sites as it was not possible to collect gas bubbles at the surface of the pelagic site.

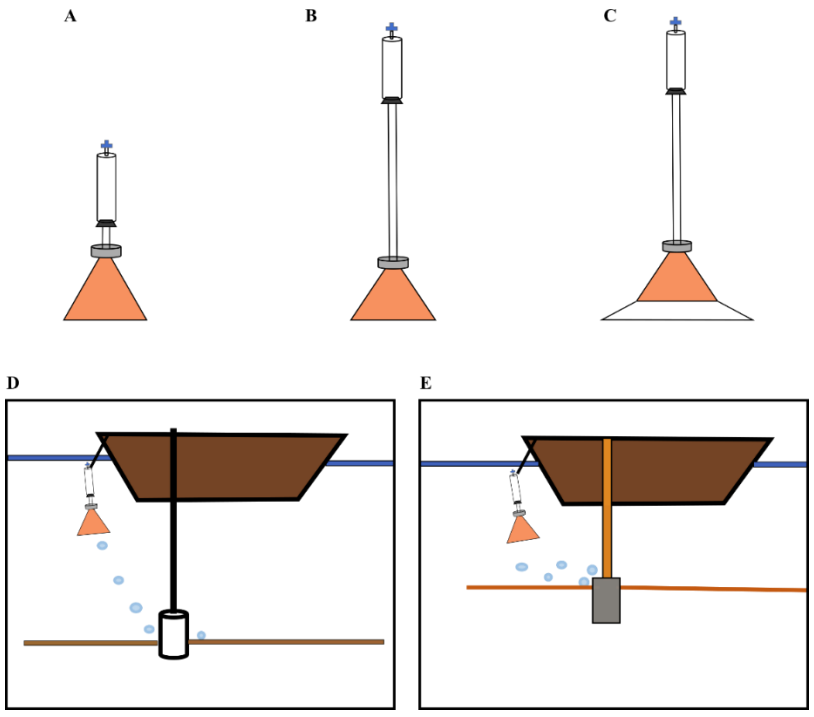

Figure 8. (A-C) Schematic setup of the bubble traps. The bubble traps consisted of an inverted funnel connected to a syringe, which was equipped with a three-way valve, via a plastic tube. A weight fitted atop of the inverted funnel ensured a vertical position when placed in water. (A) The bubble trap fitted with a short plastic tube was used at the shallow littoral site, (B) the bubble trap fitted with the longer plastic tube was used at the deeper pelagic and slope sites and (C) the bubble trap which was complemented with a metal frame to extent its surface area was used during the measurement of ebullition flux rates during November 2020. A schematic overview of the method used for (D) generating gas bubbles with a weight and catching gas bubbles at the slope site and (E) generating gas bubbles using a rudder and catching gas bubbles at the littoral site.

2.3 Stable isotope definitions and applied stable isotope techniques

2.3.1 Definition of stable isotope values and isotope fractionation

In the investigations of this study, a particular focus lay on the stable carbon and hydrogen isotope composition of CH_4. Stable isotopes are of great use and an important tool to investigate CH_4 cycles and sources in diverse ecosystems as different CH_4 sources and formation or degradation processes are often characterised by unique isotopic signatures and distinct changes in the stable isotopic composition, respectively (e.g., Hayes, 2001).

In the present study the ^{13}C- and ^{2}H- isotope ratios are reported in the conventional "delta notation" (Eq. (4)) and expressed in the recommended terms after Coplen (2011). The "delta notation" is defined as the difference of the ratio of the heavy (^{i}E) to the light isotope (^{j}E) of a sample ($R(\,^{i}E/\,^{j}E)_{\text{sample}}$) compared to the difference in the ratio of the heavy to the light isotope of an international measurement standard ($R(\,^{i}E/\,^{j}E)_{\text{standard}}$). The reference material for carbon isotopes is Vienna Peedee Belemnite (V-PDB) and Vienna Standard Mean Ocean Water (V-SMOW) for hydrogen isotopes.

$$\delta\ ^{i}E = \frac{R(\,^{i}E/\,^{j}E)_{\text{sample}}}{R(\,^{i}E/\,^{j}E)_{\text{standard}}} - 1 \tag{4}$$

In order to characterise the distribution of the stable isotope composition of an educt and product, e.g., the oxidation of the educt CH_4 to the product CO_2 during MOx, the isotope fractionation factor α (Eq. (5)) and isotope fractionation ε (Eq. (6)) are introduced. Both isotope fractionation factor and isotope fractionation allow the interpretation of stable isotope effects that occur during reactions and are in some cases, also characteristic for certain pathways, e.g., the formation of CH_4 during methanogenesis via the hydrogenotrophic or acetoclastic pathway. Please note that changes in the isotopic values of a compound during reactions are often very complex and part of numerous or still unknown pathways. Therefore, in this study α and ε are referred to as the apparent fractionation factor and the apparent fractionation in order to account for this uncertainty as suggested by Coplen (2011). Besides, α and ε also Λ, which is defined as the ratio of isotopic fractionation between carbon and hydrogen ($\varepsilon_H/\varepsilon_C$) of CH_4 during MOx is introduced (Eq. (7)).

$$\alpha\ ^{i}E_{educt/product} = \frac{R(\,^{i}E/\,^{j}E)_{\text{educt}}}{R(\,^{i}E/\,^{j}E)_{\text{product}}} \tag{5}$$

$$\varepsilon\ ^{i}E_{educt/product} = \alpha\ ^{i}E_{educt/product} - 1 \tag{6}$$

$$\Lambda = \varepsilon_H/\varepsilon_C \tag{7}$$

2.3.2 Keeling plot method for determining $\delta^{13}C$- and $\delta^{2}H$-CH_4 source values from water surface methane emissions

Isotopic source values of released CH_4 via diffusion cannot be measured directly with the applied method (section 2.2.6 for method description), as at the beginning of flux measurements, atmospheric air with a background mixing ratio of ≈ 1.8 ppmv, and atmospheric $\delta^{13}C$-CH_4 and $\delta^{2}H$-CH_4 values are already present in the headspace of the floating chamber. Thus, the $\delta^{13}C$-CH_4 and $\delta^{2}H$-CH_4 source values of CH_4 released via diffusion at the atmosphere-water interface were determined using the keeling plot method (Keeling, 1958) (Eq. (8)).

$$\delta\ {}^{i}E_a = c_b(\delta\ {}^{i}E_b - \delta\ {}^{i}E_s)\left(\frac{1}{c_a}\right) + \delta\ {}^{i}E_s \qquad (8)$$

where c_a is the headspace CH_4 mixing ratio of the floating chamber, $\delta\ {}^{i}E_a$ the $\delta^{13}C$ or $\delta^{2}H$ value of CH_4, c_b the headspace CH_4 mixing ratio of background CH_4 present in the floating chamber prior to the start of diffusion measurements, $\delta\ {}^{i}E_b$ the $\delta^{13}C$ or $\delta^{2}H$ values of CH_4 in the background, and $\delta\ {}^{i}E_s$ the $\delta^{13}C$-CH_4 or $\delta^{2}H$-CH_4 source value.

The keeling plot method is based on mass conservation and applied to account for the mixture of background CH_4 mixing ratios with a certain stable isotope composition and an additional CH_4 source characterised by another stable isotope composition. In this study the additional CH_4 source is diffusive CH_4 emissions at the water-air interface. Application of Eq. (8) allows to determine the $\delta^{13}C$-CH_4 and $\delta^{2}H$-CH_4 source values of CH_4 released via diffusion. Based on Eq. (8), a linear regression was used to estimate stable isotope source values of CH_4. Here, the inverse CH_4 mixing ratios of the individual sampling points at the x-axis were plotted against their $\delta^{13}C$- or $\delta^{2}H$-CH_4 values at the y-axis and a linear regression was employed. The intercept of this linear regression with the y-axis, then represents the $\delta^{13}C$- or $\delta^{2}H$-CH_4 source value as in this scenario the proportion of CH_4 originating from the additional source is very large ($1/[CH_4] = 0$) and therefore equals the $\delta^{13}C$- or $\delta^{2}H$-CH_4 source value of the additional source.

$\delta^{13}C$-CH_4 and $\delta^{2}H$-CH_4 source signatures were calculated at the pelagic, slope and littoral sampling sites for all campaigns in which diffusion rates and $\delta^{13}C$-CH_4 and $\delta^{2}H$-CH_4 values of the individual diffusion samples were analysed (Table A 1 for an overview of the campaigns in which the $\delta^{13}C$-CH_4 and $\delta^{2}H$-CH_4 source signatures of CH_4 via diffusion were examined). Results of the keeling plot method are then given after the linear regression to Eq. (8) as the intercept of the three individual sample points (of the floating chamber measurement) with the standard error of the linear regression. Determination coefficients (R^2) of the keeling plots were usually > 0.9.

2.3.3 The use of stable isotope labelling to identify precursor compounds of methane and determine rates of aerobic methane oxidation

Another frequently used stable isotope technique is stable isotope labelling in order to identify precursor compounds of CH_4 (e.g., ^{13}C-labelled methyl phosphonate or ^{2}H-labelled methionine) or to measure CH_4 oxidation rates by using ^{13}C-labelled CH_4. The basic principle of the stable isotope labelling concepts is outlined below, while more detailed information is provided in sections 2.5.2 and 2.5.3. In this study, stable isotope labelling was used in the scope of two incubation experiments. In the first incubation experiment, isotopically labelled compounds were supplemented to aliquots of sampled lake water. After the incubation experiment was finished, it was investigated whether a part of the isotopic labelling could be found in the stable isotope composition of CH_4. This was verified by an increase in $\delta^{13}C$-CH_4 or $\delta^{2}H$-CH_4 values. Therefore, an increase indicated that the isotopically labelled compound(s) were potential precursor(s) of CH_4 at Lake Willersinnweiher.

In the second incubation experiment ^{13}C-labelled CH_4 was supplemented to aliquots of sampled lake water. With this experiment it was investigated if a part of the ^{13}C-labelled CH_4 was converted to ^{13}C-CO_2 during MOx. Aerobic methane oxidation occurring during the incubation experiment were indicated by increased $\delta^{13}C$-CO_2 values of dissolved CO_2. The increase of $\delta^{13}C$-CO_2 values after different incubation periods could furthermore be used to determine MOx rates.

On the one hand, these stable isotope labelling techniques are very useful to overcome analytical hurdles as changes in stable isotope values provide a deeper understanding of biogeochemical cycling of CH_4. Therefore, stable isotope labelling was used to identify small CH_4 sources or oxidation rates of CH_4 where the amount of formed or oxidized CH_4 cannot be detected via concentration measurements alone, e.g., due to high background CH_4 concentrations. On the other hand, stable isotope labelling is often used to gain deeper insights into the processes of CH_4 formation and identifying precursor compounds of CH_4 and therefore contributes to a better understanding of occurring mechanisms and pathways. Thus, stable isotope labelling has been used in numerous studies to demonstrate CH_4 emissions and different potential precursor compounds from vegetation, cyanobacteria, and algae (e.g., Bižić et al., 2020a; Lenhart et al., 2016; Hartmann et al., 2020; Lenhart et al., 2015).

2.4 Laboratory analysis

2.4.1 Analysis of methane and carbon dioxide concentrations

A GC-FID (14B GC-FID *Shimadzu*, Japan) was used to determine headspace CH_4 concentrations in the gas samples of the water column, groundwater, and diffusion between 100 ppbv to 50 ppmv. Prior to entering the GC-FID system using a gas tight syringe, the gas sample was passed through a chemical trap filled with Drierite® (calcium sulphate) to remove water from the sample. The sample

was then introduced into the analytical system through a six-port valve and a 2 ml sample loop. The GC-FID was equipped with a stainless-steel column with a length of 2 m, and an inner diameter of 1/8 inches, where CH_4 was separated from other gas compounds. The column was filled with a 60-80 mesh molecular sieve 5A. The GC oven was operated at a constant temperature of 125 °C. Methane was quantified using two reference standards with known CH_4 concentrations of 2192 ± 5 ppbv and 9655 ± 53 ppbv in synthetic air and were measured daily in triplicate.

For the analysis of samples with CH_4 concentrations exceeding 50 ppmv, a GC-2010 Plus GC coupled to a barrier discharge ionization detector (GC-BID, *Shimadzu*, Japan) was used. An aliquot of 50 µl of the gas samples was injected into the system by an autosampler (split injection 5:1). The GC was equipped with 80/100 mesh ShinCarbon ST packed column with a length of 2 m and a diameter of 0.53 mm. The following temperature program of the GC oven was applied: the initial temperature of 30 °C was held for 6.5 min, then, with a rate of 10 °C min^{-1}, the GC oven temperature increased until it reached 75 °C and afterwards the oven temperate was regulated to increase at a rate of 30 °C min^{-1} to reach 180 °C. For quantification purposes, the GC-BID was calibrated using several reference standards with different concentrations for CH_4 (50, 100, 400, 600, 1000 ppmv and 0.5, 1, 2.5, 25, 49, 60, 73 % and 97 % by volume). All reference standards were measured as triplicates. For quality control, a 1000 ppmv CH_4 reference standard gas was measured after every 6 to 9 single measurements.

2.4.2 Analysis of stable carbon and hydrogen isotope values of methane and dissolved inorganic carbon

A DeltaPlus XL isotope ratio mass spectrometer (IRMS, *ThermoFisher Scientific*, USA) was used to analyse $\delta^{13}C\text{-}CH_4$, $\delta^{2}H\text{-}CH_4$ and $\delta^{13}C$-DIC values in lake water, pore water, diffusion, and ebullition samples. The IRMS was coupled to a HP 6890N GC (*Agilent Technologies*, USA) and a GC Combustion III Interface (GC-C; *ThermoFisher Scientific*, USA) via an oxidation reactor and a reduction reactor. The oxidation reactor (length: 320 mm, inner diameter: 1.0 mm) consisted of a ceramic tube filled with Ni/Pt wires activated by O_2 and was operated at a reactor temperature of 960 °C. The reduction reactor (length: 320 mm, inner diameter: 1.0 mm) consisted of a ceramic tube at a temperature of 1450 °C for high temperature conversion (HTC) for stable carbon and hydrogen isotope analysis, respectively. A CP-PoraPLOT Q capillary column (*Varian,* Palo Alto, USA) with a length of 27.5 m, an inner diameter of 0.25 mm and a film thickness of 8 µm was installed in the GC. A cryogenic pre-concentration unit was connected to the GC-C-IRMS system for $\delta^{13}C\text{-}CH_4$ and $\delta^{2}H\text{-}CH_4$ measurements, whereas for $\delta^{13}C$-DIC analysis (headspace CO_2 of the samples prepared as described in section 2.2.3) an A200S autosampler (*CTC Analytics*, Switzerland) was applied (similar as described in Schroll et al., 2020).

For $\delta^{13}C\text{-}CH_4$ and $\delta^{2}H\text{-}CH_4$ analysis gaseous samples first passed a chemical trap filled with Ascarite® to remove CO_2. Then, gas samples entered the pre-concentration unit via an evacuated 40 ml sample loop. The pre-concentration unit consisted of cold traps cooled by liquid nitrogen, removed water and compounds with a freezing point above -150 °C and then trapped CH_4 on the polymer HayeSep D. Afterwards, the gas sample was exposed to room temperature, which caused a release from the HayeSep D, and then entered the GC. In the GC, CH_4 was separated from other gaseous compounds in the capillary column and afterwards transferred to the IRMS.

Carbon dioxide with a $\delta^{13}C\text{-}CO_2$ value of -23.6 ‰ was used as a monitor gas (carbon dioxide 4.5, *Messer Griesheim*, Germany). Before and after the measurement of samples, two working standards with $\delta^{13}C\text{-}CH_4$ values of -42.32 ‰ and -66.35 ‰ and $\delta^{2}H\text{-}CH_4$ values of -190.6 ‰ and –149.9 ‰ (*Isometric instruments*, Victoria, Canada), respectively, were measured. The two working standards were calibrated against reference substances from the National Institute of Standards and Technology (NIST) and International Atomic Energy Agency (IAEA). The sample values were then normalized according to Paul et al. (2007). H_3^+ factors were measured weekly and were in the range of 2.4 to 3.7 during the measurement period.

2.4.3 Analysis of major and trace elements

The concentration of dissolved cations of calcium (Ca^{2+}), iron (Fe^{2+}), potassium (K^+), magnesium (Mg^{2+}), manganese (Mn^{2+}) and sodium (Na^+) in the water samples were analysed using an Inductively Coupled Plasma Optical Emission Spectrometer (ICP-OES 720, *Agilent Technologies*, USA). The relative standard deviations of each element were below 2 % and were determined from the measurement of the reference material SPS-SW during the analysis of the water samples. Dissolved anion concentrations (SO_4^{2-}, NO_3^-, chloride) in water samples were measured by ion chromatography (Dionex™ ICS-1100 Ion Chromatography System, *ThermoFisher Scientific*, USA). The reference material SPS-NUTR-WW1 was analysed for quality control and yielded relative standard deviations for each element below 3 %. Concentrations of DIC were determined using a TOC-V CPH (*Shimadzu*, Japan). During the analysis, the water sample was acidified in a reactor to convert all inorganic carbon into CO_2 according to the bicarbonate buffer system. Calibration of the TOC-V-CPH was achieved by repeated analysis of an in-house standard solution prior measurement. The concentrations of S^{2-} and NH_4^+ in lake water, pore water and groundwater samples were measured using a photometer (DREL 2800, *Hach*, USA) and the Spectroquant® Sulphide Reagent Test (*Merck*, Germany). Analysis took place immediately after return from the sampling campaign (within 2 to 4 h after sampling). For quality control of the major and trace element analysis, the ionic balance of each sample was determined. Ionic balance errors generally showed values below 5 %.

2.5 Incubation experiments

2.5.1 Determination of Λ, the ratio between stable carbon and hydrogen isotope fractionation during aerobic methane oxidation

The ratio of stable carbon and hydrogen fractionation due to MOx in the water column was examined by an incubation experiment with lake water collected at the pelagic site from a depth of 6 m in July 2021. To determine zones of MOx in the water column, O_2 saturation-depth profiles acquired by Exo1 multiparameter probe measurements (section 3.2.1) as well as CH_4 concentration profiles of the water column examined a day prior to sampling were considered. The sampled water depth was chosen based on the declining CH_4 concentrations in the water column and O_2 concentrations exhibiting concentrations higher than 50 % compared to surface water so that MOx would not be limited due to lack of O_2 during incubation. Lake water from the chosen depth was sampled by a submersible pump (*COMET-Pumpen Systemtechnik GmbH &Co. KG*, Germany), filled into autoclaved 2 l glass bottles (*Schott*, Germany), and stored dark and cool until transported to the laboratory (within 2 h after sampling). In the laboratory, aliquots of the sample were transferred into 120 ml glass vials so that no gas bubbles were present and sealed with a crimp lid containing a rubber butyl septum. Until analysis, samples were kept in a climate cabinet with a temperature of 15 °C and in darkness, resembling environmental conditions in the water column of the lake. During the incubation period, the water samples were analysed in triplicates and at three points in time: at the start of the incubation period and after 3 and 20 days. Analysis of CH_4 was conducted similar to the headspace method as described in section 2.2.3. First a 50 ml He headspace was created in the glass vials. Then, the glass vials were vigorously shaken for 1.5 min and headspace was drawn from the vial, while simultaneously injecting deionized water to keep pressure conditions in the vial constant and hence to not affect dissolved CH_4 concentrations or its stable isotope values. The gas samples were then introduced into 12 ml Exetainers® (*Labco*, UK) until analysis of CH_4 concentrations, $\delta^{13}C$-CH_4 and $\delta^{2}H$-CH_4 values was conducted.

2.5.2 Determination of aerobic methane oxidation rates via incubation with ^{13}C-labelled methane

Incubation experiments were conducted in order to investigate and quantify rates of MOx in the oxic water column in July, September, October 2020 and March, July, September 2021 similar to Oswald et al. (2015). To determine the depth of MOx occurring in the water column, O_2 saturation-depth profiles acquired by Exo1 multiparameter probe measurements as well as CH_4 concentration profiles of the water column examined a day prior to sampling were considered. Based on these findings, water samples from depths between 1 m and 9 m obtained by a submersible pump (*COMET-Pumpen Systemtechnik GmbH &Co. KG*, Germany) were filled into 250 ml glass bottles (*Schott*, Germany),

which were sealed with a lid containing a septum. In the laboratory, 3 ml of 99 % ^{13}C-labelled CH_4 were added with a syringe through the septum of the lid after creating a headspace of 30 ml He gas in the bottles. This resulted in final dissolved CH_4 concentrations of ≈ 30 µM in the water samples of each bottle, which was about 100 times higher than "natural" concentrations in the water column. Thus, please note that MOx rates reported in this study represent rates of potential MOx, as actual MOx rates in the water column might have differed due to lower dissolved CH_4 concentrations. After ^{13}C-labelled CH_4 was added, the samples were shaken for 2 min to equilibrate CH_4 between the headspace and water sample. The water was then extracted from the glass bottles through the septum using a syringe, while He gas was injected. The water was filled into a 12 ml Exetainers® (*Labco*, UK) until they were completely filled and gas bubble free. The samples were stored dark and at temperatures similar to the ones in water column of Lake Willersinnweiher during the incubation period. Sampling was performed five times including the initial sample, and samples were incubated between 45 to 140 h in total. In this experiment, MOx rates were determined by production of ^{13}C-CO_2, which was formed from the ^{13}C-labelled CH_4 during MOx. According to the bicarbonate buffer system, formed CO_2 reacts with water to carbonic acid (H_2CO_3), which dissociates in two steps to bicarbonate (HCO_3^-) and carbonate (CO_3^{2-}). The sum of CO_2, HCO_3^- and CO_3^{2-} is defined as DIC, and the proportion of each species in water is dependent on the respective pH value. As ^{13}C-CO_2 produced during MOx is comprised to DIC, its concentration as well as δ^{13}C-DIC values of the samples were analysed with the methods described in sections 2.2.3 and 2.4.2. At the chosen incubation time, 10 ml of the sample was filtered through a 0.2 µm poresize filter, filled into another 12 ml Exetainer® (*Labco*, UK), and topped up with deionized water for DIC concentration analysis. Deionized water was added to the sample, as a non-equilibrium state between CO_2 in the sample and a potential headspace might alter DIC concentrations and δ^{13}C-DIC values. Additionally, 1 ml of sample was filtered into a 3 ml glass vial and prepared for δ^{13}C-DIC measurements in the same way as water column and pore water samples.

2.5.3 Incubation with ^{13}C and ^{2}H-labelled methylated compounds

In order to determine potential precursor compounds of CH_4 in the oxic water column of Lake Willersinnweiher, incubation experiments with lake water supplemented with ^{13}C-labelled MPn and ^{2}H-labelled MA, TMA and MET were conducted. Methane formation from one of these potential precursor compounds was inferred from incorporation of ^{13}C or ^{2}H into the CH_4 pool. The phosphonate MPn was investigated, as it has been reported to be a precursor compound of CH_4 in the oceans by various studies (e.g., Karl et al., 2008; Repeta et al., 2016), while the amines MA and TMA were also investigated for their potential to act as CH_4 precursors in the aquatic environment according to several studies (Bižić-Ionescu et al., 2018; Wang et al., 2021). The amino acid MET was examined, as its role as a precursor of CH_4 has been linked to several CH_4 sources in aquatic as well as terrestrial environments (Lenhart et al., 2012, 2015, 2016).

Incubation experiments were executed in July 2020 for ^{13}C-labelled MPn and in September 2021 for ^{2}H-labelled MA, TMA and MET (Table A 1). Based on CH_4 concentration measurements in the water column of the pelagic site a day prior to sampling, water samples were collected just below the thermocline, where elevated CH_4 concentrations were found compared to the surface water. Water samples were taken using a submersible pump (*COMET-Pumpen Systemtechnik GmbH &Co. KG*, Germany) and transferred into 2 l glass bottles (*Schott*, Germany) that were autoclaved prior to sampling. Samples were immediately transported into the laboratory and transferred bubble free into 50 ml glass vials, which were closed with a lid containing a septum. Additionally, controls were generated by filtering aliquots of the water samples through a 0.2 µm filter before being transferred into the glass vials. Afterwards, the different potential precursor compound solutions were added to separate vials to generate the different treatments "water", "water filtered", "water + precursor", and "water + precursor filtered". The final concentration and isotope labelled proportion of the compounds in each glass vial after supplementation was 50 nmol l^{-1} of 5 % ^{13}C-labelled MPn, 100 µmol l^{-1} of 99 % ^{2}H-labelled MA, 118 µmol l^{-1} of 99 % ^{2}H-labelled TMA and 28 µmol l^{-1} of 99 % ^{2}H-labelled MET. All treatments were prepared in triplicates except for filtered samples which included only single samples. During incubation, the samples were kept in a climate cabinet with temperatures resembling those of the water column of the sampled depth. Sampling of gas was performed four times including initial sampling for MPn during a total incubation period of 190 h and two times for MA, TMA and MET during the incubation period of 275 h. Analysis of CH_4 was conducted similar to the headspace method as described in section 2.2.3. First a 25 ml He headspace was created in the glass vials via a syringe. Then, the glass vials were vigorously shaken for 1.5 min and headspace was drawn from the vial while simultaneously injecting deionized water to keep pressure conditions in the vial constant and hence to not affect dissolved CH_4 concentrations or its isotopic values. The gas samples were then introduced into 12 ml Exetainers® (*Labco*, UK) until analysis of CH_4 concentrations and analysis of δ^{13}C-CH_4 and δ^{2}H-CH_4 values were conducted.

2.6 Calculations

2.6.1 Ionic balance

In order to qualitatively control the results of total dissolved ion composition in water samples, the ionic balance (IB) was calculated as the sum of major cation and anion concentrations (Eq. (9)).

$$IB = \frac{\sum cations - \sum anions}{\sum cations + \sum anions} \qquad [\text{x } 10^2] \qquad (9)$$

where $\sum cations/anions$ is given in [meq l^{-1}] and corresponds to the sum of cations and anions in the sample, respectively. Deviations in the ionic balance were usually below 5 %, indicating good quality of analyses and a comprehensive acquisition of dissolved ions in the water samples.

2.6.2 Dissolved methane concentrations

Methane concentrations in water samples were calculated based on Henry's law. It describes that the partial pressure of a gas above the water is proportional to its dissolved concentration (Sander, 2015). This is expressed by the solubility coefficient (K) [dimensionless] of CH_4, which is dependent on temperature and salinity of the water and was used after Yamamoto et al. (1976). The total volume of dissolved CH_4 within the sample ($V_{tot}^{CH_4}$) [ml] was calculated by using Eq. (10).

$$V_{tot}^{CH_4} = V_{HS}^{CH_4} * \left(\frac{V_{aq}}{V_{HS}} * K + 1\right) \quad (10)$$

where $V_{HS}^{CH_4}$ [ml] is the volume of CH_4 in the headspace and $V_{aq/HS}$ [ml] correspond to the volume of water and headspace, respectively. Subsequently, the concentration of CH_4 (c_{CH_4}) [µmol l^{-1}] within the water was determined based on the ideal gas equation (Eq. (11)):

$$c_{CH_4} = \frac{p * V_{tot}^{CH_4}}{R * T * V_{aq}} \quad (11)$$

where p corresponds to the atmospheric pressure [bar], R to the ideal gas constant [bar l mol^{-1} K^{-1}], and T [K] to the according temperature. For the determination of CH_4 concentrations within the pore water of the lake sediment, the porosity and water content of the sediment were considered by weighing the sediment before and after drying for at least 48 h at 105 °C.

2.6.3 Fluxes in the water column and sediment

The pore water and water column fluxes of CH_4, O_2, Mn^{2+}, DIC, SO_4^{2-} and S^{2-} were calculated based on concentration changes with depth and presuming steady-state conditions using Fick's first law (Eq. (12)).

$$J = -D_W * \frac{\partial c}{\partial x} \quad (12)$$

where J [mmol m^{-2} s^{-1}] corresponds to the diffusive flux, c [mol m^{-3}] to the concentration and x [m] to the sediment/water depth. D_w [m^2 s^{-1}] is the diffusion coefficient for each individual compound in water calculated after Boudreau (1997).

For the calculation of pore water fluxes (Eq. (13)), the porosity $\emptyset$ [dimensionless] of the sediment was included. Furthermore, the diffusion coefficient of pore water D_s was determined using Eq. (14) based on the porosity dependent tortuosity θ [dimensionless] (Eq. (15)).

$$J = -\emptyset * D_s * \frac{\partial c}{\partial x} \quad (13)$$

$$D_S = \frac{D_W}{\theta^2} \quad (14)$$

$$\theta = 1 - \ln(\emptyset^2) \quad (15)$$

The release of CH_4 at the sediment-water interface was calculated using concentration changes in the upper 3 cm of the sediment. Sedimentary consumption and production rates were determined based on local fluxes in zones of the sediment where the concentrations of CH_4, SO_4^{2-} and S^{2-} changed considerably.

2.6.4 Mass balance calculations for the estimation of oxic methane production rates

For the estimation of OMP rates at Lake Willersinnweiher, a mass balance for CH_4 in the epilimnion was calculated after Donis et al. (2017) (Eq. (16)). This approach was only used for months in which CH_4 flux rates at the sediment-water interface of the littoral site and CH_4 diffusion flux rates from the surface water into the atmosphere were recorded (August/October 2019, January/May/July/October 2020, March 2021). Aerobic methane oxidation rates as well as dissolution of CH_4 from ebullition in these months were estimated from values obtained during corresponding months in 2021. Based on the assumption of steady-state conditions ($\frac{\partial C}{\partial t}$ = 0), the mass balance approach included lateral input of CH_4 from diffusion ($F_{L\,diff}$) and ebullition ($F_{L\,ebu}$) from sediments of the littoral area (A_s), fluxes of CH_4 from the metalimnion into the epilimnion (F_z), input of CH_4 rich groundwater with the flow rate of inflowing groundwater (Q_G) and its CH_4 concentration (C_G), a CH_4 source assumed to be OMP (P_{net}) within the water volume of the epilimnion ($\forall$), MOx in the epilimnion and the diffusive CH_4 flux (F_s) across the planar lake area (A_p). An overview of the parameters, values and units used in the mass balance are given in Table 1. Lateral input from dissolution from uprising gas bubbles released via ebullition was estimated to be 10 % from the overall ebullition flux rates (after Figure 15 within McGinnis et al. (2006)) depending on the release depth of gas bubbles and average gas bubble diameters, which could not be determined in the scope of this study. Uncertainties for the calculation of P_{net} via the mass balance approach were estimated by including a 10 % uncertainty in all relevant parameters such as $F_{L\,diff}$, $F_{L\,ebu}$, F_z, C_G, MOx and F_s. These estimated uncertainties were chosen in order to account for spatial and temporal variations of these parameters.

$$\frac{\partial C}{\partial t}\forall = A_s(F_{L\,diff} + F_{L\,ebu}) + A_p F_z + P_{net}\forall + Q_G C_G - (MOx\forall + A_p F_s) \quad (16)$$

Table 1. Overview of CH_4 mass balance parameters applied for Lake Willersinnweiher based on the assumption of steady-state conditions.

Parameter	Description	Value	Units
$\frac{\partial C}{\partial t}$	Changes in CH_4 surface concentrations	0	mmol d^{-1}
$\forall$	Volume of surface mixed layer	Derived from epilimnion depth	m^3
A_s	Sediment surface in contact with littoral sediments	Derived from epilimnion depth	m^2
A_p	Planar lake area	$1.7 * 10^5$	m^2
$F_{L\,diff}$	Diffusion flux from littoral sediments	Obtained from section 3.1.2	mmol m^{-2} d^{-1}
$F_{L\,ebu}$	Ebullition flux from littoral sediments	Obtained from section 3.5.2	mmol m^{-2} d^{-1}
F_s	Diffusion flux to atmosphere	Obtained from section 3.5.1	mmol m^{-2} d^{-1}
F_z	Diffusion from metalimnion to surface mixed water layer	Obtained from section 3.2.4	mmol m^{-2} d^{-1}
Q_G	Flow rate of inflowing groundwater	Obtained from Wollschläger et al.(2007)	m^{-3} d^{-1}
C_G	CH_4 concentration of inflowing groundwater	Obtained from section 3.3	mmol m^{-3}
P_{net}	Aerobic CH_4 production	-	mmol m^{-3} d^{-1}
MOx	CH_4 oxidation rate	Obtained from section 3.2.6	mmol m^{-3}

2.6.5 Rates of aerobic methane oxidation

Aerobic methane oxidation rates were determined using the results of DIC concentrations and δ^{13}C-DIC values of the incubation experiment (section 2.5.2). The CH_4 oxidation rate equals the production rate of ^{13}C-CO_2 from ^{13}C-CH_4 since during MOx CH_4 is oxidized to CO_2. The enrichment in ^{13}C-CO_2 therefore corresponds to the oxidation of CH_4 at a ratio of 1:1. First, the δ^{13}C value of the added ^{13}C-labeled CH_4 ($\delta^{13}C_{Label}^{CH4}$) [‰] was calculated as follows (Eq. (17)):

$$\delta^{13}C_{Label}^{CH4} = \left(\frac{1}{1 - {}^{13}C} - 1\right) * \frac{1}{R_{VPDB}} - 1 \qquad [* 10^3] \tag{17}$$

, where R_{V-PDB} corresponds to the carbon isotopic ratio of the reference standard V-PDB and ^{13}C to the fraction of ^{13}C-CH_4 within the sample after adding ^{13}C-labeled CH_4. Therefore, the amount of ^{13}C-labelled CH_4 added to the sample (c_{aq}) must be known. The latter was calculated by using Eq. (18).

$$c_{aq} = \frac{m_{CH_4}}{\frac{V_{HS}}{K_C} + V_{aq}} * \frac{1}{M} \tag{18}$$

where m_{CH_4} [g] is the mass of CH_4 added and $V_{HS/aq}$ [l] to the volume of He headspace and water in the sample, respectively. M is the molar mass of CH_4 [g mol^{-1}] and K_C the solubility coefficient for CH_4. m_{CH_4} was calculated as follows (Eq. (19)):

$$m_{CH_4} = \frac{V_{CH_4}}{M\ x\ V_M} \tag{19}$$

where V_{CH_4} [l] is the volume of added ^{13}C-labeled CH_4 gas to the sample and V_M the molar volume of an ideal gas at standard temperature and pressure [l mol^{-1}]. The solubility coefficient K_C is determined according to the equation (Eq. (20)).

$$K_C = H * R * T \tag{20}$$

where H corresponds to the Henry constant of CH_4 according to Sander (2015) [mol l^{-1} bar^{1}], R to the ideal gas constant [bar l mol^{-1} K^{-1}], and T to the temperature [K].

The produced ^{13}C-DIC during the incubation experiment was then calculated from the increase of the ^{13}C proportion in the DIC pool of the incubated water samples (Eq. (21)).

$$^{13}C\text{-}DIC_{production} = c_{DIC} * \left[\left(\frac{n_{13C\text{-}DIC}}{n_{12C\text{-}DIC} + n_{13C\text{-}DIC}}\right)_{tn} - \left(\frac{n_{13C\text{-}DIC}}{n_{12C\text{-}DIC} + n_{13C\text{-}DIC}}\right)_{t0}\right] \tag{21}$$

where $^{13}C\text{-}DIC_{production}$ [mmol l^{-1}] is the produced DIC during the incubation experiment at the point in time t_n, c_{DIC} the concentration of DIC [mmol l^{-1}] in the water sample, and $n_{12/13C\text{-}DIC}$ the amount of substance of ^{12}C-DIC or ^{13}C-DIC in the water sample at the respective time point (t_n) and the start of the incubation (t_0).

The MOx rate was obtained from the slope of the linear regression between the produced ^{13}C-DIC and the incubation time. For the linear regression, only sample points were chosen in which the increase of produced ^{13}C-DIC was linear. Each sample point of the incubation experiment was conducted in triplicates for the analysis of DIC concentrations and δ^{13}C-DIC values, except for July and September 2021, where DIC concentrations and δ^{13}C-DIC values consisted of single measurements. Uncertainties of the MOx rates are given by the standard error of the linear regression.

2.6.6 Stable carbon isotope fractionation factors during methanogenesis

The apparent carbon isotopic fractionation factor $\alpha_{CH4-CO2}$ between δ^{13}C-CH_4 and δ^{13}C-CO_2 during methanogenesis in the sediment was calculated after Eq. (22). $\alpha_{CH4\text{-}CO2}$ values are indicative of the type of methanogenesis predominantly occurring in the sediment. While values between 1.050 to 1.060 indicate acetoclastic methanogenesis, values between 1.060 to 1.090 are characteristic for hydrogenotrophic methanogenesis (e.g., Conrad, 2005). $\alpha_{CH4\text{-}CO2}$ values were calculated with δ^{13}C-CH_4 values obtained from the lower part of the sediment cores, where CH_4 concentrations were either increasing or stagnant and no oxidation was apparent. δ^{13}C-CO_2 values were converted from

measured δ^{13}C-DIC values which were examined from the pore water of the sediment cores after Eq. (23) (Mook, 2000).

$$\alpha_{CH4\text{-}CO2} = \frac{(\delta^{13}C\text{-}CO_2 + 1000)}{(\delta^{13}C\text{-}CH_4 + 1000)} \quad (22)$$

$$\delta^{13}C\text{-}CO_2 = \delta^{13}C\text{-}DIC - 8.16\ ‰ \quad (23)$$

2.6.7 Stable carbon and hydrogen isotope fractionation factors during aerobic and anaerobic methane oxidation

The carbon and hydrogen isotopic fractionation factor α was determined for AOM and MOx using the Rayleigh model for closed systems after Bastviken et al. (2002) (Eq. (24)).

$$\ln(1-f) = \left[\ln(\delta_p + 1000) - \ln(\delta_{ox} + 1000)\right]/[\alpha - 1] \quad (24)$$

where f is the fraction of oxidized CH_4, δ_b the δ^{13}C-CH_4 or δ^2H-CH_4 value of CH_4 in the near-bottom water and the zone of CH_4 production in the sediment, respectively, and δ_{ox} the δ^{13}C-CH_4 or δ^2H-CH_4 value of CH_4 in the zone of CH_4 oxidation in the anoxic sediment or the aerobic water column, respectively.

2.6.8 Δ(2,13) values

Recently, Tsunogai et al. (2020) suggested the application of a dual-isotope approach (δ^{13}C-CH_4 and δ^2H-CH_4 values) to gain substantial insight into the sources of limnic CH_4 regardless of MOx. Thereby, the indicator Δ(2,13) [‰] was defined in order to better characterise the sources of CH_4 based on the isotopic composition of CH_4 and is determined according to the equation (Eq. (25)):

$$\Delta(2,13) = \delta\ ^2H\text{-}CH_4 - \Lambda\ x\ \delta^{13}C\text{-}CH_4 \quad (25)$$

Λ was determined to be 9.3 ± 0.3 in an aerobic methane oxidation incubation experiment from the slope of the linear regression between changes in δ^{13}C-CH_4 and δ^2H-CH_4 values during the incubation experiment (section 3.2.6). It was assumed that Λ was similar for anaerobic methane oxidation in the sediment and aerobic MOx that occurred in the water column of Lake Willersinnweiher. The concentration-weighted mean isotopic values and $\Delta(2,13)$ were calculated for the different water layers and the sediment at the three investigated sites. Summarized $\Delta(2,13)$ of the water layers are given along with the pooled standard deviation s_c (Eq. (26)):

$$s_c = \sqrt{\frac{(n_1 - 1)\ x\ {s_1}^2 + \ (n_2 - 1)\ x\ {s_2}^2 + \ldots + (n_k - 1)\ x\ {s_k}^2}{n_{tot} - k}} \quad (26)$$

where $n_1 + n_2 + \ldots = n_{tot}$ is the number of $\Delta(2,13)$ values included in the summarized $\Delta(2,13)$ of the water layer, k the number of summarized $\Delta(2,13)$ values obtained by considering the range of Λ, and s_{1-k} the according standard deviations.

2.6.9 Methane formation by ^{13}C- and ^{2}H-labelled methylated compounds

A mass balance approach was used to calculate the amount of substance of CH_4 produced from ^{13}C-and ^{2}H-labelled compounds in the incubation experiment described in section 2.5.3 (Eq. (27)):

$$c(CH_4)_b * i(CH_4)_b + c(CH_4)_p * i(CH_4)_p = c(CH_4)_t * i(CH_4)_t \quad (27)$$

where $c(CH_4)_b$, $c(CH_4)_p$ and $c(CH_4)_t$ refer to dissolved CH_4 concentrations in the background, produced CH_4 produced during the incubation experiment and total CH_4, respectively. The parameters $i(CH_4)_b$, $i(CH_4)_p$ and $i(CH_4)_t$ refer to the stable isotope values of dissolved CH_4 in the background, produced CH_4 during the incubation experiment and total CH_4, respectively. It was assumed that total dissolved CH_4 equals the sum of produced and background CH_4 (Eq. (28)). Then Eq. (28) was inserted into Eq. (27) and consequently Eq. (29) was used to calculate the amount substance of CH_4 formed from the isotopically labelled compounds.

$$c(CH_4)_t = c(CH_4)_p + c(CH_4)_b \quad (28)$$

$$c(CH_4)_p = \frac{\left(c(CH_4)_b * i(CH_4)_t\right) - \left(c(CH_4)_b * i(CH_4)_b\right)}{i(CH_4)_p - i(CH_4)_t} \quad (29)$$

2.6.10 Diffusion rates of methane at the water-atmosphere interface

Methane diffusion rates at Lake Willersinnweiher were determined using a floating chamber (method description in section 2.2.6) measuring the increase in the CH_4 mixing ratio in the headspace of the chamber with time using Eq. (30).

$$F_{diff}^{rate} = \frac{\Delta CH_4 * p_{atm} * V_{chamber} * cf_{time}}{R * T * A_{chamber} * t * cf_{unit}} \quad (30)$$

where F_{diff}^{rate} [mmol m^{-2} d^{-1}] is the diffusion flux rate, ΔCH_4 [ppmv] the change of the CH_4 mixing ratio within the headspace of the chamber, p_{atm} [bar] the atmospheric pressure, $V_{chamber}$ [m^3] the volume of the chamber, R [bar m^3 mol^{-1} K^{-1}] the ideal gas constant, T [K] the temperature, $A_{chamber}$ [m^2] the area of the chamber, t [s] the length of deployment of the chamber, cf_{time} [d s^{-1}] a time

conversion factor with a value of 86400, and cf_{unit} [mmol mol^{-1}] the unit conversion factor with a value of 1000.

The overall spatial CH_4 diffusion flux for whole Lake Willersinnweiher during a field campaign was calculated using Eq. (31).

$$F_{diff} = (F^{rate}_{diff\ pelagic} * A_{pelagic} + F^{rate}_{diff\ slope} * A_{slope} + F^{rate}_{diff\ littoral} * A_{littoral}) * cf_{unit} \quad (31)$$

where F_{diff} [mol d^{-1}] is the daily CH_4 flux and F^{rate}_{diff} [mmol m^{-2} d^{-1}] and A [m^2] are the diffusion flux rates and areas of the respective pelagic, slope and littoral zones and cf_{unit} [mol mmol^{-1}] the unit conversion factor with a value of 0.001. The areas of the pelagic (depth = 10 to 21 m), slope (depth = 4 to 10 m) and littoral (depth = 0 to 4 m) zones were adapted from bathymetric map calculations (Table A 3).

2.6.11 Ebullition rates of methane

Ebullition rates of CH_4 were calculated using the measured volume of uprising gas bubbles from the sediment via bubble traps at the pelagic, slope and littoral sites, and their measured CH_4 concentrations using Eq. (32).

$$F^{rate}_{ebu} = \frac{V_{bubble} * c^{bubble}_{CH4} * p_{atm} * cf_{unit}}{R * T * A_{bubble\ trap} * t} \quad (32)$$

where F^{rate}_{ebu} [mmol m^{-2} d^{-1}] is the ebullition flux rate of CH_4, V_{bubble} [l] the volume of bubbles caught with the bubble trap, c^{bubble}_{CH4} [dimensionless] the CH_4 concentration of uprising gas bubbles, p_{atm} [bar] the atmospheric pressure, cf_{unit} [mmol mol^{-1}] the unit conversion factor with a value of 1000, R [bar l mol^{-1} K^{-1}] the ideal gas constant, T [K] the temperature, $A_{bubble\ trap}$ [m^2] the area of the bubble trap, t [d] the duration of the deployment of the bubble trap.

The overall spatial CH_4 ebullition flux of whole Lake Willersinnweiher during a field campaign was calculated using Eq. (33).

$$F_{ebu} = (F^{rate}_{ebu\ pelagic} * A_{pelagic} + F^{rate}_{ebu\ slope} * A_{slope} + F^{rate}_{ebu\ littoral} * A_{littoral}) * cf_{unit} \quad (33)$$

where F_{ebu} [mol d^{-1}] is the daily CH_4 flux, and F^{rate}_{ebu} [mmol m^{-2} d^{-1}] and A [m^2] are the ebullition flux rates and areas of the respective pelagic, slope and littoral zones and cf_{unit} [mol mmol^{-1}] the unit conversion factor with a value of 0.001. Similar to the diffusion fluxes the areas of the pelagic, slope and littoral zones were adapted from bathymetric map calculations (Table A 3).

2.7 Statistics

Various statistical methods were used in the scope of this study to analyse the obtained data. Arithmetic means, standard deviations (SD; used throughout the whole study), pooled standard deviations (used for Δ(2,13) values; section 3.4) and linear regression analysis were performed using Microsoft Excel (Microsoft Office 365 MSO). Linear regression analysis was conducted for the determination of MOx rates (section 3.2.6), the calculation of flux rates within the water column and sediment (sections 3.2.4 and 3.1.2), and the determination of $\delta^{13}C\text{-}CH_4$ and $\delta^{2}H\text{-}CH_4$ values of CH_4 released via diffusion (section 3.5.1.2). The R square value (R^2) was used to describe how well the linear regression model matched the input data. The standard error of the linear regression was used as an indicator for the uncertainty of the results of the model. *P*-values were obtained from unpaired two tailed *t*-tests to identify differences between the mean values of two treatment groups using the software SigmaPlot (SigmaPlot 12.2.0.45, *Systat Software*, USA). *P*-values were also used during incubation experiments with potential precursor compounds (section 3.2.6). Even though numerous statistical methods were used within the scope of this study, please note that as suggested by the American Statistical Association (ASA) the term “statistically significant” was avoided. Furthermore, statistical parameters (e.g. *p*-values) were not used as the exclusive criteria for conveying conclusions from the results of this study (Wasserstein et al., 2019).

3 Results

Firstly, results from the investigation of the lake sediment (section 3.1) are described, followed by the water column (section 3.2) and groundwater (section 3.3). Finally, all investigated CH_4 sources of Lake Willersinnweiher were characterised by the novel Δ(2,13) indicator (section 3.4), and seasonal CH_4 emissions and their stable isotope composition of CH_4 (section 3.5) are presented.

3.1 Seasonal characteristics of pore water in the sediment

3.1.1 Pore water parameters[3]

Figure 9 shows various parameters for the profiles of water column (blue) and sediment cores (brown) of pelagic (A-J), slope (K-T) and littoral sites (U-AD) for two sampling dates during the stratification period (July 2020) and the mixing period in winter (March 2021). In this section the pore water parameters of the sediment sampled between May 2019 and March 2021 are described. The results of the parameters of the water column are subject of section 3.2.

In the sediment CH_4 concentrations ranged from 10 to 6000 µmol l^{-1} at all three investigates sites (pelagic, slope and littoral) of Lake Willersinnweiher (Figure 9 B, G, L, Q, V, AA) and were between 50 to 10,000 times higher compared to the water column. Methane concentrations were usually 1.5 to 50 times higher at the pelagic site compared to slope and littoral sites. In the upper part of sediment, decreasing CH_4 concentrations towards the water sediment interface were found at all sites, while in the lower part of the sediment CH_4 increased steadily until constant concentrations were reached. Measured $\delta^{13}C$-CH_4 values were comparable for the pelagic and slope sites ranging from -80.2 ‰ to -38.7 ‰, while at the littoral site higher values from -64.3 ‰ to -52.0 ‰ were found throughout the sampling period. A similar observation was made for $\delta^{2}H$-CH_4 values at the littoral site, which showed more positive values compared to the deeper sites ranging from -336 ‰ to -215 ‰, while $\delta^{2}H$-CH_4 values at the slope and pelagic sites were more negative ranging from -344 ‰ to -80 ‰.

Sulphate concentrations of up to 3.31 mmol l^{-1} in the sediment cores at all sites were characterised by a strong decrease in the upper part of the cores until most SO_4^{2-} was consumed. The decrease in the SO_4^{2-} concentrations was mostly accompanied by an increase in S^{2-} concentrations in the upper part of the sediment cores reaching concentrations of up to 3.22 mmol l^{-1}, 1.71 mmol l^{-1} and 5.47 mmol l^{-1} for the pelagic, slope and littoral site, respectively. Dissolved inorganic carbon concentrations and $\delta^{13}C$-DIC values increased distinctively with depth at all sites ranging from 1.46 to 13.18 mmol l^{-1} and -17.7 ‰ to +8,00 ‰, respectively. However, while DIC concentrations were in similar range at all

[3] Please note that parts of this section are taken from Einzmann et al. (2022).

three sites, the δ^{13}C-DIC values were usually up to 10 ‰ more positive at the littoral site compared to the pelagic and slope sites. In the upper part of the sediment Fe^{2+} concentrations were generally low and mostly increased in depths below 16 cm. Therefore, at all sites Fe^{2+} concentrations in the sediment cores accounted for up to 17.0 µmol l^{-1}. Concentrations of Mn^{2+} showed values of up to 146 µmol l^{-1} and reached maximum concentrations in the upper part of the sediment cores, while concentrations remained stagnant or decreased slightly with depth. Nitrate concentrations in the sediment showed only little variation throughout the depth of sediment cores mostly below 15 µmol l^{-1}. However, in individual sediment cores (e.g., at the pelagic site in September 2019, Table A 4), comparatively high concentrations up to 50 µmol l^{-1} were detected in the topmost part of the sediment, which decreased to background values within a few centimetres.

In every investigated sediment core, zones, where both stable isotope values of CH_4 showed one or multiple excursions towards more positive values, occurred (Figure 9B, G, L, Q, V, AA). Interestingly, positive stable isotope excursions were less pronounced for δ^2H-CH_4 than for δ^{13}C-CH_4 values. Furthermore, in these zones, stable isotope excursions of CH_4 coincided with an increase in DIC and S^{2-} concentrations, a decrease in δ^{13}C-DIC values, CH_4 maxima and SO_4^{2-} minima. Here, these zones are classified as sulphate-methane transition zones (SMTZ, Figure 9 yellow zones).

3.1.2 Sedimentary fluxes

Seasonal sedimentary fluxes of CH_4, SO_4^{2-}, S^{2-}, DIC and Mn^{2+} for the pelagic (A, D, G), slope (B, E, H) and littoral (C, F, I) sites are shown in Figure 10. Sediment flux rates were determined for fluxes of CH_4, Mn^{2+} and DIC released from the sediment-water interface into the water column (indicated in Figure 10 by the addendum “release”) and for CH_4, SO_4^{2-} and S^{2-} fluxes within the zones of SMTZ (yellow zones of the sediment cores in Figure 9 and indicated in Figure 10 by the addendum “SMTZ”).

Across the three investigated pelagic, slope and littoral sites CH_4 release from the sediment into the water column showed large variations ranging from 0.07 to 2.56 mmol m^{-2} d^{-1} (Figure 10A-C). At the littoral site CH_4 release into the water column ranged from 0.14 to 2.28 mmol m^{-2} d^{-1}, while at the deeper located pelagic and slope sites release rates were in a similar magnitude ranging from 0.07 to 2.12 mmol m^{-2} d^{-1} and 0.42 to 2.56 mmol m^{-2} d^{-1}. Distinctively higher CH_4 release into the water column was observed during late-stage stratification periods compared to early-stage stratification periods and the mixing period for all study sites. Methane decline rates in the SMTZ were in the range of 0.14 to 2.59 mmol m^{-2} d^{-1} during sampling periods at all three sites (Figure 10A-C). The highest downward fluxes of CH_4 in the sediment were determined at the pelagic and littoral sites during the late-stage stratification and the mixing period.

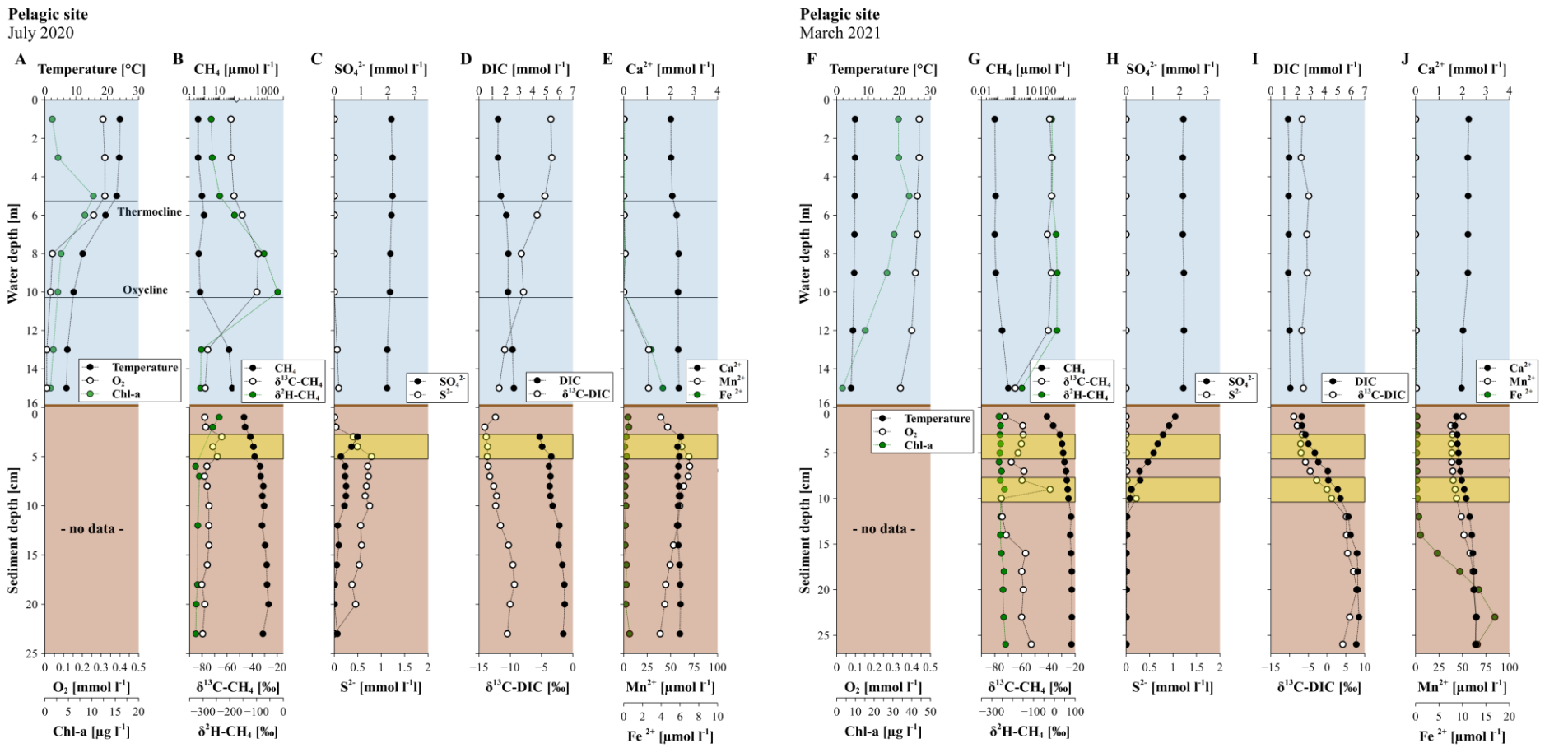

Figure 9. Methane concentrations, $\delta^{13}C\text{-}CH_4$ and $\delta^{2}H\text{-}CH_4$ values, Chl-a concentrations along with SO_4^{2-}, S^{2-}, DIC concentrations, $\delta^{13}C$-DIC values, Ca^{2+}, Fe^{2+} and Mn^{2+} concentrations at the (A-E) pelagic, (K-O) slope and (U-Y) littoral site during the stratified period (July 2020) and at the (F-J) pelagic, (P-T) slope and (Z-AD) littoral site during the mixing period (March 2021). Water column profiles are shown by blue background colours, sediment core profiles are indicated by brown background colours and yellow bars imply the occurrence of SMTZs (modified after Einzmann et al., 2022).

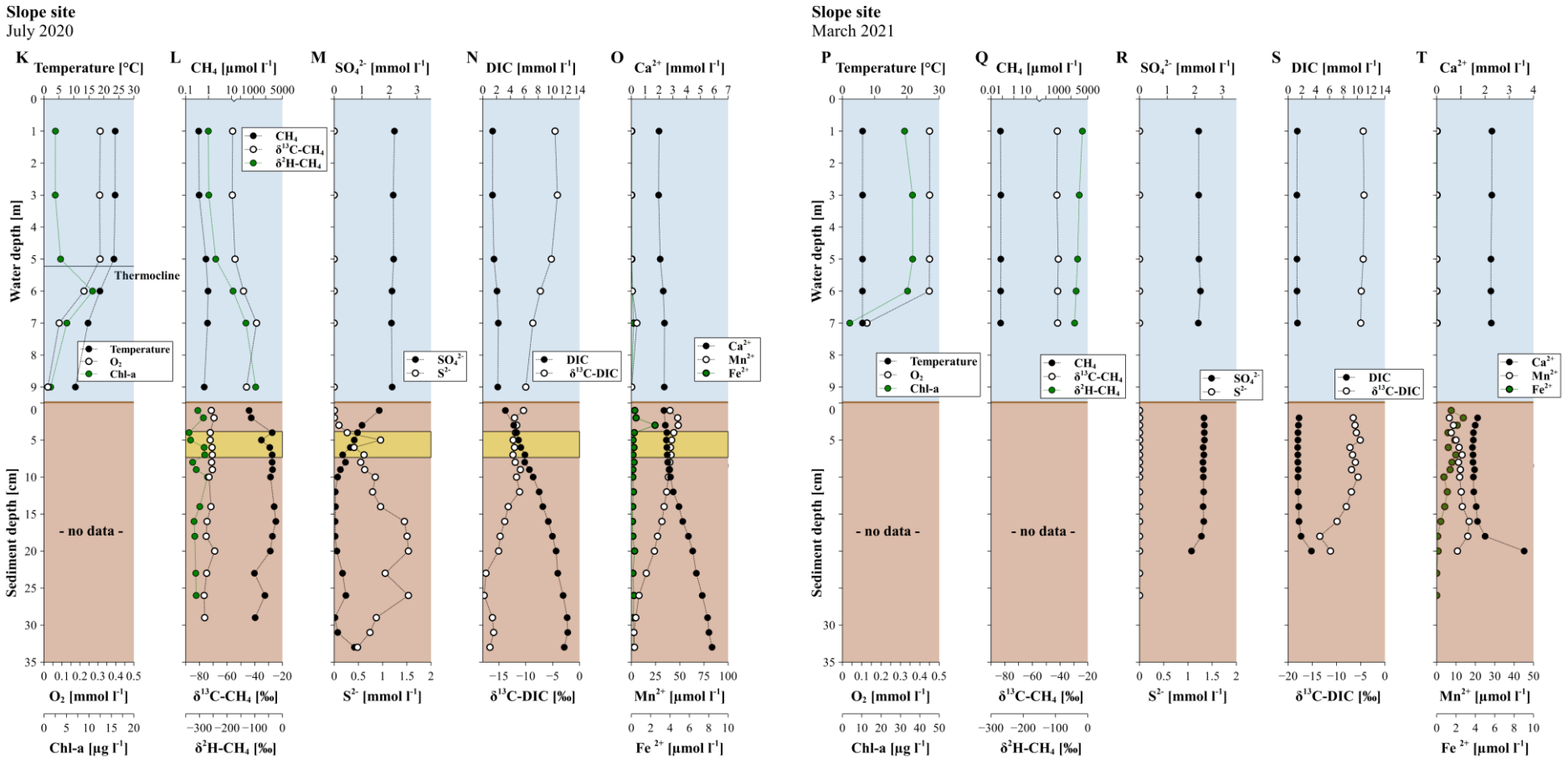

Figure 9. (continued).

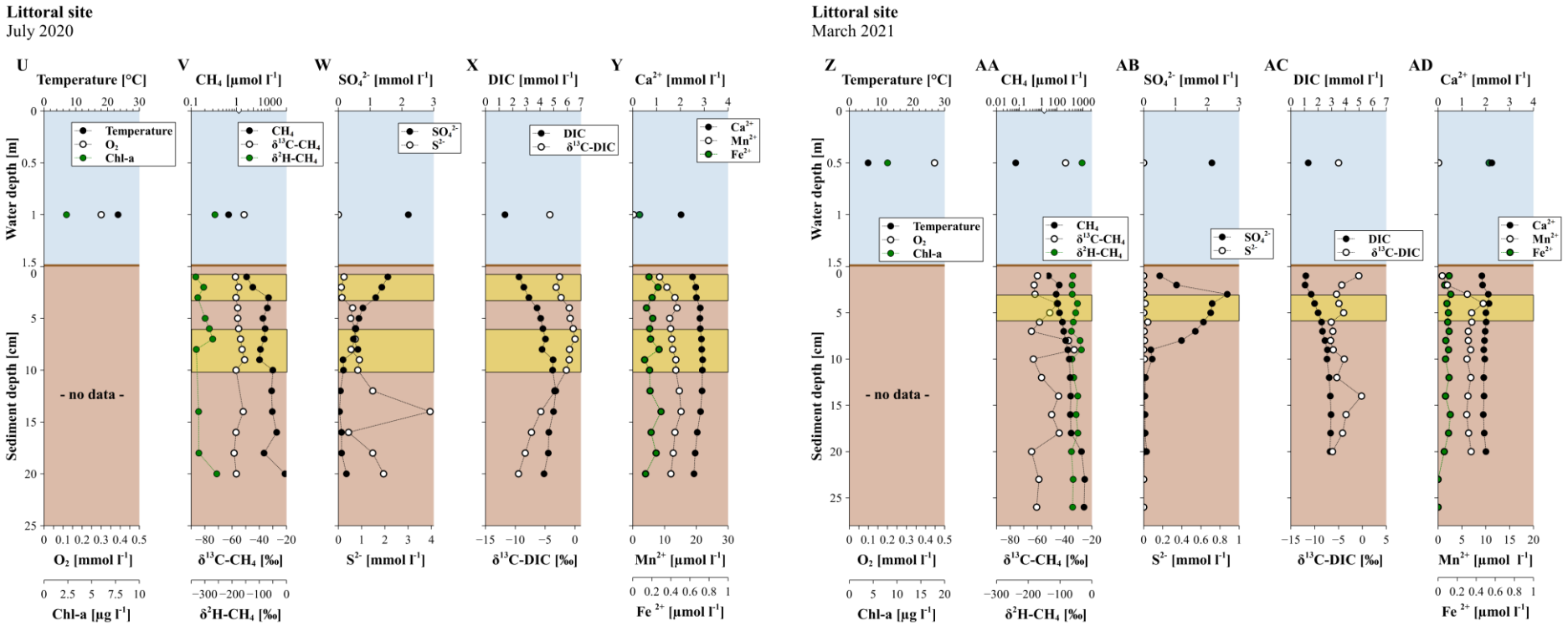

Figure 9. (continued).

Flux rates of SO_4^{2-} and fluxes of S^{2-} in the sediment were closely linked, as higher SO_4^{2-} fluxes coincided with higher S^{2-} fluxes and vice versa at all sites (Figure 10D-F). Fluxes of these two parameters ranged from 0.23 to 1.75 mmol m^{-2} d^{-1} and 0.10 to 3.72 mmol m^{-2} d^{-1} for SO_4^{2-} and S^{2-}, respectively, while no clear seasonality was observed. Dissolved inorganic carbon flux rates at the water-sediment interface were in the range of 0.11 to 3.64 mmol m^{-2} d^{-1} at all three sites (Figure 10G-I). A trend towards higher flux rates of DIC during the late-stage stratification was observed at all sites, while smaller rates were found during the early-stage stratification and the mixing period. Flux rates of Mn^{2+} at the water-sediment interface varied between -30.2 µmol m^{-2} d^{-1} and +30.7 µmol m^{-2} d^{-1} throughout the examined months at all three sites (Figure 10G-I).

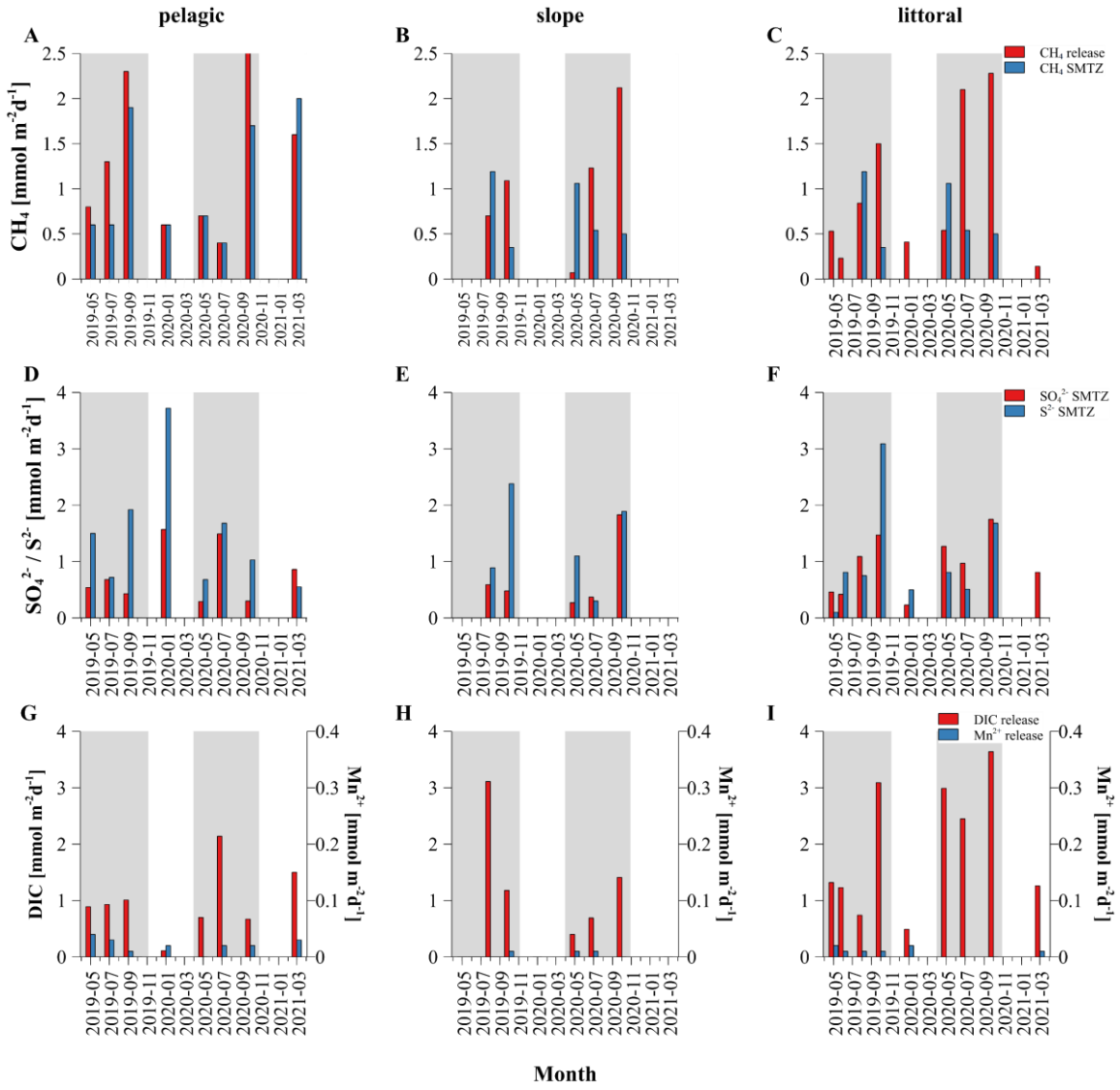

Figure 10. Fluxes of CH_4, SO_4^{2-} and S^{2-} in the SMTZ in the sediment and fluxes of CH_4, DIC and Mn^{2+} released from the sediment into the water column of Lake Willersinnweiher at the (A, D, G) pelagic, (B, E, H) slope and (C, F, I) littoral sites from May 2019 to March 2021. Grey background colours indicate the stratification period and white background colours represent the mixing period.

3.1.3 Stable isotope fractionation during methanogenesis and anaerobic methane oxidation[4]

The isotopic fractionation factor $\alpha_{CO2\text{-}CH4}$ between CO_2 and CH_4 during anaerobic methanogenesis in the sediment were similar in magnitude for each respective site (Table 2). However, the highest values were observed at the pelagic site (1.062 ± 0.009 to 1.067 ± 0.007; n = 3 to 7), while smaller values were determined for the slope site (1.055 ± 0.002 to 1.057 ± 0.009; n = 5 to 8) and the littoral site (1.041 ± 0.004 to 1.052 ± 0.001; n = 4 to 6). Contrary to the strong differences in the $\alpha_{CO2\text{-}CH4}$ values depending on the observed site, $\alpha_{CO2\text{-}CH4}$ values did not show strong seasonal variations throughout the year between May 2020 and March 2021.

Isotope fractionation factors for carbon ($^{13}\alpha$) and hydrogen ($^{2}\alpha$) during AOM were calculated to be in the range of 1.031 to 1.051 and 0.980 to 1.143 at the pelagic site, 1.000 to 1.058 and 1.007 to 1.460 at the slope site and 1.012 to 1.087 and 1.067 to 1.169 at the littoral site, respectively (Table 2). Thus, $^{2}\alpha$ values were mostly higher compared to $^{13}\alpha$ values. Furthermore, $^{13}\alpha$ and $^{2}\alpha$ values were characterised by large variations of up to 0.087 for $^{13}\alpha$ and 0.480 for $^{2}\alpha$, and, therefore, did not show any seasonal trend.

Table 2. Apparent carbon isotope fractionation factor ($\alpha_{CO2\text{-}CH4}$) between CO_2 and CH_4 during anaerobic methanogenesis and isotope fractionation factors of carbon and hydrogen during AOM in the lake sediment of the pelagic, slope and littoral sites during May, July, October 2020, and March 2021. Values for $\alpha_{CO2\text{-}CH4}$ are given as the mean ± SD (n = 3 to 8).

Site	Month	$\alpha_{CO2\text{-}CH4}$	$^{13}\alpha$	$^{2}\alpha$
pelagic	May 2020	1.062 ± 0.009	-	-
	July 2020	1.062 ± 0.003	1.031	1.143
	October 2020	1.067 ± 0.002	1.037	0.980
	March 2021	1.067 ± 0.007	1.051	1.015
slope	May 2020	1.057 ± 0.009	1.005	1.007
	July 2020	1.055 ± 0.002	1.058	1.460
	October 2020	1.055 ± 0.002	1.000	1.057
	March 2021		-	-
littoral	May 2020	1.041 ± 0.004	1.039	1.067
	July 2020	1.044 ± 0.004	1.012	1.124
	October 2020	1.052 ± 0.001	1.015	-
	March 2021	1.044 ± 0.008	1.087	1.169

[4] Please note that parts of this section are taken from Einzmann et al. (2022).

3.2 Seasonal characteristics of the water column[5]

3.2.1 Water column properties

The water column of Lake Willersinnweiher between May 2019 and September 2021 was characterised by a strong thermal stratification between April/May to November/December (stratification period) and thorough mixing of the water column from November/December to March/April (mixing period, Figure 11A). During the period of thermal stratification, the water column was divided into a epilimnion, metalimnion and hypolimnion. In the epilimnion, water temperatures were similar throughout the whole lake. However, water temperatures in the epilimnion ranged between 13 °C and 27 °C in the early and late stages of the stratification, respectively (Figure 11A). The thickness of the epilimnion varied between depths of 3 to 7 m in spring and autumn, respectively. During the stratification period, the epilimnion was further characterised by pH values in the range of 7 and 9 (Figure 11B) and O_2 concentrations ranging from 0.25 mmol l^{-1} up to 0.50 mmol l^{-1} (Figure 11C).

The subjacent metalimnion was found to extend between a depth of 4 m and 11 m. Within the metalimnion the water temperature declined substantially, while O_2 concentrations and pH values often increased in the upper epilimnion with maximum O_2 concentrations of 0.60 mmol l^{-1} and pH values of 8.7 and then decreased towards the lower metalimnion with minimum O_2 concentrations of 0.001 mmol l^{-1} and pH values of 5.9 (Figure 11B, C). In the upper metalimnion Chl-a concentrations in the of up to 100 µg l^{-1} and in single months up to 1000 µg l^{-1} were observed in one or two peaks (Figure 11D).

The transition between metalimnion and hypolimnion was characterised by the occurrence of an oxycline and chemocline where O_2 was no longer present (below mmol l^{-1}) while temperatures (average of 7 °C) and pH values remained constant (average of pH = 7). Generally, during the course of the summer higher water temperature led to a stronger stratification, an upwards shift of the O_2 depletion zone and an increase in the thickness of the hypolimnion to up to 12 m. Towards the end of summer and autumn, decreasing water temperatures led to a substantial extension of the epilimnion and hypolimnion due to the weakening of the stratification. The thickness of the metalimnion shrank until full mixing of the water column was established in early winter to early spring. At the slope site, the water column was only divided into an epilimnion and metalimnion during periods of strong stratification. At the beginning (April/May) and the end (September/October) of the stratification period, the water column usually consisted only of the epilimnion due to its extended thickness and the mere ≈ 8 m depth at the slope site. The water column at the littoral site did not show any stratification due to its shallow depth of about 1.5 m. Water parameters at the slope and littoral sites were very similar to those at the pelagic site and are therefore shown in the appendix (Table A 5). The mixing

[5] Please note that parts of this section are taken from Einzmann et al. (2022).

period was characterised by similar values of the above-mentioned parameters temperature (≈ 5.5 °C), pH (≈ 6.8), O_2 (≈ 0.27 mmol l^{-1}) concentrations throughout the whole water column, except for O_2 concentrations and pH values decreasing in the lowermost observed depths towards the sediment water interface in March 2021.

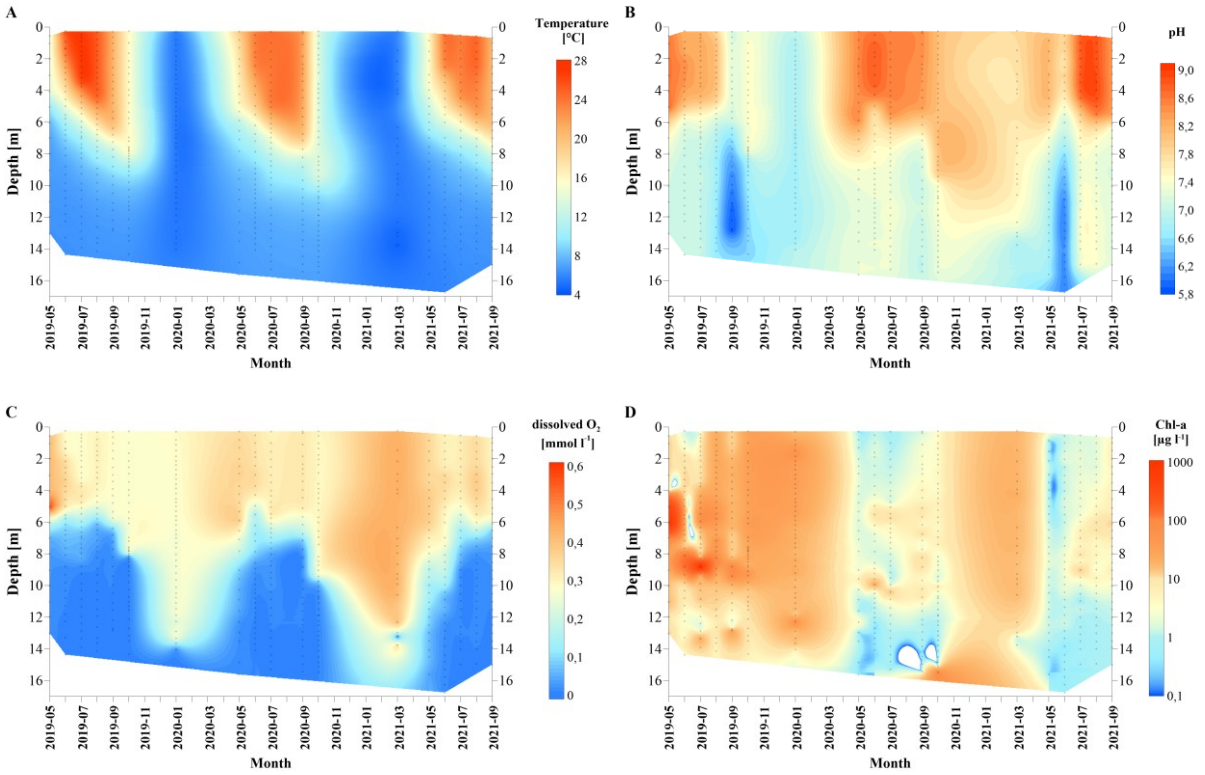

Figure 11. (A) Water temperature, (B) pH values, (C) dissolved O_2 and (D) Chl-a concentrations in the water column of the pelagic site at Lake Willersinnweiher interpolated for the period between May 2019 and September 2021. Gray dots indicate sampled depths.

3.2.2 Major ion composition of the water column

For all campaigns between May 2019 and September 2021, major ion concentrations were analysed for the water column of the pelagic, slope and littoral sites. The results of the major ions are described only for the pelagic site, where an epilimnion, metalimnion and hypolimnion were observed. Data of the profiles of the slope and littoral sites are shown in the appendix Table A 5. In Figure 12, the interpolated concentrations of the major ions Ca^{2+}, DIC, NO_3^- and SO_4^{2-} during the whole observation period (May 2019 to September 2021) are illustrated. Individual profiles of these parameters and additional results for δ^{13}C-DIC values, Fe^{2+} and Mn^{2+} concentrations at the pelagic site during the stratification period (July 2020) and the mixing period (March 2021) are shown in Figure 9C, D, E, H, I, J.

During periods of stratification, the concentrations of Ca^{2+} in the epilimnion were lower compared to the metalimnion and hypolimnion, ranging between 1.6 to 2.5 mmol l^{-1} (Figure 12A). Similarly, DIC concentrations were lower in the epilimnion but increased with depth and towards the end of

stratification with concentrations ranging from 1.0 to 3.2 mmol l^{-1} (Figure 12B). During the mixing period, DIC concentrations were much lower compared to the stratification period ranging from 1.9 to 2.3 mmol l^{-1}. δ^{13}C-DIC values in the epilimnion were found to show only little variation with values between -6 ‰ and -3 ‰, while δ^{13}C-DIC values became more negative with depth and increasing DIC concentrations reaching values of up to -11 ‰ (Figure 9D, I). During mixing period however, δ^{13}C-DIC values were more positive compared to stratification period ranging from -7 ‰ to -4 ‰.

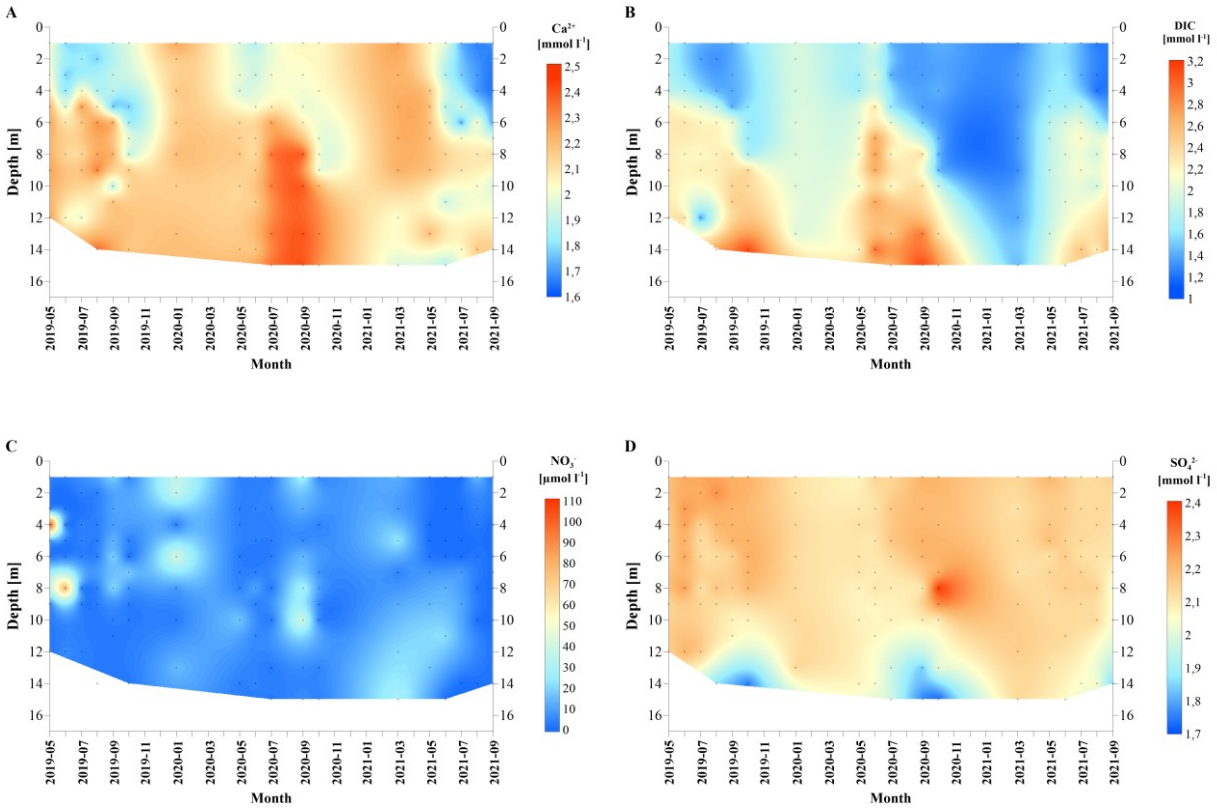

Figure 12. (A) Calcium ion, (B) DIC, (C) NO_3^- and (D) SO_4^{2-} concentrations in the water column of Lake Willersinnweiher interpolated for the period between May 2019 and September 2021. Gray dots indicate sampled depths.

Nitrate concentrations were uniformly distributed and usually accounted for less than 10 µmol l^{-1} except for a few single instants where concentrations reached up to 110 µmol l^{-1} (Figure 12C). Sulphate concentrations in the epilimnion of Lake Willersinnweiher showed only little variation throughout the year ranging from 2.0 to 2.4 mmol l^{-1} (Figure 12D). However, a decrease of up to 0.6 mmol l^{-1} was observed during periods of strong stratification in the hypolimnion. Coinciding with the SO_4^{2-} decrease was an increase in S^{2-} concentrations to up to 2 mmol l^{-1} in the anoxic hypolimnion that intensified during stratification period and the duration of anoxic conditions in the hypolimnion (Figure 9C, H).

In the epilimnion Fe^{2+} and Mn^{2+} were found with concentrations reaching up to 0.3 µmol l^{-1} and 1.0 µmol l^{-1}, respectively (Figure 9E, J, O, T, Y, AD, appendix Table A 5). However, in the metalimnion especially around the depth of the redoxcline elevated Fe^{2+} and Mn^{2+} concentrations were

detected during stratification period, which increased in the hypolimnion with concentrations reaching up to 4 µmol l^{-1} and 50 µmol l^{-1}, respectively.

3.2.3 Methane concentration and stable isotope composition

When compared to the atmospheric equilibrium levels in Lake Willersinnweiher supersaturated CH_4 concentrations were found throughout the whole observation period between May 2019 and September 2021 (Figure 13A).

Lowest and evenly distributed CH_4 concentrations were detected during the mixing periods (January 2020 and March 2021) ranging from 0.05 µmol l^{-1} to 0.07 µmol l^{-1} and up to 0.4 µmol l^{-1} in the bottom water. Stable carbon and hydrogen isotope values of CH_4 (Figure 13B, C) in the upper water column during the mixing period were characterised by a strong enrichment in ^{13}C and ^{2}H leading to $\delta^{13}C$-CH_4 values of -30 ‰ to -42 ‰ and $\delta^{2}H$-CH_4 values of -40 ‰ to +20 ‰. In March 2021, the lowermost sample point showed a small increase in its CH_4 concentration compared to the rest of the water column and more negative $\delta^{13}C$-CH_4 and $\delta^{2}H$-CH_4 values (-65 ‰ and -12 ‰, respectively).

During stratification periods, up to 1200 times higher CH_4 concentrations were detected in the water column of Lake Willersinnweiher compared to mixing period (Figure 13). In the epilimnion, CH_4 concentrations increased with progression of the stratification period and CH_4 concentrations, $\delta^{13}C$-CH_4 and $\delta^{2}H$-CH_4 values ranged from 0.1µmol l^{-1} to 1.6 µmol l^{-1}, -56 ‰ to -38 ‰ and -317 ‰ to -90 ‰, respectively. In the upper part of the metalimnion, an increase in CH_4 concentrations of up to 1 µmol l^{-1} was observed during the stratification period in most months, accompanied by an increase in Chl-a concentrations and O_2 concentrations. Below this peak CH_4 concentrations decreased considerably to as little as 0.03 µmol l^{-1} in the lower part of the metalimnion. This strong decrease in CH_4 concentrations was also concomitant with a decrease in O_2 concentrations and a strong increase in $\delta^{13}C$-CH_4 and $\delta^{2}H$-CH_4 values reaching values of up to -9 ‰ and +140 ‰, respectively (Figure 13B, C). Methane concentrations (Figure 13A) in the hypolimnion were generally characterised by a strong increase towards the sediment-water interface and also incremented with the length of the stratification period ranging from 0.7 µmol l^{-1} during early stratification to 120 µmol l^{-1} during late-stage stratification. Hypolimnic $\delta^{13}C$-CH_4 and $\delta^{2}H$-CH_4 values (Figure 13B, C) became more negative with increasing CH_4 concentrations and were in the range of -80 ‰ to -55 ‰ and -320 ‰ to -175 ‰, respectively.

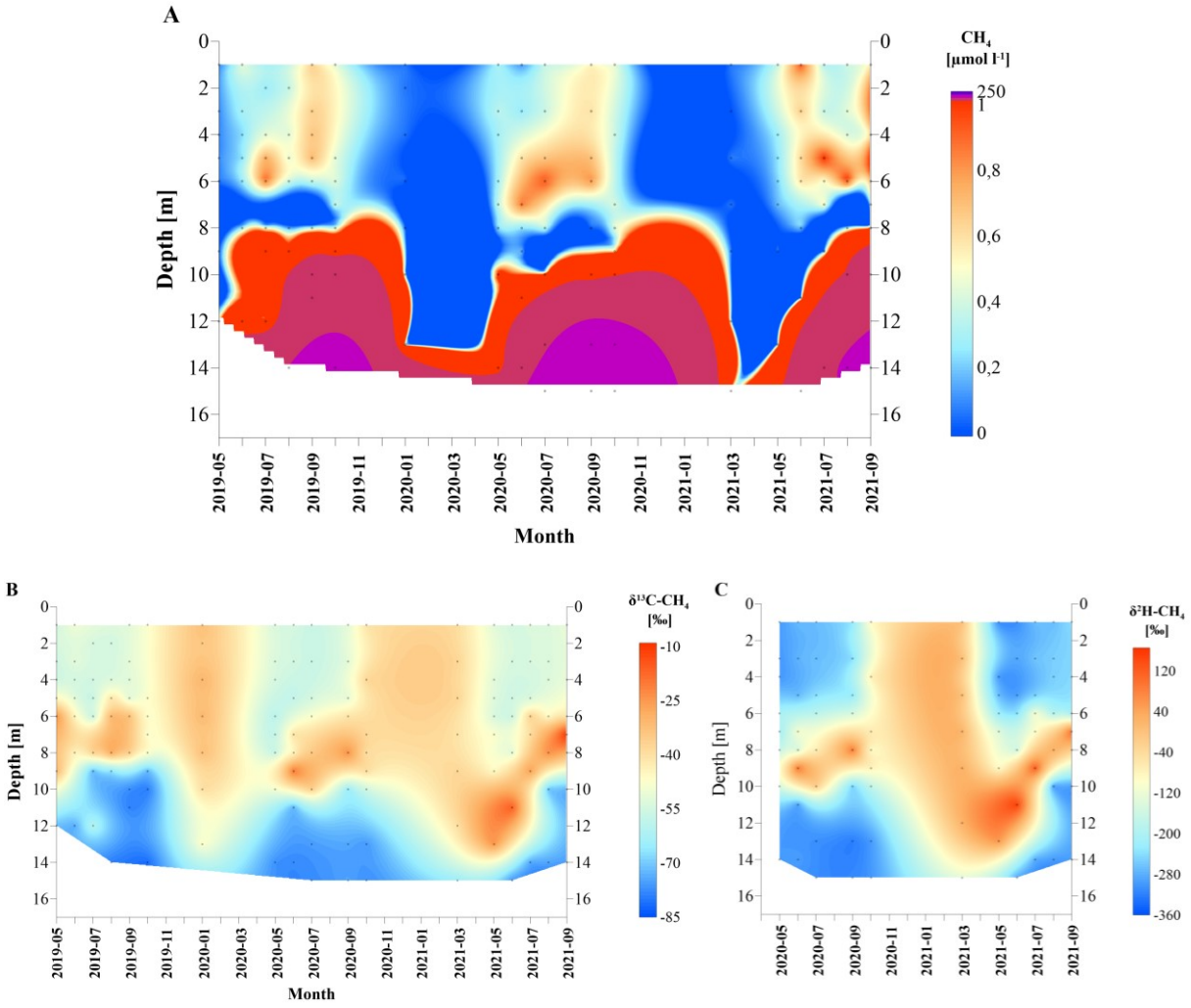

Figure 13. (A) Methane concentrations, (B) δ^{13}C-CH_4 values in the water column of Lake Willersinnweiher interpolated for the period between May 2019 and September 2021, and (C) δ^{2}H-CH_4 values in the water column of Lake Willersinnweiher interpolated for the period between May 2020 and September 2021. Gray dots indicate sampled depths.

3.2.4 Methane production rates and fluxes of methane and oxygen in the water column

Seasonal CH_4 production rates in the epilimnion as well as flux rates of CH_4 and O_2 from the metalimnion into the oxycline and flux rates of CH_4 from the metalimnion into the epilimnion are shown in Figure 14 for the pelagic and slope sites. No fluxes could be determined for the littoral site due to its shallow depth of ≈ 1.5 m. Methane production rates in the epilimnion were determined by a mass balance approach for 7 months (August and October 2019, January, May, July and October 2020, and March 2021), in which, relevant parameters (CH_4 diffusion from the sediments into the water column, from the metalimnion into the epilimnion and from the water column into the atmosphere, input of CH_4 rich groundwater; dissolution of CH_4 from ebullition and MOx; section 2.6.4) were determined.

Methane production in the epilimnion of Lake Willersinnweiher was in the range of 0 to 129 ± 36 nmol l^{-1} d^{-1} (Figure 14A) and was only present at the beginning and end of the stratification period with production rates of 52 ± 14 nmol l^{-1} d^{-1} and 47 ± 27 nmol l^{-1} d^{-1} in May 2020 and October 2020, respectively. When stratification of the water column was strongly developed in August 2019 and July 2020 and during the mixing period (January 2020 and March 2021), the CH_4 mass balance of these months inferred that no CH_4 production rates in the epilimnion was needed to sustain the observed CH_4 supersaturation.

Decreasing CH_4 and O_2 concentrations from the metalimnion towards the oxycline or from the metalimnion towards epilimnion were indicated by positive fluxes, whereas increasing concentrations of CH_4 are reflected by negative fluxes. Methane flux rates into the oxycline were higher at the pelagic site accounting for up to 1.99 mmol m^{-2} d^{-1} compared to the slope site with flux rates up to 0.59 mmol m^{-2} d^{-1} (Figure 14B). While CH_4 flux rates into the oxycline were constantly observed during the stratification period at the pelagic site, flux rates at the slope site were only present in a few months between July to October 2019 and May 2020.

Methane flux rates from the metalimnion into the oxycline increased with length of the stratification period compared to early-stage stratification and mixing periods for both sites. A similar pattern was also found for O_2 fluxes, where flux rates were highest during late-stage stratification (16 to 52 mmol m^{-2} d^{-1}) and lower during early-stage stratification and mixing periods (up to 20 mmol m^{-2} d^{-1}) (Figure 14C). Furthermore, O_2 fluxes showed also higher rates at the pelagic site compared to the slope site most of the times, except for May 2020 and March 2021 (0.5 to 39 mmol m^{-2} d^{-1}).

Methane fluxes from the metalimnion to the epilimnion (up to 20 µmol m^{-2} d^{-1}) were about one order of magnitude smaller compared to CH_4 fluxes from the metalimnion into the oxycline (Figure 14D). Contrastingly, CH_4 fluxes into the epilimnion did not increase with the duration of the stratification period but showed the highest values during summer when the lake stratification was strongly developed. During most months, an upwards flux of CH_4 from the metalimnion to the epilimnion was found. However, during the mixing period and early stratification period in 2021 (March/May 2021) downwards directed fluxes from the epilimnion into the metalimnion were found. Methane fluxes into the epilimnion at the pelagic site (-3 to 21 µmol m^{-2} d^{-1}) were in the same order of magnitude but mostly slightly smaller compared to the rates determined for the slope site (-2 to 20 µmol m^{-2} d^{-1}).

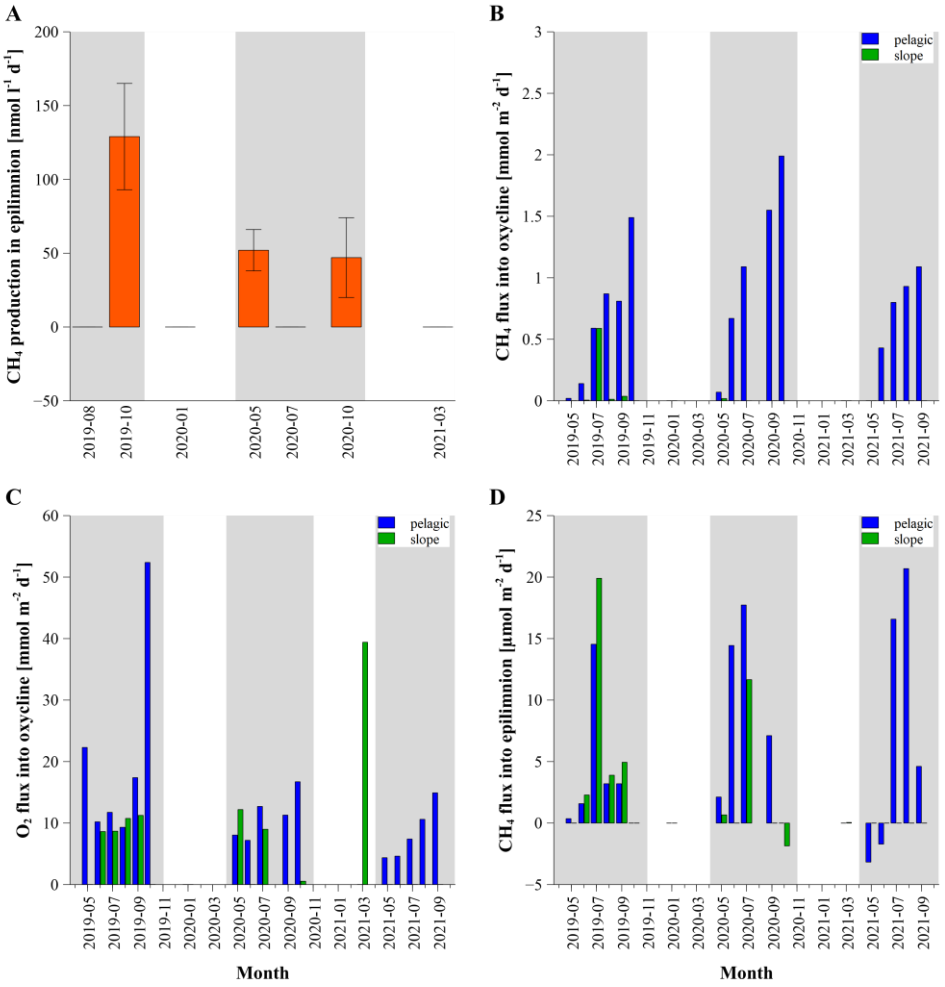

Figure 14. (A) Estimated rates of CH_4 production in the epilimnion of Lake Willersinnweiher (orange), fluxes of (B) CH_4 and (C) O_2 into the oxycline (downwards) and fluxes of (D) CH_4 from the metalimnion into the epilimnion (upwards) at the pelagic (blue) and slope (green) sites at Lake Willersinnweiher. Grey background colours indicate the stratification period and white background colours represent the mixing period.

3.2.5 Spatial distribution of methane in the epilimnion

The spatial distribution of CH_4 concentrations in a water depth of 1 m was investigated at Lake Willersinnweiher in July, September and October 2020 and March 2021 (Figure 15). Methane concentrations throughout Lake Willersinnweiher showed distinct differences between the examined months and were in the range of 342 ± 25, 622 ± 50, 454 ± 68 nmol l^{-1} and 74 ± 4, 370 ± 16, 1024 ± 155, 345 ± 13 nmol l^{-1} for July, September, October 2020 and March, May, June, and July 2021, respectively. Spatial variations of the CH_4 concentrations within one sampling campaign were highest in June 2021, where also highest CH_4 concentrations were recorded (ranging from 524 to 2249 nmol l^{-1}). In contrast smallest spatial variations were measured during the mixing period in March 2021 with values ranging from 62 to 75 nmol l^{-1}. A trend towards higher CH_4 concentrations in the north-eastern part and lower concentrations in the south-western part of Lake Willersinnweiher were found for most investigated months except for May and June 2021, where surface water CH_4 was

distributed more evenly and higher CH_4 concentrations appeared to rather derive from point sources in the north-eastern part of the lake. In Figure 15, CH_4 concentrations of sample points in the epilimnion were related to their distance to shore and lake depth at their lake positions to determine potential patterns and influences of these parameters to CH_4 supersaturation. Neither the distance to the shore, nor the lake depth seemed to strongly influence CH_4 concentrations in the epilimnion during all observed months, which was indicated by $R^2 < 0.06$ and $R^2 < 0.15$, respectively. Due to the used methodical approach (section 2.2.4), littoral areas with only a shallow depth smaller than 2 m could not be analysed. Therefore, their influence on CH_4 concentrations in surface water could not be evaluated.

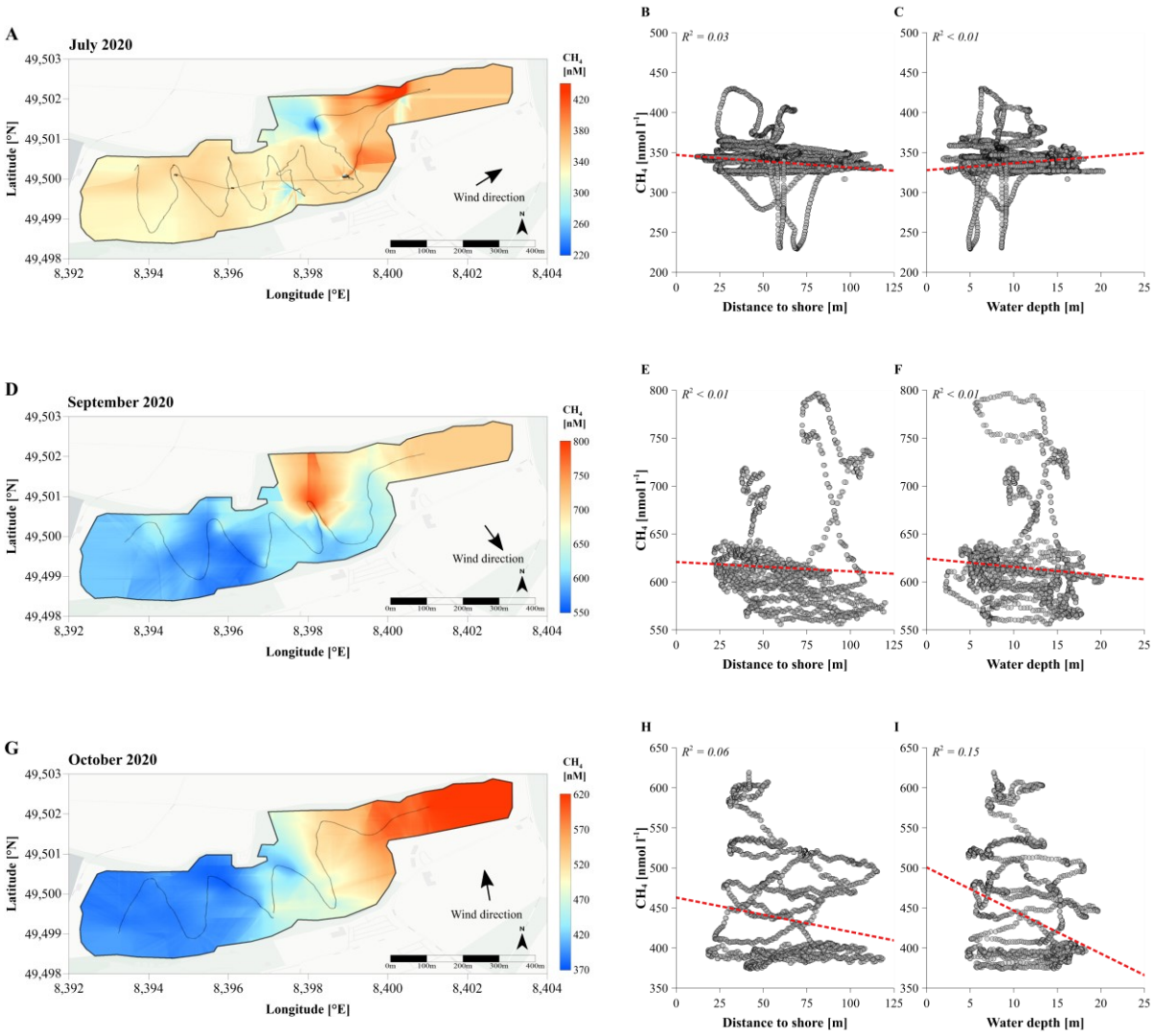

Figure 15. (A, D, G, J, M, P, S) Interpolated spatial distribution of CH_4 in the epilimnion of Lake Willersinnweiher (depth = 1 m). Average daily wind directions are indicated by a black arrow. Gray dots indicate the location of water samples. (B, E, H, K, N, Q, T) Relation of the CH_4 concentration and the distance to the shore of each sample point (dotted red line) and (C, G, I, L, O, R, U) relation of the CH_4 concentration and the water depth at each sample point (dotted red line). Data for the wind direction was obtained from a nearby weather station. R^2 values were calculated using a simple linear regression.

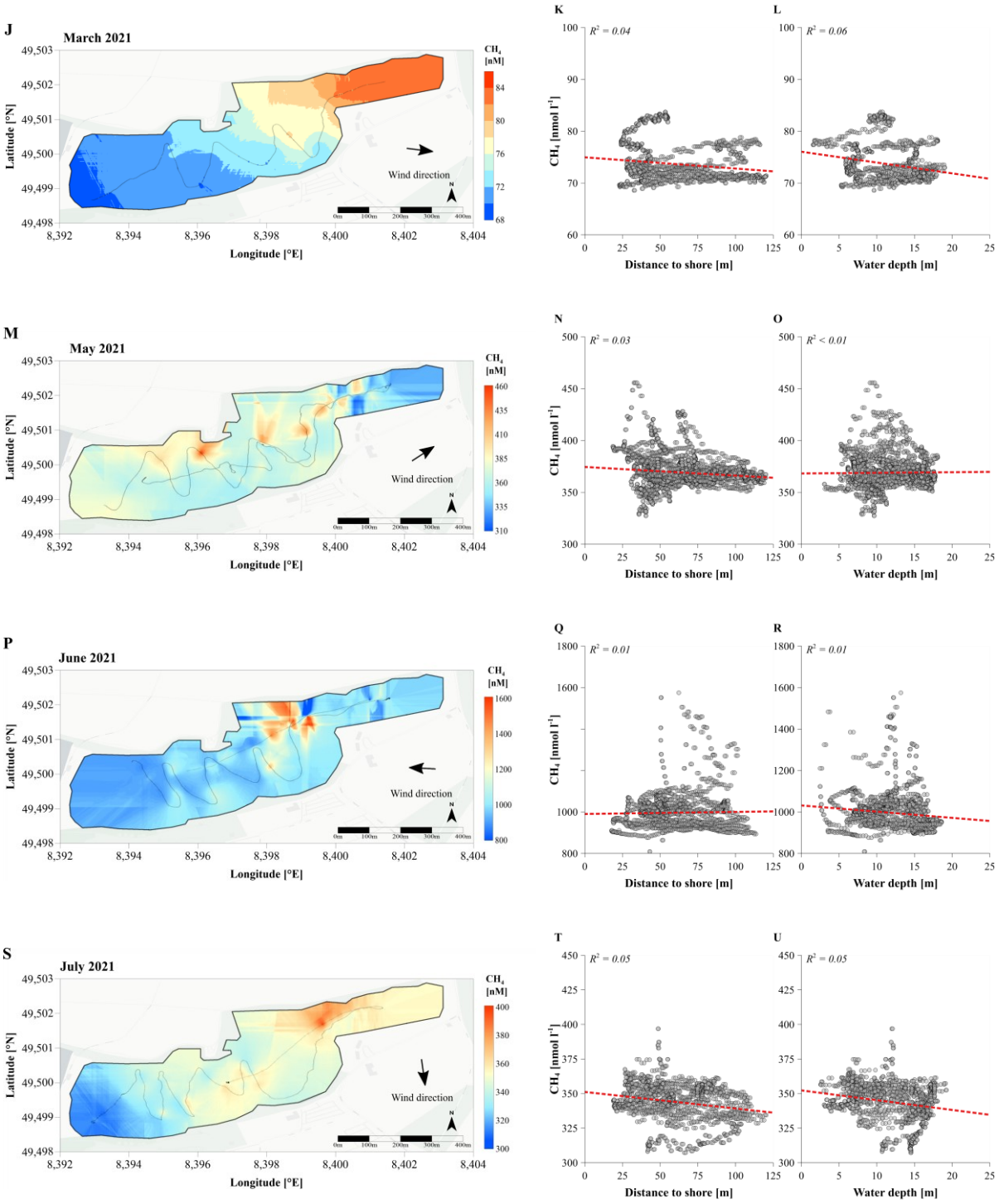

Figure 15. (continued).

Contrastingly to the results shown in Figure 15, where only small correlations between water depth and distance to shore was found for surface CH_4 concentrations, the comparison of CH_4 concentrations of the pelagic, slope and the shallowest littoral site (≈ 1.5 m depth), showed a strong bias towards higher CH_4 concentrations at the littoral site compared to the two deeper sites nearly throughout the whole year (Figure 16). This disparity was especially developed during stratification period, where

concentrations were up to three times higher at the littoral site compared to the other two sites, while during the mixing period CH_4 concentrations were in the same order of magnitude at all three sites.

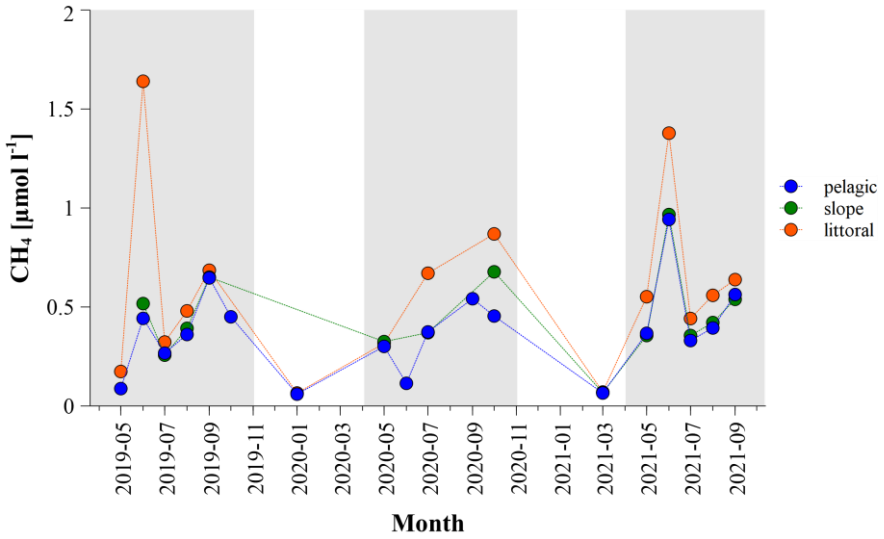

Figure 16. Dissolved CH_4 concentrations in the epilimnion at the pelagic (depth = 1 m; blue), slope (depth = 1 m; green) and littoral (depth = 0.5 m; orange) sites from May 2019 to September 2021. Grey background colours indicate the stratification period and white background colours represent the mixing period.

3.2.6 Aerobic methane oxidation and associated stable isotope fractionation

Aerobic methane oxidation rates in the water column of Lake Willersinnweiher were determined between July 2020 and September 2021. In the months of July, September, October 2020 and March 2021 MOx rates were only determined for one depth (appendix Table A 6), while in July and September 2021, two profiles of MOx rates were analysed in four different depths of the epilimnion and metalimnion (Figure 17A, B). Aerobic methane oxidation rates at Lake Willersinnweiher were in the range of 43 ± 5 to 950 ± 149 nmol l^{-1} d^{-1}. A trend towards increasing MOx rates in the water column were observed with increased duration of the stratification period. During 2020, where MOx was determined for only one depth, increasing MOx rates from 49 ± 5 nmol l^{-1} d^{-1} in July to 109 ± 7 nmol l^{-1} d^{-1} in September and 251 ± 13 nmol l^{-1} d^{-1} in October were observed. A similar pattern was found for MOx profiles obtained during stratification period in 2021 (Figure 17A, B). In both profiles higher MOx rates were found with increasing water depth and decreasing proximity to the oxycline. Furthermore, higher MOx rates coincided with decreasing CH_4 concentrations in the metalimnion. An exception of the latter observation was the MOx rate in a depth of 8 m in September 2021, which did not increase but decrease towards the oxycline. Interestingly, even though no decrease in CH_4 concentrations in the water column was observed during the mixing period in March 2021 (Figure 9G), a MOx rate of 89 ± 13 nmol l^{-1} d^{-1} was determined in a water depth of 8 m.

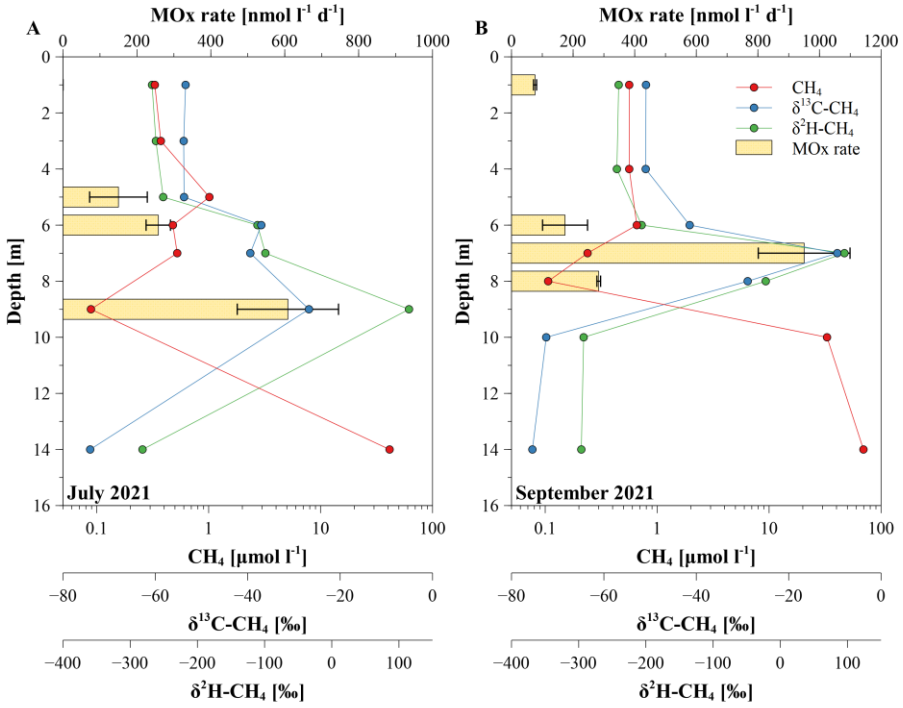

Figure 17. Profiles of CH_4 concentration (red), $\delta^{13}C$-CH_4 values (blue), $\delta^{2}H$-CH_4 values (green) and MOx rates (yellow) at the pelagic site in (A) July 2021 and (B) September 2021. Error bars of the MOx rates indicate the standard error of the linear regression used to calculate MOx rates (section 2.6.5).

Carbon ($^{13}\alpha$) and hydrogen ($^{2}\alpha$) isotope fractionation factors of CH_4 due to MOx are shown in Table 3. Throughout the observation period (May 2019 to September 2021), $^{13}\alpha$ values were very similar and did not show large variation ranging from 1.006 to 1.013 with an average value of 1.009 ± 0.002. Values of $^{2}\alpha$ were determined in the field campaigns during the years 2020 and 2021. They were distinctively higher than $^{13}\alpha$ values (up to 0.080 higher) and ranged from 1.051 to 1.095 with an average value of 1.068 ± 0.015. Furthermore, a seasonal trend towards decreasing $^{2}\alpha$ values from June 2020/2021 to October 2020/September 2021 was found.

In the months May 2019, January and May 2020, March and May 2020 no isotopic fractionation factors could be determined for MOx since the water column recorded a steady CH_4 concentration and isotopic signature with depth (Figure 9G and appendix Table A 5)

The incubation experiment in which Λ, the relation between $^{13}\alpha$ and $^{2}\alpha$ values during MOx was determined, was conducted in July 2021. During the incubation experiment CH_4 concentrations decreased from 694 ± 7 (n = 3) to 290 ± 18 nmol l^{-1} (n = 3) (Figure 18A). Stable carbon isotope values of CH_4 increased from -33.8 ± 0.2 ‰ (n = 3) to -11.6 ± 1.5 ‰ (n = 3), while a stronger increase in $\delta^{2}H$-CH_4 values compared to $\delta^{13}C$-CH_4 values was observed ranging from -79 ± 2 ‰ (n = 3) to 127 ± 17 ‰ (n = 3). The relation between $\delta^{13}C$-CH_4 and $\delta^{2}H$-CH_4 values is displayed in Figure 18B, reveals a high correlation of R^2 = 0.99 between both values and showed that CH_4 became 9.3 times more enriched in ^{2}H compared to ^{13}C during MOx.

Table 3. Carbon ($^{13}\alpha$) and hydrogen ($^{2}\alpha$) isotope fractionation factors of CH_4 due to MOx between May 2019 and September 2021. $^{2}\alpha$ values were not determined (n.d.) in the year 2019.

Month	$^{13}\alpha$	$^{2}\alpha$
May 2019	-	n.d.
June 2019	1.009	n.d.
July 2019	1.011	n.d.
August 2019	1.009	n.d.
September 2019	1.009	n.d.
October 2019	1.006	n.d.
January 2020	-	-
May 2020	-	-
June 2020	1.007	1.087
July 2020	1.009	1.057
September 2020	1.007	1.064
October 2020	1.007	1.052
March 2021	-	-
May 2021	-	-
June 2021	1.013	1.095
July 2021	1.008	1.072
August 2021	1.009	1.067
September 2021	1.008	1.051

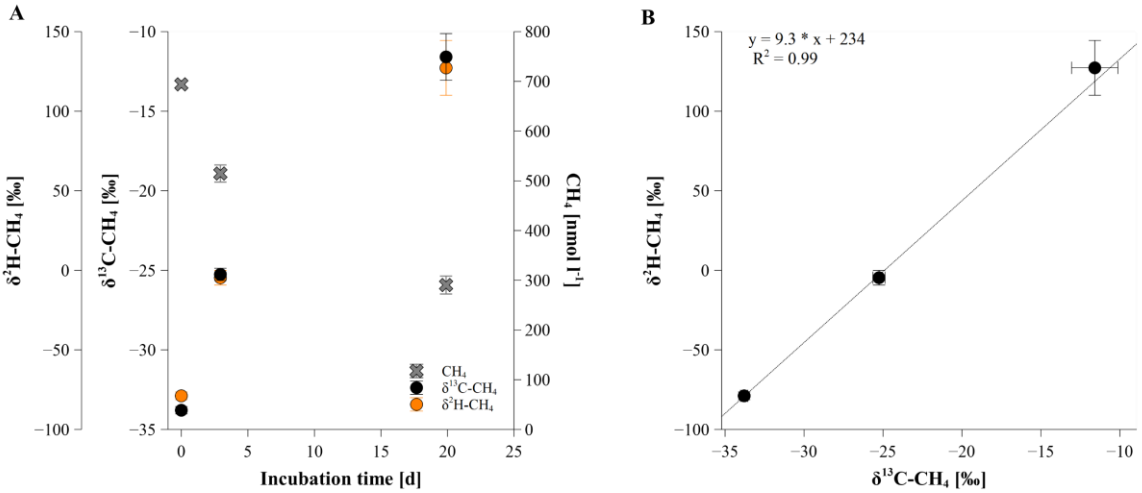

Figure 18. (A) Methane concentrations, δ^{13}C-CH_4 and δ^{2}H-CH_4 values during the incubation experiment to determine Λ. (B) Relationship between δ^{13}C-CH_4 and δ^{2}H-CH_4 values during MOx. Data show mean values with SD (n = 3). Where no error bars are visible, they lie within the data point symbol.

3.2.7 Methane formation from $\delta^{13}C$ and $\delta^{2}H$-labelled methylated compounds

Methyl phosphonate, MA, TMA and MET were tested for their potential as precursor compounds of OMP within the water column of Lake Willersinnweiher. Therefore, incubation experiments, where the methyl group of MPn was labelled with ^{13}C (September 2020) and the methyl groups of MA, TMA and MET were labelled with ^{2}H (September 2021) were conducted with water samples from the metalimnion in a water depth of 6 m and 7 m, respectively (O_2 was present; Figure 11C).

Figure 19A, displays the $\delta^{13}C$-CH_4 values during the incubation experiment with supplemented ^{13}C-MPn. Stable carbon isotope values of CH_4 in the treatments "Control" and "Control filtered" show only small differences during the incubations with values ranging between -34 ± 7 ‰ to -38 ± 6 ‰ (n = 3) and -27 ± 9 ‰ to -34 ± 3 ‰ (n = 3, $p = 0.702$ between "Control" and "Control filtered") at the beginning and the end of the incubations, respectively. In contrast in the treatment "^{13}C-MPn" $\delta^{13}C$-CH_4 values increased gradually from -37 ± 8 ‰ to +100 ± 14 ‰ (n = 3, $p < 0.001$ compared to "Control"). The treatment "^{13}C-MPn filtered" $\delta^{13}C$-CH_4 values showed only minor changes in the first 42 hours of the incubation however, subsequent samples were lost due to technical issues.

The results of $\delta^{2}H$-CH_4 values during the incubation experiment with ^{2}H-labelled MA, TMA and MET are illustrated in Figure 19C. Stable hydrogen isotope values of CH_4 showed only little changes during the incubation in the control treatments "Control" (n = 3) and "Control filtered" (n = 1) ranging from +104 ± 4 ‰ to +127 ± 9 ‰ and +157 to + 142 ‰, respectively. When the ^{2}H-labelled substances were incubated $\delta^{2}H$-values increased from +138 ± 7 ‰ to +928 ± 56 ‰ (n = 3, p = 0.002 compared to treatment "Control") for "^{2}H-MA" and from +183 ± 45 ‰ to +4813 ± 653 ‰ (n = 3, $p = 0.029$ compared to treatment "Control") for "^{2}H-MET". In the treatment "^{2}H-TMA" changes in the range of the SD were observed (+136 ± 16 ‰ to +130 ± 24 ‰, n = 3, $p = 0.931$ compared to "Control").

All filtered treatments showed only minor changes of the $\delta^{2}H$-CH_4 values during the incubation period from +159 ‰ to +184 ‰ (n = 1) and +106 to +177 ‰ (n = 1) for the treatments "^{2}H-TMA filtered" and "^{2}H-MET filtered". The final sample of the treatment "^{2}H-MA filtered" at the end of the incubation was lost due to technical issues.

The results of the incubation experiments unambiguously showed that MPn, MA and MET constituted potential precursor compounds of CH_4 in Lake Willersinnweiher. Based on the changes of $\delta^{13}C$-CH_4 and $\delta^{2}H$-CH_4 values during incubation experiments, 17.4 ± 2.0 nmol l^{-1} ^{13}C-CH_4 as well as 0.14 ± 0.01 pmol l^{-1} and 0.80 ± 0.11 pmol l^{-1} ^{2}H-CH_4 were produced from the labelled precursor compounds MPn, MA and MET, respectively.

The dissolved CH_4 concentrations during the incubation experiment are shown in Figure 19B for the incubation with ^{13}C-MPn and in Figure 19D for the incubation experiment with ^{2}H-MA, ^{2}H-TMA and ^{2}H-MET. In both incubation experiments dissolved CH_4 concentrations were up to 33 % smaller in samples of filtered treatments compared to non-filtered treatments due to partial degassing while

filtering the water samples. Therefore, only the trends of the CH_4 concentrations are described. In the MPn incubation experiment a decrease in CH_4 concentrations was observed for the non-filtered treatments "Control" (n = 3) and "^{13}C-MPn" (n = 3), while for the filtered treatments "Control filtered" (n = 3) and "^{13}C-MPn filtered" (n = 3) CH_4 concentration changes were within their respective SD. Similar to the MPn incubation experiment, CH_4 concentrations decreased (up to 10 %) in the samples of the non-filtered treatments "Control", "^{2}H-MA", "^{2}H-TMA" and "^{2}H-MET" (n = 3 each), while only minor changes were observed for samples of filtered treatments (n = 1).

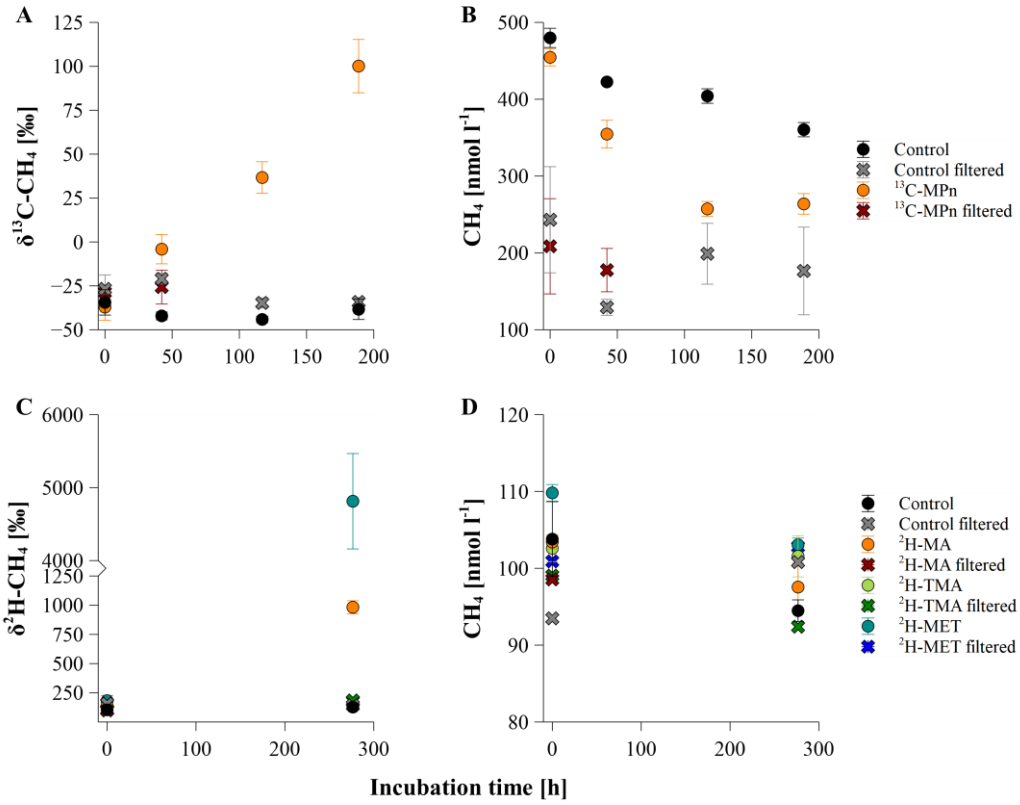

Figure 19. Stable carbon and hydrogen isotope values of CH_4 and CH_4 concentrations during the incubation experiments of the precursor compounds (A, B) MPn and (C, D) MA, TMA and MET. Data show mean values with SD (n = 3) for all treatments, except "filtered" treatments (n = 1). Where no error bars are visible, they lie within the data point symbol or belong to the "filtered" treatments.

3.3 Groundwater characteristics

Groundwater from the three wells (GW West out, GW East out and GW West in) around Lake Willersinnweiher was investigated. Details of the location are shown in Figure 5C. The general flow direction of the groundwater was directed from southwest to northeast (Figure 5B). Inflowing groundwater was thereby represented by GW West in, while outflowing groundwater was represented by GW West out and GW East out. Please note that within the scope of this study flow directions of the groundwater were not investigated and current flow regimes might have changed compared to

previous studies (Wollschläger et al., 2007). Physiochemical properties, as well as concentrations of dissolved CH_4 and other investigated ions showed distinctive differences between inflowing and outflowing groundwater, which is outlined in the following three chapters.

3.3.1 Physiochemical properties of groundwater

The physiochemical properties of in- and outflowing groundwater is illustrated in Figure 20. Groundwater temperatures showed only small variances for GW West out and GW West in ranging from 12.8 to 13.8 °C and 13.5 to 14.7 °C, respectively, while higher seasonal variations, especially between late 2019 and early 2020, were observed for GW East out ranging between 11.7 to 15.7 °C. In all observed months, the groundwater was suboxic and pH values were constant with 7.3 ± 0.1, 7.8 ± 0.1 and 7.3 ± 0.1 for GW West out, GW East out and GW West in, respectively.

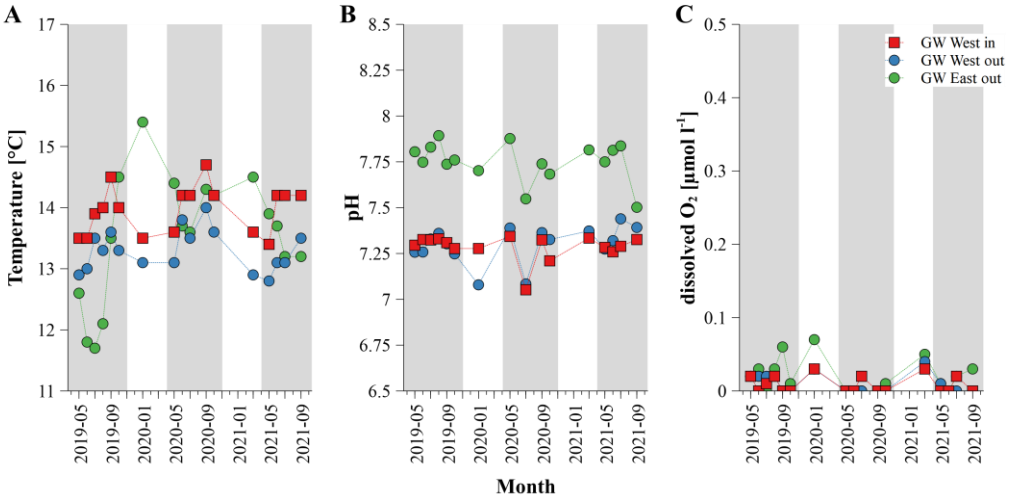

Figure 20. (A) Water temperature, (B) pH values and (C) dissolved O_2 concentrations of inflowing groundwater at GW West in (red) as well as outflowing groundwater at GW West out (blue) and GW East out (green) at Lake Willersinnweiher from May 2019 to September 2021. Grey background colours indicate the stratification period and white background colours represent the mixing period.

3.3.2 Major ion composition of the groundwater

An overview of major ion concentrations at all three groundwater wells is shown in Figure 21. Groundwater at Lake Willersinnweiher was characterised by SO_4^{2-} concentrations reaching up to 2.5 mmol l^{-1} (Figure 21A). For inflowing groundwater at GW West in, on average higher SO_4^{2-} concentrations (2.52 ± 0.06 mmol l^{-1}) compared to outflowing groundwater at GW West out (1.75 ± 0.06 mmol l^{-1}) and GW East out (2.04 ± 0.30 mmol l^{-1}) were found during the observation period from May 2019 to September 2021. However, at GW East out SO_4^{2-} concentrations showed a strong seasonal variation with lower values during the mixing period and higher values during stratification period. Concentrations of NO_3^- in inflowing and outflowing groundwater were usually

below a concentration of ≈ 10 µmol l^{-1} throughout the sampling period at all groundwater wells except for punctual strong increases, reaching up to 250 µmol l^{-1} at GW West in (Figure 21B).

Concentrations of Fe^{2+} were on average between 1.5 to 7 times higher in inflowing groundwater at GW West in (42.4 ± 11.0 µmol l^{-1}) compared to outflowing groundwater at GW West out (30.0 ± 11.9 µmol l^{-1}) and GW East out (5.5 ± 2.0 µmol l^{-1}). Contrastingly to Fe^{2+} concentrations, average Mn^{2+} concentrations were up to 33 % lower in inflowing groundwater at GW West in, ranging from 12.7 ± 1.0 µmol l^{-1} compared to outflowing groundwater at GW West out and GW East out with concentrations ranging between 19.1 ± 4.7 µmol l^{-1} and 17.6 ± 6.8 µmol l^{-1}, respectively (Figure 21D). Furthermore, a seasonal variation with lower Mn^{2+} concentrations during the mixing period and higher ones during stratification period were observed for outflowing groundwater.

Average DIC concentrations were up to 25 % higher in inflowing groundwater at GW West in (4.10 ± 0.44 mmol l^{-1}) compared to outflowing groundwater at GW West out (3.74 ± 0.42 mmol l^{-1}) and GW East out (3.01 ± 0.63 mmol l^{-1}; Figure 21E). However, high seasonal variations of up to 2 mmol l^{-1} were found.

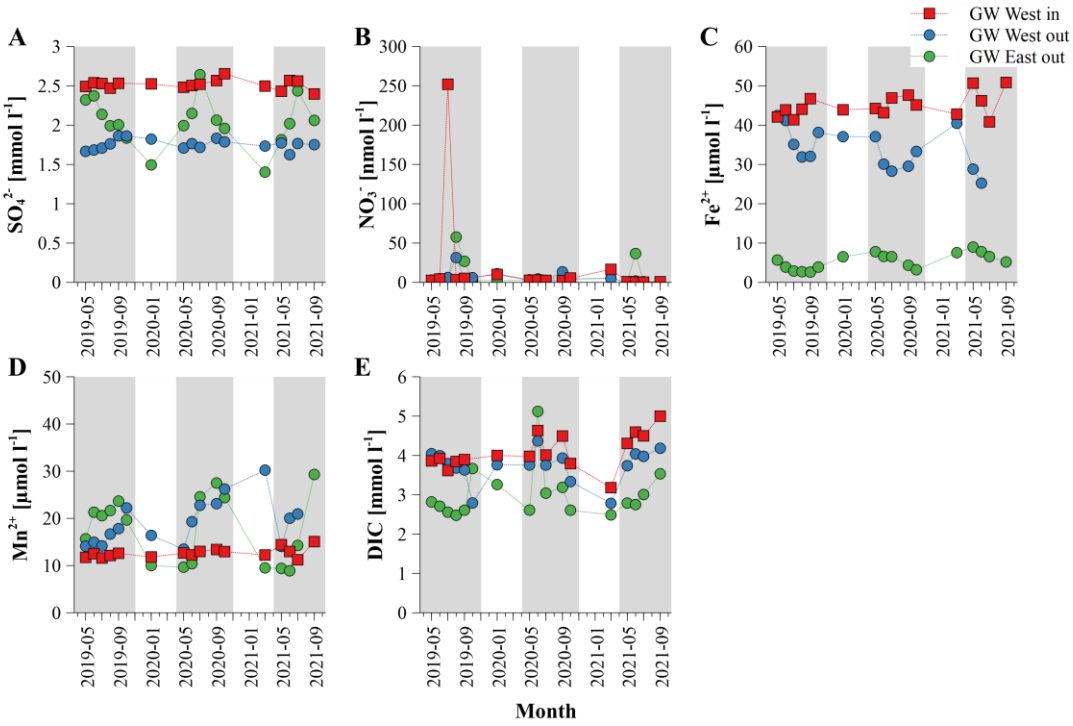

Figure 21. (A) Sulphate, (B) NO_3^- , (C) Fe^{2+}, (D) Mn^{2+} and (E) DIC concentrations of inflowing groundwater at GW West in (red) as well as outflowing groundwater at GW West out (blue) and GW East out (green) at Lake Willersinnweiher from May 2019 to September 2021. Grey background colours indicate the stratification period and white background colours represent the mixing period.

3.3.3 Methane concentrations and its stable isotope composition

The observed CH_4 concentrations, $\delta^{13}C$-CH_4 and $\delta^{2}H$-CH_4 values determined for groundwater at Lake Willersinnweiher are illustrated in Figure 22. Methane concentrations at GW West out and GW West in showed less variation compared to GW East out throughout the observation period and ranged from 0.62 to 2.71 µmol l^{-1} and 0.95 to 2.06 µmol l^{-1}, respectively (Figure 22A). At GW East out, CH_4 concentrations were higher at most times compared to GW West out and GW West in ranging from 0.59 up to 30.8 µmol l^{-1}. Two periods of elevated CH_4 concentrations at GW East out were detected between July 2019 to May 2020 and October 2020 to August 2021, which also coincided with low SO_4^{2-} and Mn^{2+} concentrations at this groundwater well (Figure 21A, D).

Stable carbon isotope values of CH_4 showed distinct characteristics between the three groundwater wells (Figure 22B). The most negative $\delta^{13}C$-CH_4 values were measured for outflowing groundwater at GW East out ranging from -61.2 to -31.1 ‰. Furthermore, at this site two periods (between September 2019 to May 2020 and September 2020 to May 2021) of distinct increases in $\delta^{13}C$-CH_4 values were observed that partly coincided with the periods of elevated CH_4 concentrations (Figure 22A). Stable carbon isotope values of CH_4 at GW West in were more positive compared to GW East out with observed values between -36.8 ‰ and -4.01 ‰. Even more positive $\delta^{13}C$-CH_4 values were found at GW West out ranging from -37.2 to +40.6 ‰.

Stable hydrogen isotope values of CH_4 showed a similar pattern compared to the $\delta^{13}C$-CH_4 values with most negative $\delta^{2}H$-CH_4 values measured at GW East out and most positive values measured at GW West out ranging from -24 ‰ to +660 ‰, -296 ‰ to -184 ‰ and +83 ‰ to +185 ‰ for GW West out, GW East out and GW West in, respectively (Figure 22C). A small increase in $\delta^{2}H$-CH_4 values was found between March 2020 to July 2020 and March 2021 to June 2021 at GW East out; however, it was not as distinct as the one observed for $\delta^{13}C$-CH_4 values.

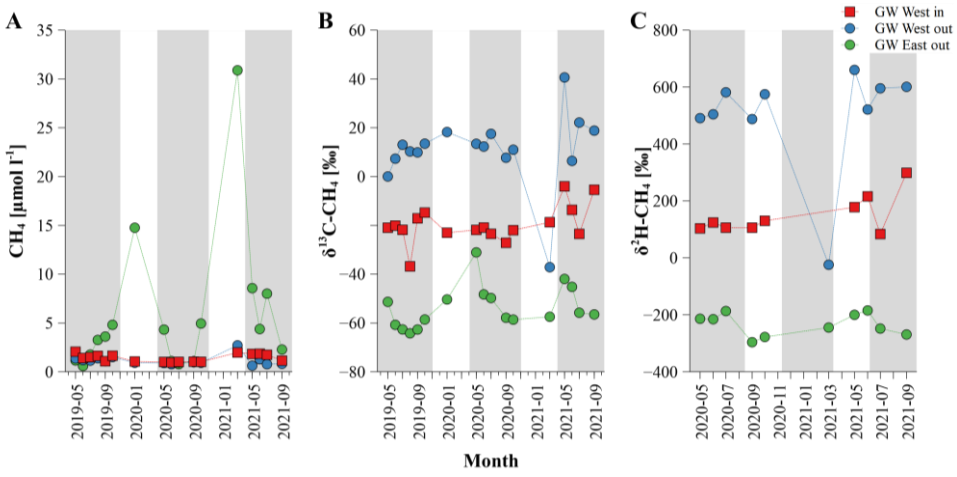

Figure 22. (A) Methane concentrations, (B) $\delta^{13}C$-CH_4 and (C) $\delta^{2}H$-CH_4 values of inflowing groundwater at GW West in (red) as well as outflowing groundwater at GW West out (blue) and GW East out (green) at Lake Willersinnweiher from May 2019 to September 2021. Grey background colours indicate the stratification period and white background colours represent the mixing period.

3.4 Characterisation of methane sources via Δ(2,13) values[6]

Concentration weighted mean Δ(2,13) values were calculated after Tsunogai et al. (2020) using Eq. (25) for dissolved CH_4 in the epilimnion, metalimnion, hypolimnion, sediment and inflowing groundwater at Lake Willersinnweiher for May, July and October 2020 and May 2021 (Figure 23).

In the sediment Δ(2,13) values showed large variabilities based on the sampling site (pelagic, slope or littoral). Highest Δ(2,13) values were observed for the pelagic sediment, where values were in a similar range for May, July and October (415 ± 58 ‰ to 395 ± 39 ‰) but decreased in March (320 ± 76 ‰). At the slope an opposing pattern in Δ(2,13) values was observed as values increased from May to October, yielding values from 293 ± 49 ‰ to 369 ± 17 ‰, respectively. No Δ(2,13) values for sedimentary CH_4 could be determined due to technical issues at the slope site during sampling in March. Δ(2,13) values found at the littoral site were lowest compared to the sedimentary values of the other two sites and showed only minor seasonal changes, thus showing Δ(2,13) values of 203 ± 32 ‰ to 232 ± 65 ‰ between May 2020 and March 2021.

Throughout the sampling period a hypolimnion was only present at the pelagic site. However, the hypolimnion in March 2021 was not anoxic, as observed in the other months but was oxic. Nevertheless, it was characterised by elevated CH_4 concentrations compared to the rest of the water column (Figure 9G). Δ(2,13) values of the hypolimnion overlapped with sedimentary Δ(2,13) values for all investigated months but March 2021, where hypolimnic values were 25 % higher compared to sedimentary ones. Between May and October 2020 hypolimnic Δ(2,13) values were very similar ranging between 415 ± 18 ‰ and 411 ± 15 ‰. However, in March Δ(2,13) values in the bottom water of the lake were higher compared to the previous months accounting for 477 ± 18 ‰.

A metalimnion in the water column of Lake Willersinnweiher was only present at the pelagic and slope site in May and July 2020. Metalimnic Δ(2,13) values decreased from May to July at the pelagic site ranging from 342 ± 12 ‰ to 276 ± 25 ‰, while at the slope site Δ(2,13) values slightly decreased but within their respective errors (311 ± 47 ‰ to 271 ± 40 ‰).

Δ(2,13) values in the epilimnion of Lake Willersinnweiher showed a strong increase at all three sampling sites from May 2020 to March 2021. Thus, epilimnic Δ(2,13) values were in the range of 203 ± 3 ‰ to 381 ± 17 ‰ at the pelagic site, 204 ± 2 ‰ to 359 ± 10 ‰ at the slope site and 183 ± 12 ‰ to 335 ± 9 ‰ at the littoral site. Interestingly, Δ(2,13) values at the littoral site overlapped with values from the littoral sediment for all months except March 2021.

The inflowing groundwater was characterised by similar but slightly increasing Δ(2,13) values during the observation period, ranging from 307 ± 5 ‰ in May 2020 to 335 ± 5 ‰ in October 2020. Due to technical issues the δ^2H-CH_4 value of inflowing groundwater in March 2021 could not be measured. Therefore, its Δ(2,13) value could not be calculated. However, as the $\delta^{13}C$-CH_4 values of October

[6] Please note that parts of this section are taken from Einzmann et al. (2022).

2020 (-23.4 ‰) and March 2021 (-22.0 ‰) were very similar, the Δ(2,13) value of inflowing groundwater was estimated to be similar to the one in October 2020 (335 ± 5 ‰).

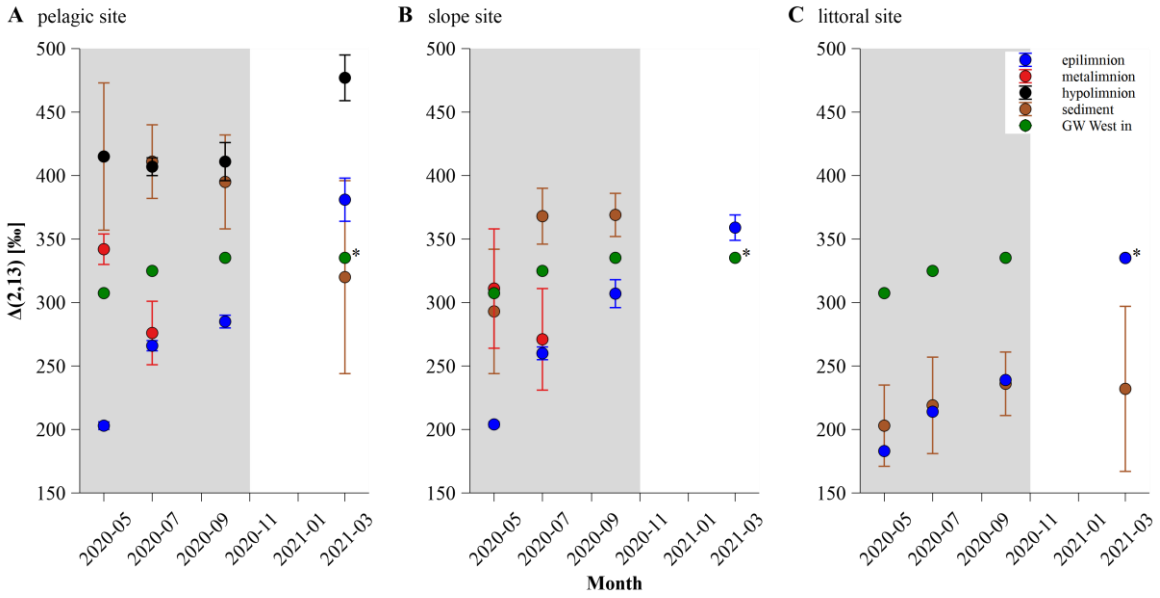

Figure 23. Δ(2,13) values found in the epilimnion (blue), metalimnion (red), hypolimnion (black), sediment (brown) and inflowing groundwater (green) at the (A) pelagic, (B) slope and (C) littoral sites at Lake Willersinnweiher for May, July, October 2020 and March 2021. Δ(2,13) values are shown as concentration-weighted means (n = 3 to 5) with pooled standard deviations. The asterisk indicates that the Δ(2,13) value of GW West in shown for March 2021 is estimated from similar stable carbon isotope values of methane from October 2020. Grey background colours indicate the stratification period and white background colours represent the mixing period.

3.5 Seasonal methane emissions

3.5.1 Diffusion

Diffusion rates of CH_4 at the atmosphere-water interface were measured in the period from August 2019 to September 2021. Methane diffusion rates were determined at the pelagic, slope and littoral sites for each sampled month. In some months diffusion rate data is missing due to technical problems or the trapping of gas bubbles with high CH_4 concentrations that influenced the CH_4 mixing ratio in the headspace of the floating chamber. Samples for the determination of diffusive $\delta^{13}C$-CH_4 and $\delta^{2}H$-CH_4 values of CH_4 emissions were collected between March and September 2021 and calculated applying the Keeling plot method (section 2.3.2).

3.5.1.1 Diffusion rates of methane

Diffusion flux rates of CH_4 measured at Lake Willersinnweiher are shown in Figure 24 and ranged from 0.030 to 0.827 mmol m^{-2} d^{-1}, 0.125 to 0.578 mmol m^{-2} d^{-1} and 0.019 to 0.904 mmol m^{-2} d^{-1} for the pelagic, slope and littoral sites, respectively. Methane diffusion flux rates showed large variations;

however, higher rates during the stratification period compared to the mixing period were determined. The highest diffusion rate was observed at the littoral site in October 2019 accounting for 0.904 mmol m^{-2} d^{-1}, while the smallest rate was found at the littoral site in March 2021 with 0.019 mmol m^{-2} d^{-1}. Methane diffusion rates were highest at the littoral site during late-stage stratification in 2019 and 2020, while they were much smaller compared to diffusion rates at the pelagic and slope site in 2021. Conversely, diffusion rates recorded at the pelagic site in 2021 were usually highest, followed by diffusion rates obtained at the slope site.

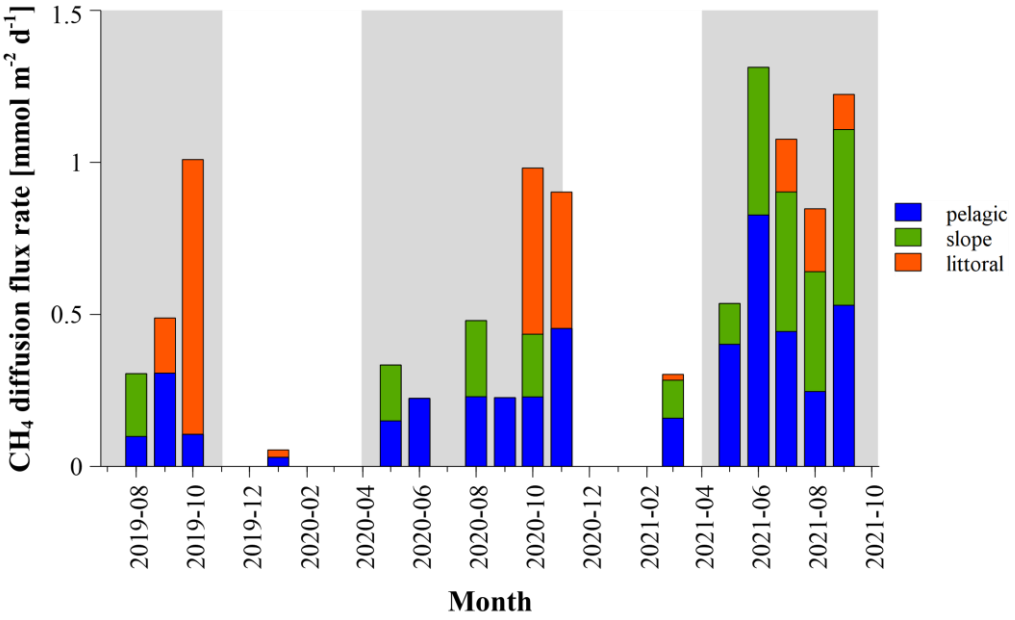

Figure 24. Diffusive CH_4 flux rates at the pelagic (blue), slope (green) and littoral (orange) site of Lake Willersinnweiher from August 2019 to September 2021. Data where diffusive CH_4 flux rates of only one or two site(s) are shown indicate that no flux rate(s) were determined at the missing site(s) due to technical issues. Grey background colours indicate the stratification period and white background colours represent the mixing period.

3.5.1.2 Stable carbon and hydrogen isotope values of methane emitted via diffusion[7]

Methane released via diffusion from the lake at the water-atmosphere interface during the stratification period (May 2021 to September 2021) recorded similar δ^{13}C-CH_4 values at the three sampled sites varying between -52 ‰ and -58 ‰ (Table 4). δ^{2}H-CH_4 values, however, showed higher variations ranging from -195 ‰ to -310 ‰ at the different sites. The highest δ^{2}H-CH_4 values of CH_4 released from the surface water during stratification period were recorded at the littoral site in August 2021 (-195 ± 22 ‰). During the mixing period (March 2021), CH_4 emitted from the lake was significantly enriched in the heavier isotopes compared to the stratification period at all three sites ranging from -36 ‰ to -42 ‰ and δ^{2}H-CH_4 values from 1 ‰ to 26 ‰.

[7] Please note that parts of this section are taken from Einzmann et al. (2022).

Table 4. Stable carbon and hydrogen isotope values of CH_4 released from the lake surface water into atmosphere via diffusion. SDs are given as the standard error of the linear regression using the Keeling plot method (taken from Einzmann et al. (2022)).

Month	Site	$\delta^{13}C\text{-}CH_{4\ diffusion}$ [‰]	$\delta^{2}H\text{-}CH_{4\ diffusion}$ [‰]
March 2021	pelagic	-37 ± 1	1 ± 34
May 2021		-56 ± 1	-
June 2021		-59 ± 1	-310 ± 8
July 2021		-52 ± 1	-208 ± 3
August 2021		-54 ± 1	-250 ± 25
September 2021		-53 ± 1	-271 ± 4
March 2021	slope	-42 ± 1	26
May 2021		-53 ± 2	-
June 2021		-58 ± 1	-306 ± 13
July 2021		-53 ± 2	-205 ± 14
August 2021		-53 ± 1	-
September 2021		-52 ± 1	-220 ± 11
March 2021	littoral	-36 ± 8	-
May 2021		-	-
June 2021		-	-
July 2021		-53 ± 1	-250 ± 14
August 2021		-51 ± 1	-195 ± 22
September 2021		-55 ± 2	-224 ± 4

3.5.2 Ebullition

Concentrations of CH_4 in uprising gas bubbles were measured during field campaigns in November 2020 and September 2021, while ebullition flux rates were determined in November 2020 and May, June, July and August 2021 via inverted funnel traps (section 2.2.7). Methane concentrations of uprising gas bubbles could not be analysed for the pelagic site, as it was not possible to collect gas bubbles at the surface after releasing CH_4 bubbles at the deepest site. Hence, in the rest of this study concentration of ebullitive CH_4 at the pelagic site were assumed to be similar to the ones at the slope site due to similar concentrations and isotopic compositions of CH_4 in the sediment of these two sites. In July 2020 and March 2021 and ebullitive CH_4 could not be collected due to logistical reasons. However, the stratification period is represented by data from September 2021 and the mixing period by data from November 2020.

3.5.2.1 Ebullition rates of methane

Rates of CH_4 emitted by ebullition ranged from 0.002 to 8.83 mmol m^{-2} d^{-1} and were very variable throughout the sampled months at the three sites (Figure 25). Ebullitive CH_4 flux rates were up to 70 times higher during the stratification period when compared to the flux rate obtained during the mixing period in November 2020. Highest ebullitive CH_4 flux rates throughout all sampled months were found at the littoral site during the stratification period ranging from 3.95 to 8.83 mmol m^{-2} d^{-1}. At the pelagic and slope sites, ebullitive CH_4 fluxes were much more variable accounting for 0.130 to 3.78 mmol m^{-2} d^{-1} at the pelagic and 0.300 to 2.77 mmol m^{-2} d^{-1} at the slope site.

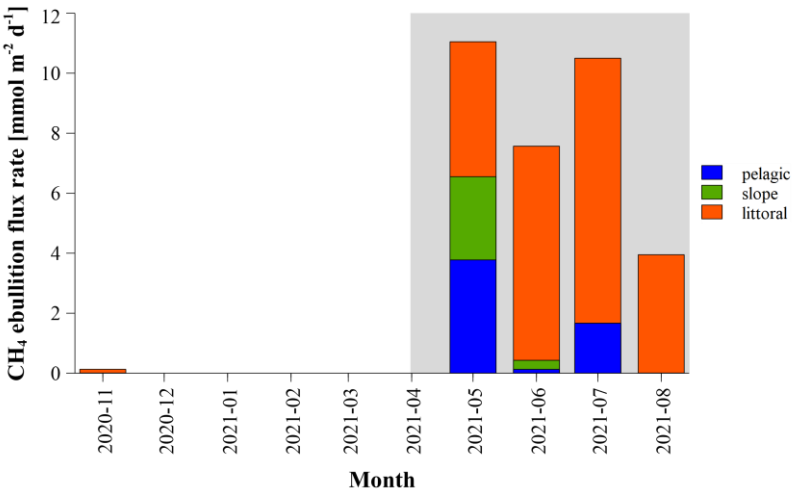

Figure 25. Ebullitive CH_4 flux rates at the pelagic (blue), slope (green) and littoral (orange) sites of Lake Willersinnweiher from November 2020 to September 2021. Grey background colours indicate the stratification period and white background colours represent the mixing period.

3.5.2.2 Concentration and stable isotope composition of ebullitive methane[8]

During the stratification period in September, CH_4 concentrations in uprising gas bubbles reached up to 80.8 ± 4.5 % at the littoral site (Table 5). During mixing period in March 2021, CH_4 concentrations in the gas bubbles were smaller accounting for 62.1 ± 7.4 % at the littoral site and 66.3 ± 1.2 % at the slope site.

Ebullitive $\delta^{13}C$-CH_4 values showed distinct differences between the slope and littoral sites. The most negative $\delta^{13}C$-CH_4 values were found at the slope site in November 2020 (-73.7 ± 1.0 ‰, n = 3). At the littoral site, $\delta^{13}C$-CH_4 values were less negative compared to the slope site. While in November 2020 $\delta^{13}C$-values accounted for -50.0 ± 11.6 ‰ (n = 3), they showed more negative values in September 2021 yielding -58.0 ± 0.3 ‰ (n = 3). Contrastingly, only small differences in the $\delta^{2}H$-CH_4 values of CH_4 released by ebullition were observed. However, $\delta^{2}H$-CH_4 values were slightly more negative at the slope site in November 2020 with values of -317 ± 0.1 ‰ (n = 3) when compared with $\delta^{2}H$-CH_4 values determined for the littoral site with values of -326 ± 4 ‰ for November 2020 and -323 ± 3 ‰ for September 2021.

Table 5. Methane concentrations, $\delta^{13}C$-CH_4 and $\delta^{2}H$-CH_4 values of CH_4 released via ebullition at the slope and littoral sites of Lake Willersinnweiher in November 2020 and at the littoral site in September 2021. Data show mean values with SD (n = 3) (taken from Einzmann et al. (2022)).

Month	Site	CH_4 mixing ratio [%]	$\delta^{13}C$-CH_4 [‰]	$\delta^{2}H$-CH_4 [‰]
November 2020	slope	66.3 ± 1.2	-73.7 ± 1.0	-317 ± 0.1
November 2020	littoral	62.1 ± 7.4	-50 ± 11.6	-326 ± 4
September 2021	littoral	80.8 ± 4.5	-58 ± 0.3	-323 ± 3

[8] Please note that parts of this section are taken from Einzmann et al. (2022).

4 Discussion

4.1 Methane dynamics in the sediment[9]

4.1.1 Anaerobic methanogenesis

The analysis of CH_4 concentrations, $\delta^{13}C$-CH_4 and $\delta^{2}H$-CH_4 values in pore water at the pelagic, slope and littoral sites were carried out in order to determine CH_4 release rates at the sediment-water interface and distinguish between pathways of CH_4 formation via methanogenesis in the anoxic sediment of Lake Willersinnweiher based on their stable isotope composition. Additionally, isotope fractionation factors of carbon between CH_4 and CO_2 were utilized as a tool to differentiate between these different pathways. Generally, two major metabolic pathways are known to be involved in anaerobic methanogenesis in anoxic sediments: acetate fermentation and carbon dioxide reduction via H_2. Acetate fermentation is usually more common in freshwater environments, while CO_2 reduction is the most abundant pathway in marine systems (Whiticar, 2020). Additional to the two major pathways there is also the methylotrophic pathway, where methanogens use e.g., methanol or methylamines as substrates for methanogenesis (Conrad, 2005). However, the contribution of the methylotrophic pathway was evaluated to below 6 % in previous studies (Lovley and Klug, 1983) and thus its contribution to methanogenesis at Lake Willersinnweiher is likely minor and not discussed within this study.

High SO_4^{2-} concentrations of up to 2.5 mmol l^{-1} prevailed in the water column and the upper sediment layers of Lake Willersinnweiher due to the input from SO_4^{2-} rich groundwater. A feature that is rare for freshwater environments. Sulphate in the groundwater originated from pyrite oxidation in the Quaternary river sediments of Rhine, which occurs in the catchment upstream of the lake (Isenbeck-Schröter et al., 2016; Schröder, 2004). Previous studies found that high SO_4^{2-} concentration in the sediment (Figure 9C, G, M, R, W, AB) effectively inhibit methanogenesis, due to the competition for prevailing H_2 as substrate between SRB and methanogenic archaea (Holmer and Storkholm, 2001; Reeburgh, 2007; Schubert et al., 2011). Moreover, decreasing SO_4^{2-} and CH_4 concentrations in the upper part of the sediment indicated the occurrence of SO_4^{2-}-dependent AOM at Lake Willersinnweiher, that effectively limited CH_4 release from the sediment into the water column. (Kleint et al., 2021; section 4.1.2 for further discussion of AOM). Thus, CH_4 concentrations found in the sediment cores of all three sampling sites were usually higher in the lower part of the sediment,

[9] Please note that parts of this section are taken from Einzmann et al. (2022).

where SO_4^{2-} concentrations were low or not present at all (Figure 9B, F, L, O, V, AA). Hence, the below discussed methanogenesis is most likely limited to the lower part of the sediment.

Nevertheless, sediments of Lake Willersinnweiher were found to release CH_4 to the water column all year. At all three investigated sites (pelagic, slope, littoral) a trend towards higher rates was found with succession of the stratification period (Figure 10A, B, C). This increase in CH_4 release rates was most likely caused by elevated temperatures and subsequently higher microbial activities in the sediment in the course of the summer (Natchimuthu et al., 2016). Even though changes in temperature during the observed months were highest in the shallow littoral zone, CH_4 release rates from the sediments were smaller compared to the ones observed at the pelagic site. This observation is in agreement with a recent study by Kleint et al. (2021) and indicates that the conversion of organic matter and thus methanogenesis was more intensive in greater water depths. Furthermore, observed CH_4 release rates at the sediment-water interface were well within the range of rates reported in other studies, e.g., by Schubert et al. (2011) (1.12 mmol m^{-2} d^{-1}) for lake Cadagno, Norði et al. (2013) (1.8 ± 0.2 mmol m^{-2} d^{-1}) for lake Ørn, Bastviken et al. (2004) 3.87 to 5.05 mmol m^{-2} d^{-1} for various northern lakes and (Kelly and Chynoweth (1981) (2.5 to 15.2) mmol m^{-2} d^{-1} for two northern lakes and previous reported rates for Lake Willersinnweiher ranging from 0.04 to 0.96 (Kleint et al., 2021).

Methanogenic pathways can be inferred by utilizing $\delta^{13}C\text{-}CH_4$ and $\delta^{2}H\text{-}CH_4$ values, as CH_4 produced via the acetate formation pathway is usually characterised by $\delta^{13}C\text{-}CH_4$ values between -60 ‰ to -40 ‰ and $\delta^{2}H\text{-}CH_4$ values ranging from -400 ‰ to -250 ‰ (Whiticar, 2020). Based on $\delta^{13}C\text{-}CH_4$ values in the pore water at the pelagic site (Figure 9B, G) CO_2 reduction via H_2 was the predominant pathway of methanogenesis there. In shallower areas of the lake (slope and littoral sites) a shift towards more positive $\delta^{13}C\text{-}CH_4$ values in the lower part of the sediment was apparent. Therefore, CH_4 more enriched in ^{13}C at the shallower sites compared to the pelagic site indicated a shift towards a higher contribution of CH_4 formation from the acetate pathway. Contrary to $\delta^{13}C\text{-}CH_4$ values, $\delta^{2}H\text{-}CH_4$ values were not influenced by the water depth of sampling site and showed similar values at the pelagic, slope and littoral sites. Thus, the measured $\delta^{2}H\text{-}CH_4$ values suggest that they yield only little information about the methanogenic pathway in sediments but might rather depend on $\delta^{2}H$ values of the coexisting source water (not measured in this study; Waldron et al., 1998; Nakagawa et al., 2002; Sugimoto and Wada, 1995).

Additionally, to stable isotope measurements of CH_4, $\alpha_{CO2\text{-}CH4}$ is a useful tool to differentiate between the occurring methanogenic pathways. Calculated $\alpha_{CO2\text{-}CH4}$ values for Lake Willersinnweiher were in the range of 1.062 ± 0.009 to 1.067 ± 0.007 at the pelagic site, 1.055 ± 0.002 to 1.057 ± 0.009 at the slope site and 1.041 ± 0.004 to 1.052 ± 0.001 at the littoral site. These values were well in the range of $\alpha_{CH4\text{-}CO2}$ values reported for different methanogenic cultures ranging from 1.021 to 1.071 for hydrogenotrophic methanogenesis and 1.007 to 1.021 for acetate-dependent methanogenesis (Conrad, 2005).

Moreover, $\alpha_{CH4\text{-}CO2}$ values in the sediment cores of Lake Willersinnweiher showed an increase from the pelagic site (1.062 ± 0.009 to 1.067 ± 0.007) towards shallower littoral site (1.041 ± 0.004 to 1.052 ± 0.001). Similar to sedimentary $\delta^{13}C\text{-}CH_4$ values, this increase in $\alpha_{CH4\text{-}CO2}$ values from the pelagic to the littoral sites indicates a stronger contribution of acetate dependant methanogenesis pathway at shallower sites compared to hydrogenotrophic methanogenesis as the predominant methanogenesis pathway at the deeper pelagic site. Additionally, whether the lake was stratified or completely mixed did not seem to influence observed $\alpha_{CH4\text{-}CO2}$ values, thus inferring that the stratification mode of the lake did not influence prevailing methanogenesis pathways at the respective sites.

However, apart from the methanogenesis, there were various further parameters and processes that potentially influenced the stable isotope composition of CH_4 in the sediment. One factor influencing the $\delta^{13}C\text{-}CH_4$ and $\delta^{2}H\text{-}CH_4$ values of CH_4 from methanogenesis might be the isotopic signature of fresh organic matter input. It is reasonable to assume that organic matter input and conversion varies considerably with water depth. At the littoral site, fresh organic matter from aquatic vegetation and the shore most likely promoted the occurrence of more ^{13}C- and $^{2}H\text{-}CH_4$ enriched CH_4, thus indicating methanogenesis predominantly via the acetate pathway. Whereas at the deeper pelagic and slope sites, organic matter input was likely scarce and consisted of relatively decomposed material which might have been the main driver of a shift towards higher contribution of hydrogenotrophic methanogenesis with greater water depth (Bouchard et al., 2015; Thottathil and Prairie, 2021; Wik et al., 2020).

Less negative $\delta^{13}C\text{-}CH_4$ and $\delta^{2}H\text{-}CH_4$ values at the littoral site compared to the slope and pelagic sites could possibly arise from oxidation at the oxic-anoxic interface through the contact of O_2 rich water masses of the epilimnion with the uppermost sediment layers. Thus, sedimentary CH_4 diffusing upwards in the sediment was likely partially consumed by MOx leading to an enrichment in $^{13}C\text{-}CH_4$ and $^{2}H\text{-}CH_4$ values. This isotopic enrichment, however, could also be caused by SO_4^{2-}-dependent AOM taking place in the upper part of the sediment cores, where high SO_4^{2-} concentrations prevailed (Wegener et al., 2021; Whiticar, 2020; Tsunogai et al., 2020;section 4.1.2 for further discussion about AOM)

Additionally, $\delta^{13}C$- and $\delta^{2}H\text{-}CH_4$ values in the sediment at the littoral site might be more easily influenced by mixing of pore water with lake water, as the littoral sediment is composed of more sandy components compared to the sediment at the pelagic/slope sites which facilitated potential mixing.

4.1.2 Anaerobic methane oxidation - sulphate-methane transition zones

Evidence for the occurrence of CH_4 oxidation in the sediment of Lake Willersinnweiher was found similar to a recent study by Kleint et al. (2021). Due to the anoxic character of the sediment, CH_4 oxidation in the sediment likely took place via AOM through anaerobic methanotrophic archaea (ANME). Due to high prevailing SO_4^{2-} concentrations in Lake Willersinnweiher ANME were presumably associated with SRB leading to decreasing CH_4 and SO_4^{2-} concentrations in the upper sediment (Boetius et al., 2000; Su et al., 2020; Weber et al., 2017). Anaerobic methane oxidation counteracts methanogenesis, which occurs in the lower part of the sediment where SO_4^{2-} concentrations and the activity of SRB are low (section 4.1.1 and references therein). In the upper part of the sediment, methanogenesis was likely inhibited by high SO_4^{2-} concentrations and SRB thermodynamically outcompeting methanogens for available substrates such as H_2 (Holmer and Storkholm, 2001; Reeburgh, 2007; Schubert et al., 2011). Thus, CH_4 diffusion from the sediment into the water column was effectively limited (Bastviken et al., 2002; Kleint et al., 2021; Norði et al., 2013). In this study, CH_4 release from the sediment was thereby reduced by 30 to 90 %, a range that is similar to values recently reported by Hartmann (2018) where a reduction between 60 to 90 % was found.

In the sediment of Lake Willersinnweiher, several parameters indicated the existence of a zone of AOM in the sediment that was observed throughout the whole year. Methane concentration profiles and flux calculations of sediment cores showed that SO_4^{2-} concentrations strongly declined in the pore water of the upper part of the sediment implying the presence of SRB and identifying the sediment as a sink for SO_4^{2-} as also reported by Kleint et al. (2021) (e.g., Figure 9C, H). Simultaneously, CH_4 concentrations also decreased towards the sediment-water interface, thereby strongly indicating SO_4^{2-}-dependent AOM and the existence of SMTZs. Sulphate-methane transition zones are rarely found in freshwater environment due to mostly low prevailing SO_4^{2-} concentrations and have only been described in a few limnic environments including e.g., lake Cadagno (Schubert et al., 2011) and Lake Willersinnweiher Kleint et al. (2021). However, SMTZs are very common in marine environments due to the high SO_4^{2-} concentrations in the ocean (Whiticar, 2020). The conversion of CH_4 via SO_4^{2-}-dependent AOM led to the increase of S^{2-} and DIC concentrations according to Eq. (34). Thus, AOM and other reactions involved in DIC production (indicated by increasing DIC concentrations) due to the conversion of organic matter, DIC was released from the sediment-water interface all year round (Figure 10G, H, I). Furthermore, DIC produced via this reaction then likely led to the formation of carbonates in the upper part of the sediment, which was indicated by coincidingly decreased Ca^{2+} concentrations (e.g., Figure 9E, J; Knittel and Boetius, 2009; Schubert et al., 2011).

$$CH_4 + SO_4^{2-} + Ca^{2+} \rightarrow CaCO_3 + H_2\,S + H_2\,O \quad (34)$$

The increase in DIC concentrations with increased sediment depth was further linked to a shift towards more negative δ^{13}C-DIC values in the zone of the sediment where AOM was present (Fig. 9,

yellow bars). This shift was caused by the preferential oxidation and conversion of lighter ^{12}C-CH_4 by methanogens and subsequent implementation of ^{12}C into DIC leading to more negative $\delta^{13}C$-DIC values (Knittel and Boetius, 2009; Schubert et al., 2011). However, this shift might have also been influenced by remineralization of fresh relatively undecomposed organic matter, which predominantly comprises ^{12}C (Schubert et al., 2011). Below the zone of AOM an increase in $\delta^{13}C$-DIC values was usually observed. This increase probably originated from production of CH_4 via hydrogenotrophic methanogenesis, which led to an enrichment of ^{13}C-DIC in the remaining DIC (Schubert et al., 2011) through the preferred metabolization of ^{12}C-DIC.

Another indication for AOM was examined by the investigation of $\delta^{13}C$-CH_4 and $\delta^{2}H$-CH_4 values of pore water in the sediments. More positive stable isotope values of CH_4 in the SMTZ compared to the rest of the sediment were characterised by an increase of $\delta^{13}C$-CH_4 and $\delta^{2}H$-CH_4 values of up to 25 ‰ and 60 ‰, respectively (Figure 9B, G, L, Q, V, AA). However, in some sediment profiles no increase in $\delta^{13}C$-CH_4 or $\delta^{2}H$-CH_4 values typical for AOM was present. Possible reasons for this observation are: 1) methanogenesis and AOM occurred simultaneously. Thus, if CH_4 production rates were substantially higher compared to AOM rates, this would have resulted in more negative or no change in $\delta^{13}C$-CH_4 and $\delta^{2}H$-CH_4 values. 2) CH_4 with more negative $\delta^{13}C$-CH_4 and ^{2}H-CH_4 values could potentially be converted by ANME and SRB to more depleted ^{13}C-DIC, which again would result in the production of relatively negative $\delta^{13}C$-CH_4 values by methanogens (Su et al., 2020). 3) A carbon isotope equilibrium between CH_4 and CO_2 could be established by microorganisms caused by forward and backward AOM in the SMTZ (Chuang et al., 2019; Yoshinaga et al., 2014). 4) Isotope fractionation factors of carbon and hydrogen during AOM are dependent on prevailing SO_4^{2-} concentrations. Thus, even a depletion in ^{13}C of residual CH_4 ($^{13}\alpha = 0.977$) was reported in laboratory incubations for SO_4^{2-}-dependent AOM and SO_4^{2-} concentrations similar to Lake Willersinnweiher (1.5 mmol l^{-1}). Contrastingly, for higher SO_4^{2-} concentrations an enrichment in ^{13}C of the residual CH_4 was found (10 mmol l^{-1}; $^{13}\alpha = 1.155$) (Wegener et al., 2021).

In the zones of the sediment Lake Willersinnweiher that were characterised by decreasing CH_4 concentrations and increasing $\delta^{13}C$-CH_4 and $\delta^{2}H$-CH_4 values, thus AOM was supposedly present, apparent fractionation factors ranged between 1.000 to 1.087 for $^{13}\alpha$ and 0.980 to 1.460 for $^{2}\alpha$. Isotopic fractionation factors of AOM determined from *in situ* isotopic signatures have to be considered with care since methanogenesis and AOM might coexist and overlap in the sediment. Furthermore, carbon isotope equilibrium effects might in opposite ways affect the isotopic composition of sedimentary CH_4. Nevertheless, isotopic fractionation values determined for Lake Willersinnweiher are in a similar range as previously reported isotopic fractionation factors for other limnic, marine, brackish and lab culture studies. In Lake Cadagno, a freshwater lake, where SO_4^{2-}-dependent AOM and SMTZ was reported, $^{13}\alpha$ values were estimated to be 1.031 (Schubert et al., 2011), while in marine and brackish environments $^{13}\alpha$ and $^{2}\alpha$ values were found to range from 1.009 to 1.024 and 1.120 to 1.157, respectively (Knittel and Boetius, 2009; Whiticar et al., 1986). In lab culture studies, Holler et al.

(2009) found similar fractionation factors compared to Lake Willersinnweiher ranging from 1.012 to 1.039 for $^{13}\alpha$ and 1.109 to 1.315 for $^{2}\alpha$.

Input of SO_4^{2-} rich groundwater from below the lake sediments might be a further factor influencing AOM in Lake Willersinnweiher. Sulphate was completely consumed below the SMTZ. However, in the lowermost depths of the sediment core, an increase of SO_4^{2-} was frequently observed indicating the potential input of SO_4^{2-} by groundwater. Thus, higher SO_4^{2-} concentrations in the lowermost sediment potentially inhibited methanogenesis similarly to the upper part of the sediment where SO_4^{2-} was present. This provided potential for a further zone of AOM in the lowermost part of the sediment.

Besides SO_4^{2-}, a succession of other different compounds (NO_3^-, NO_2^-, Fe^{2+}, Mn^{2+}) can be utilized as terminal electron donors by methanotrophs in order to gain energy from the oxidation of CH_4. At Lake Willersinnweiher, other potential electron donors such as, NO_3^- and Fe^{2+} showed only small concentrations in the pore water compared to SO_4^{2-}. Therefore, their impact was likely negligible, even though thermodynamically these compounds would be preferentially converted (Kleint et al., 2021; Schröder, 2004).

However, Mn^{2+} was abundant in the pore water and determination of fluxes showed that Mn^{2+} was released at the sediment-water interface throughout the year (Figure 10G, H, I). Thus, Mn^{2+} -dependent AOM yields another possibility besides SO_4^{2-}-dependent AOM (Kleint et al., 2021). However, due to the dominance of SO_4^{2-} compared Mn^{2+} concentrations the contribution of Mn^{2+}-dependent AOM was likely subsidiary. Nonetheless, similar to a proposition by Su et al. (2020) for lake Cadagno, Mn^{2+} at lake Willersinnweiher could be potentially involved in SO_4^{2-}-dependent AOM by re-oxidizing reduced sulphur compounds to SO_4^{2-} via the reduction of MnO_2 (Figure 26; Kleint et al., 2021). In past studies this process has also been described for limnic and marine systems, where AOM was coupled to re-oxidation of sulphur compounds via iron(III)-oxide reduction (Chuang et al., 2019; Holmkvist et al., 2011; Norði et al., 2013).

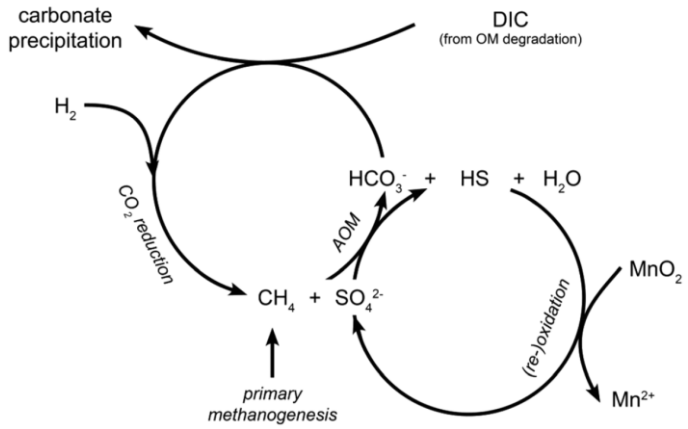

Figure 26. Scheme of the reaction pathways and interaction of carbon, sulphur, and manganese compounds as well as AOM and MOx in the sediment of Lake Willersinnweiher (taken from Kleint et al., 2021).

4.2 Methane dynamics in the water column[10]

4.2.1 Aerobic methane oxidation

Aerobic methane oxidation was a prominent process in the water column of Lake Willersinnweiher throughout the year. It was investigated both via concentration and isotopic measurements in the water column of the pelagic site and incubations experiments with water samples from the pelagic site. Aerobic methane oxidation occurred especially in the metalimnion and was indicated by decreasing CH_4 and O_2 concentrations as well as a concomitant increase in $\delta^{13}C\text{-}CH_4$ and $\delta^{2}H\text{-}CH_4$ values (Figure 17). During stratification period sedimentary CH_4 migrating upwards in the water column was almost completely oxidized at the bottom of the oxycline. Thus, MOx diminished CH_4 fluxes from the anoxic hypolimnion towards the epilimnion, thereby prevented higher contribution of hypolimnic CH_4 to the meta- and epilimnion, and consequently to higher CH_4 fluxes from the surface water layer to the atmosphere (e.g., Reeburgh, 1996; King, 1992).

In the lower metalimnion, strongly enriched $^{13}C\text{-}CH_4$ and $^{2}H\text{-}CH_4$ and low CH_4 concentrations compared to the rest of the water column, clearly implied the presence of MOB and occurring MOx. The shift towards increasing $\delta^{13}C\text{-}CH_4$ and $\delta^{2}H\text{-}CH_4$ values is a result of the preference of MOB to consume the thermodynamically more favourable, lighter $^{12}C\text{-}CH_4$ / $^{1}H\text{-}CH_4$ isotopologues. This process led to the enrichment of the heavier isotopologues $^{13}C\text{-}CH_4$ and $^{2}H\text{-}CH_4$ in the residual CH_4 pool and is therefore characteristic for MOx (e.g., Coleman et al., 1981; Barker and Fritz, 1981).

Thus, carbon (α_C) and hydrogen (α_H) isotopic fractionation factors of 1.009 ± 0.002 and 1.068 ± 0.015 also expressing stable isotope enrichment of $^{13}C\text{-}CH_4$ and $^{2}H\text{-}CH_4$ were determined. While values obtained for α_C were in the same order of magnitude as α_C values determined in experimental studies (1.003-1.039; Templeton et al., 2006), α_H values obtained were substantially lower compared to the ones reported in closed culture studies (1.103-1.325; Coleman et al., 1981). However, stronger isotopic enrichment of ^{2}H compared to ^{13}C ($\approx$ 6 times higher) during MOx at Lake Willersinnweiher was identified by the higher α_H compared α_C values, as also shown in numerous previous studies (e.g., Coleman et al., 1981; Feisthauer et al., 2011).

A further indicator of MOx was the increase of DIC and concomitant decrease in $\delta^{13}C\text{-}DIC$ values (e.g., Figure 9X, AC). Oxidation of CH_4 led to the formation of CO_2, which was mainly converted to HCO_3^- due to pH $\approx$ 7 in these water depths. Since MOB preferably metabolize the lighter $^{12}C\text{-}CH_4$, the resulting DIC showed more negative $\delta^{13}C\text{-}DIC$ values compared to epilimnic DIC. In the hypolimnion, DIC concentrations increased and $\delta^{13}C\text{-}DIC$ decreased further due to DIC released via the remineralization of organic matter at the sediment surface and from sedimentary DIC fluxes that were observed all year at Lake Willersinnweiher.

[10] Please note that parts of this section are taken from Einzmann et al. (2022).

MOx rates determined via incubation experiments demonstrated that MOx occurred throughout the epilimnion and metalimnion during stratification periods. Two profiles of MOx rates determined in July and September 2021 accounted for up to 950 ± 149 nmol l^{-1} d^{-1} and showed an increase towards the oxycline as well as length of the stratification period. An increase of O_2 and CH_4 fluxes towards the oxycline furthermore supported the occurrence of higher MOx rates towards the end of the stratification period (Figure 14B, C). Highest MOx rates in both profiles were furthermore characterised by the most positive $\delta^{13}C$-CH_4 and $\delta^{2}H$-CH_4 values as well as lowest CH_4 concentrations. Compared to MOx rates of other lakes, the ones found at Lake Willersinnweiher are in the upper range (Table 6).

Table 6. Aerobic methane oxidation rates reported for different lakes.

Lake	Aerobic methane oxidation rate [nmol l^{-1} d^{-1}]	Reference
Lake Willersinnweiher	44 ± 5 to 950 ± 149	This study
Lake Biwa	0.33 to 55	Murase and Sugimoto (2005)
Mono Lake	59 to 123	Carini et al. (2005)
Lake Gek-Gel	18 to 25	Pimenov et al. (2010)
Lake Rotsee	5000	Schubert et al. (2010)
Lake Rotsee	15 to 146	Oswald et al. (2015)
Lake Stechlin	89 to 103	Tang et al. (2016)
Five northern lakes	10 to 540	Thottathil et al. (2019)

The occurrence of MOx in the water column was dependent on several factors. The observation that highest MOx rates were found at the chemocline suggests that MOB were most active at low O_2 levels and that their presence was restricted by higher O_2 concentrations in the upper water body (Rudd et al., 1976). Apart from O_2 concentration, the light availability in the photic zone was shown to be another controlling factor of MOx. Murase and Sugimoto (2005) found that MOx was inhibited under light conditions, which might explain the observation of lower MOx rates determined for lower water depths at Lake Willersinnweiher (Figure 17). Opposingly, Oswald et al. (2015) linked MOx to photosynthesis driven O_2 production and therefore also reported a light dependency of MOx. Moreover, in contrast to methanogenesis, MOx was also found to be rather insensitive to temperature (Sepulveda-Jauregui et al., 2018).

Interestingly, during the mixing period, the whole water body of Lake Willersinnweiher was characterised by low CH_4 concentrations (between 0.05 µmol l^{-1} to 0.07 µmol l^{-1}) compared to the stratification periods. Isotope values, strongly enriched in ^{13}C-CH_4 and ^{2}H-CH_4 (ranging from -30 ‰ to -42 ‰ and -40 ‰ to +20 ‰, respectively) indicated extensive MOx, but O_2 concentrations were high and in equilibrium with the atmosphere. Furthermore, MOx rates of 140 nmol l^{-1} were determined at a depth of 7 m during March 2021 showing that MOx was present in the water column, even though

O_2 concentrations were high, thus challenging the previously discussed O_2 sensitivity of MOx. Due to the lack of MOx rates determined in the upper water column during the stratification period it is hard to assess the potential role of light driven inhibition of MOx. However, based on the determination of MOx rates during mixing period light dependent inhibition of MOx seemed more plausible at Lake Willersinnweiher than O_2-dependent MOx inhibition. Nevertheless, more detailed research in the future is needed to assess potential inhibitions of MOx at Lake Willersinnweiher. Compared to the MOx rates during the stratification period the rates during the mixing period (at the corresponding depths) were smaller but still in the range of MOx rates discussed above.

Even though MOx was present during the mixing period, CH_4 was still supersaturated in the whole water column, thus indicating one or more CH_4 sources contributing to dissolved CH_4 concentrations. Potential CH_4 sources during mixing period include diffusion from the sediment and inflowing groundwater. Interestingly, CH_4 input from groundwater was characterised by high concentrations ($\approx$ 1 to 2 µmol l^{-1}) and unusually positive $\delta^{13}C$-CH_4 and $\delta^{2}H$-CH_4 values (-36.8 ‰ to -4.01 ‰ and +83 ‰ to +185 ‰, respectively) reported only for few other groundwater systems (Schloemer et al., 2016). Thus, groundwater input in addition to MOx might have also significantly contributed to CH_4 concentration dynamics and its stable isotope composition in the water column of Lake Willersinnweiher during the mixing period.

4.2.2 Oxic methane production and potential precursor compounds

Oxic methane production in oxygenated water layers has been reported in numerous studies despite the long-standing paradigm that methanogenesis only occurs under anaerobic conditions (e.g., Grossart et al., 2011; Donis et al., 2017; Günthel et al., 2019, 2020; Hartmann et al., 2020; Bižić et al., 2020a; Klintzsch et al., 2019; Lenhart et al., 2016; León-Palmero et al., 2020). Thus, OMP might play an important factor for CH_4 emissions of limnic and marine systems, because CH_4 produced in the oxic water column is produced near the water surface and thus potentially circumvents MOx in the water column of lakes (Hartmann et al., 2020; Tang et al., 2016). Oxic methane production is associated with CH_4 formation from inter alia algae and cyanobacteria in freshwater and marine environments and therefore coupling of OMP and primary production has been proposed in several studies (Bogard et al., 2014; Grossart et al., 2011; Hartmann et al., 2020; Klintzsch et al., 2019; Lenhart et al., 2016; León-Palmero et al., 2020; Morana et al., 2020; Wang et al., 2017, 2021).

Interestingly, a local CH_4 concentration peak that was frequently observed in the upper metalimnion of Lake Willersinnweiher usually coincided with a peak in Chl-a, also indicating a linkage between CH_4 production and phytoplankton activity (Figure 9A, B and Figure 11D). Nevertheless, local CH_4 peaks in the upper metalimnion could also be caused by physical processes such as lateral transport from CH_4 from the littoral area (Donis et al., 2017). Furthermore, density flows generated by differential cooling of the lake water, meaning that water from shallower areas of the lake cools faster than the

water masses at the pelagic areas might lead to a mixture of water masses from the shallower and deeper part of the lake and therefore contribute to the formation of local CH_4 peaks in the upper metalimnion (Doda et al., 2022).

Therefore, due to the multiple possible pathways contributing to CH_4 concentrations in the epilimnion of lakes, a mass balance approach was applied in order to disentangle these different CH_4 sources and evaluate the occurrence of CH_4 production in this water layer. Hence, CH_4 production rates in the epilimnion of Lake Willersinnweiher were estimated via a mass balance approach similar to Donis et al. (2017) and Günthel et al. (2019), considering steady-state conditions. Methane production rates in the epilimnion accounted for 47 ± 27 to 129 ± 36 nmol l^{-1} d^{-1} at the beginning (May 2020) and end of stratification season (October 2020), while no CH_4 production was clearly obvious when stratification was most strongly developed and during the mixing period (Figure 14). The estimated CH_4 production rates are in accordance with previously reported ones for Lake Willersinnweiher (65 ± 50 to 280 ± 200 nmol l^{-1} d^{-1}; Hartmann, 2018), but also other lakes (Table 7). As no methods for directly measuring OMP rates exist as of yet, mass balances are an important approach to estimate OMP in lakes. However, large uncertainties still prevail in the mass balance derived estimations of OMP, due to the complex interplay of CH_4 sources and sinks in limnic systems. Nevertheless, further research about the spatial and temporal variations of CH_4 sources and sinks will reduce these uncertainties in future studies. The mass balance approach combined with further evidence (precursor compounds of OMP; discussed below), strongly suggested that CH_4 production in the oxygenated water layer occurred at least seasonally and might have played an important role in the CH_4 cycle of Lake Willersinnweiher. However, even though estimations of CH_4 production in the surface water of various lakes were found, there is still a lack of knowledge about the mechanisms and processes underlying this CH_4 production and involved processes might vary substantially between different lakes and/or aquatic systems.

Table 7. Rates of OMP reported for different lakes.

Lake	Methane production rate [nmol l^{-1} d^{-1}]	Reference
Lake Willersinnweiher	47 ± 27 to 129 ± 36	This study
Lake Willersinnweiher	65 ± 50 to 280 ± 200	Hartmann (2018)
Lake Stechlin	38 to 210	Grossart et al. (2011), Günthel et al. (2019), Hartmann et al. (2020)
Lake Cromwell	210 to 240	Bogard et al. (2014)
Lake Hallwil	110	Donis et al. (2017)
Yellowstone Lake	0.2 to 0.7	Wang et al. (2017)
Lake Bonney	54 to 257	Li et al. (2020)

To better understand the mechanisms and processes involved OMP, stable isotope analysis and characterisation constitute an important tool to potentially distinguish between CH_4 originating from OMP or other sources such as anoxic methanogenesis.

At Lake Willersinnweiher $\delta^{13}C\text{-}CH_4$ values in the upper metalimnion, which were characterised by a local CH_4 and Chl-a peak during stratification period ranged from -40 ‰ to -48 ‰ (Figure 13). Hence, CH_4 there was enriched in ^{13}C compared to CH_4 originating from anoxic methanogenesis. Similar observations were made in several other lakes, e.g., Lake Stechlin (-49 ‰ to 52 ‰, Hartmann et al., 2020), Lake Cromwell (-40 ‰, Bogard et al., 2014), Lake Hallwil (-60 ‰, Donis et al., 2017) and Lake Biwa (-50 ‰, Tsunogai et al., 2020), which all showed CH_4 enriched in ^{13}C in the oxygenated water column compared to sedimentary CH_4. The isotopic source signatures of CH_4 produced in the oxygenated water column, e.g., via phytoplankton might therefore give important insight about the possible contribution of OMP to surface CH_4 supersaturation. However, for limnic systems, no data for the stable isotopic source signatures of $\delta^{13}C\text{-}CH_4$ and $\delta^{2}H\text{-}CH_4$ values of OMP are available yet. However, recently Klintzsch (2021) reported that $\delta^{13}C\text{-}CH_4$ values of CH_4 produced by three marine algae were in the range of -43.2 ‰ to -21.6 ‰. If similar $\delta^{13}C\text{-}CH_4$ and $\delta^{2}H\text{-}CH_4$ values prevailed for CH_4 produced by limnic phytoplankton, contribution of OMP to the epilimnic CH_4 pool might at least partially explain the observed CH_4 enriched in ^{13}C in various lakes. Therefore, in future studies, the investigation of the isotopic source signatures of CH_4 produced via OMP might become a crucial tool in distinguishing this source from other CH_4 sources. However, the observed stable isotope composition of CH_4 in the water column might also be influenced by enrichment of $^{13}C\text{-}CH_4$ and $^{2}H\text{-}CH_4$ due to MOx (Donis et al., 2017). Thus, in future studies, incubation experiments in which MOx is inhibited might give further insight into the origin of isotopic enrichment of CH_4 in the upper metalimnion of lakes.

In order to identify precursor compounds of CH_4 potentially contributing to OMP in Lake Willersinnweiher, incubation experiments of lake water with the addition of ^{13}C- and ^{2}H-labelled compounds were conducted (section 3.2.7). Due to the association of OMP with phytoplankton in previous studies, lake water was chosen that exhibited the highest Chl-a concentrations and was characterised by a local CH_4 peak. The addition of ^{13}C-labelled MPn, ^{2}H-labelled MA and MET resulted in a strong increase in the $\delta^{13}C\text{-}CH_4$ and $\delta^{2}H\text{-}CH_4$ values in the water samples. This showed that the isotopically labelled methyl groups of these compounds were converted to CH_4. Hence, MPn, MA and MET were identified as potentially important precursor compounds contributing to OMP at Lake Willersinnweiher. The quantitative contribution of these compounds to CH_4 in the oxic water column of Lake Willersinnweiher, however, remains unknown, as the concentration of these compounds in the lake water could not be analysed in the scope of this study. The increase in $\delta^{13}C\text{-}CH_4$ or $\delta^{2}H\text{-}CH_4$ values during the incubation experiments suggested that 1.7 % of the added ^{13}C-MPn and less than 0.001% of added ^{2}H-MA, and ^{2}H-MET, respectively, were converted to $^{13}C\text{-}CH_4$/ $^{2}H\text{-}CH_4$. Supplementing ^{2}H-labelled TMA to lake water samples did not cause an increase in

the water samples and hence was not considered to be a potential precursor compound of CH_4 in the oxic water column of Lake Willersinnweiher. In the scope of the incubation experiment also water samples filtered through a 0.2 µm pore size filter and supplemented with ^{13}C- or ^{2}H-labelled substances, were investigated. In these filtered water samples similar to the controls, no formation of ^{13}C-CH_4 and ^{2}H-CH_4 was detected. Therefore, the formation of CH_4 in the water samples of Lake Willersinnweiher was attributed to prevailing phytoplankton and microorganisms, thus providing further evidence for the possible linkage between OMP and phytoplankton. In the following paragraphs the investigated precursor compounds of OMP are discussed.

MPn has been linked to OMP and supersaturation of the oxygenated water column in limnic and marine environments by several studies (Karl and Tilbrook, 1994; Khatun et al., 2019; Repeta et al., 2016; Wang et al., 2017). Methane is formed from MPn via the microbial cleavage of the C-P bond resulting in the dissociation of the methyl group from MPn (Kamat et al., 2013). However, CH_4 is merely a by-product, as microorganisms probably developed this mechanism in order to release phosphorous from MPn since it is often the limiting nutrient in aquatic environments (Dyhrman et al., 2009). In the freshwater environment genes for the C-P lyase pathway have been detected in heterotrophic bacteria and cyanobacteria (Kutovaya et al., 2013; Wang et al., 2017; Yao et al., 2016), but these genes are only expressed under phosphorous limited conditions. Moreover, the degradation of MPn might not only lead to the formation of CH_4 but also other compounds such as formate (Sosa et al., 2019). In incubation experiments with water from the oxygenated water column of lake Stechlin Grossart et al. (2011) reported no increase in CH_4 production rates when MPn was added. On the contrary, CH_4 production rates were enhanced when MPn was supplemented in similar experiments by (Bižić-Ionescu et al., 2018) suggesting that MPn constituted a potential source of CH_4 in lake Stechlin. These conflicting observations might be caused by the differences in the availability of phosphorous between the two incubation experiments; however exact reasons for this disparity remain unknown. Phosphorous limiting conditions in the oxic water column also prevailed in Lake Willersinnweiher (Table A 5). In the environment MPn is known to be produced in marine and limnic systems by archaea and bacteria (Ju et al., 2015; Metcalf et al., 2012; White and Metcalf, 2007). Therefore, CH_4 formation via MPn might be an occurring pathway in the lake. However, due to the lack of knowledge about the microbial occurrences and natural abundance concentrations of MPn in the water column of Lake Willersinnweiher an evaluation of the importance of this CH_4 formation pathways is not possible and demands more detailed investigations in the future studies.

The second group of investigated precursor compounds were the methylamines MA and TMA. Methylamines are frequently abundant in aquatic systems (Cai et al., 2003; Gibb et al., 1999; Osadchyy et al., 2016; Sun et al., 2019) as they are formed during degradation of organic matter of inter alia algae and cyanobacteria, and concentrations of up to 180 mg l^{-1} were found in proximity to phytoplankton blooms (de Angelis and Lee, 1994; Herrmann and Jüttner, 1977; Osadchyy et al., 2016; Rolle et al., 1977). Traditionally, methylamines have been associated with CH_4 production by anoxic

methanogenesis, e.g., in the lake sediments (Conrad, 2005). However, more recently they were also linked to OMP in the oxygenated water layers of different lakes (Bižić-Ionescu et al., 2018; Tang et al., 2016; Wang et al., 2021). According to Tang et al. (2016), non-methanogenic bacteria possess all genes necessary for the conversion of methylamines to CH_4. In laboratory investigations at lake Stechlin CH_4 production from TMA was detected in the scope of incubation experiments conducted with lake water enrichment cultures that were supplemented with the TMA (Bižić-Ionescu et al., 2018). As no methanogens were found in their experiment, their results strongly indicated that the produced CH_4 derived from the conversion of TMA via a non-archaeal pathway. Apart from TMA, incubation experiments conducted by Wang et al. (2021) found evidence for the microbiological conversion of MA to CH_4. Similar to the isotope labelling experiment in this study (section 3.2.7), water samples from Yellowstone Lake were supplemented with ^{13}C-labelled MA, which led to the formation of ^{13}C-CH_4. Furthermore, Wang et al. (2021) identified a proteome and gene involved in OMP via MA. Thus, the pathway of CH_4 formation via methylamines presents another possibility of CH_4 production in oxygenated waters, which could be potentially relevant and widespread across aquatic environments, especially in association with algal blooms. However, the occurrence of this pathway might also be dependent on the presence of the respective microbial communities, which might therefore be the reason for the observed CH_4 formation via MA but not TMA within this study (Bižić-Ionescu et al., 2018; Wang et al., 2021). More detailed research concerning the microbial communities at Lake Willersinnweiher might therefore yield further insight into the importance of methylamines as potential precursor compounds at Lake Willersinnweiher.

Another potential precursor compound of CH_4 formation by eukaryotes and procaryotes is MET, which has been shown for plants, marine algae, fungi (Lenhart et al., 2012, 2015, 2016), and marine and limnic cyanobacteria (Klintzsch, 2021). Furthermore, supplementation of ^{13}C-labelled MET to water samples of a tropical lake led to an increase in δ^{13}C-CH_4 values, thus implying the that the methyl group of MET was converted of CH_4 in this lake (Morana et al., 2020). Methionine is an essential amino acid and therefore a ubiquitous compound in the environment and organisms. Additionally, MET is a precursor of several methylated sulphur compounds such as dimethyl sulphoxide (DMSO), dimethyl sulphide (DMS), methyl sulphoxide (MSO) and methanethiol in the marine environment, and to a lower extent also in freshwater systems (Damm et al., 2010; Gage et al., 1997; Steinke et al., 2018; Summers et al., 1998).

In recent studies, methylated nitrogen (methylamines) and sulphur (e.g., MET) compounds have been identified as potential precursor compounds of CH_4 formation in bacteria, cyanobacteria, and algae (Bižić-Ionescu et al., 2018; Klintzsch, 2021; Lenhart et al., 2016; Wang et al., 2021). A possible mechanism of CH_4 formation from methylamines and MET was described by Althoff et al. (2014) and Benzing et al. (2017). The authors detected CH_4 formation from methyl ethers, sulphoxides and methylamines in chemical reactions catalysed by non-hem iron oxo (IV) species. Non-heme

iron oxo (IV) species are the catalytic centre of many enzymes, hence this pathway might exist similarly in living cells and thus possibly also occurs in non-archaeal bacteria or phytoplankton.

Just recently, Ernst et al. (2022) proposed another reaction mechanism for CH_4 formation that might occur across all living organisms. Methylated nitrogen und sulphur compounds react with ROS and free iron on a cellular level to form CH_4. Moreover, when higher levels of oxidative stress were applied to the investigated organisms, higher CH_4 formation rates were detected. Interestingly, elevated CH_4 formation under increased oxidative stress (indicated by increased light intensities compared to the dark) was also shown for three marine algal species (Klintzsch et al., 2020) and during incubation experiments of lake water with supplemented MET (Morana et al., 2020). This indicates that the mechanism proposed by Ernst et al. (2022) might be involved in the CH_4 production by aquatic organisms and likely, at least partially, controls CH_4 formation, along with light intensity and other physiological and environmental factors.

4.2.3 Groundwater

Inflowing groundwater that was characterised by high CH_4 concentrations (0.95 to 2.06 µmol l^{-1}) and unusually and rarely observed positive $\delta^{13}C\text{-}CH_4$ and $\delta^{2}H\text{-}CH_4$ values (-36.8 ‰ and -4.01 ‰ and +83 ‰ to +185 ‰, respectively) constituted another potentially important contributor to CH_4 supersaturation in the water column of Lake Willersinnweiher (Schloemer et al., 2016). In previous studies groundwater inflow rates were found to range between 530 m^3 d^{-1} and 970 m^3 d^{-1} (Kluge et al., 2007; Wollschläger et al., 2007). Kluge et al. (2007) reported that up to 60 % of groundwater infiltrates into the epilimnion of Lake Willersinnweiher, and, therefore, CH_4-rich groundwater contributes both to the CH_4 concentration in the epilimnion as well as the $\delta^{13}C\text{-}CH_4$ and $\delta^{2}H\text{-}CH_4$ values observed in surface waters. Furthermore, beyond adding CH_4 to the water column of Lake Willersinnweiher, inflowing groundwater was characterised by SO_4^{2-} concentrations of around 2.5 mmol l^{-1} (Figure 21A) and therefore provides SO_4^{2-} for AOM in the sediment (Kleint et al., 2021).

The origin of CH_4 in the groundwater however is uncertain. For a detailed overview of potential pathways and accumulation of CH_4 in groundwater flowing into Willersinnweiher please refer to the study by Kleint et al. (2021). Briefly, pathways contributing to the observed CH_4 characteristics of inflowing groundwater include (1) diffusion from deeper aquifers, where CH_4 likely originates from thermogenic origin or sediments containing lignite, (2) methanogenesis in the sediments of dead stream branches, (3) surface infiltration of CH_4 rich water from an open nearby gravel pit and (4) anoxic methanogenesis in the littoral sediments of upstream lakes and subsequent infiltration into the aquifer via the porous sediment (Wollschläger et al., 2007).

However, the positive $\delta^{13}C\text{-}CH_4$ and $\delta^{2}H\text{-}CH_4$ values of the inflowing groundwater suggested that intense AOM, e.g., via SO_4^{2-}, NO_3^-, Fe^{2+} or Mn^{2+} occurred, as no O_2 was present in the groundwater (Kleint et al., 2021). Nevertheless, above-mentioned terminal electron acceptors show very low

concentrations with only small variations in the range of a few µmol l^{-1} in the inflowing groundwater, except for SO_4^{2-} (Figure 21A). Hence, if the above-mentioned electron acceptors were present upstream of the inflowing groundwater at Lake Willersinnweiher, they could potentially have been consumed in the course of AOM leading to an extreme enrichment of ^{13}C- and ^{2}H in the remaining CH_4 pool.

Outflowing groundwater at GW East out showed strong variations of CH_4 and SO_4^{2-} concentrations compared to GW West out (Figure 5C). Interestingly, water sampled at GW East out was characterised by CH_4 concentrations that were usually much higher (up to 30 times). Beyond that, more negative $\delta^{13}C$-CH_4 and $\delta^{2}H$-CH_4 values compared to the other outflowing groundwater well with isotopic signatures similar to sedimentary CH_4 with average $\delta^{13}C$-CH_4 values of -53.5 ‰ and $\delta^{2}H$-CH_4 values of -233 ‰, prevailed. The reason for the disparity between the two outflowing groundwater wells is unclear. However, it seems likely that groundwater at GW East out is more influenced by infiltration of CH_4 from the sediments, compared to GW West out, as due to the flow direction, groundwater passes only a small part of the lake before reaching GW West out, but passes all of Lake Willersinnweiher before reaching GW East out. Another possibility for the differences between both outflowing groundwater wells could constitute another groundwater source at the north-eastern basin. This which could influence the observed variabilities of CH_4 and SO_4^{2-} concentrations at GW East out and also affect the CH_4 input in the north-eastern part of Lake Willersinnweiher. However, this question could not be investigated in the scope of this study. Thus, future investigations about the origin of groundwater and its complex interplay between sediment and water column chemistry as well as influence on the CH_4 cycle are desirable.

4.3 Seasonal and spatial supersaturation of methane in the epilimnion[11]

In this chapter, the previously discussed CH_4 sources and sinks at Lake Willersinnweiher are brought together in order to discuss the CH_4 cycle at Lake Willersinnweiher as a whole. An overview of CH_4 fluxes obtained from Lake Willersinnweiher during the stratification (July 2020) and the mixing period (March 2021) are shown in Figure 27. In Lake Willersinnweiher surface CH_4 concentrations ranged from 0.1 to 1.6 µmol l^{-1} during the stratification periods and 0.05 to 0.07 µmol l^{-1} during the mixing periods (Figure 13A). This showed an oversaturation of CH_4 of up to ≈ 500 times compared to equilibrium with the atmosphere (0.003 µmol l^{-1}; Wiesenburg and Guinasso, 1979) and revealed Lake Willersinnweiher as a constant source of CH_4 to the atmosphere.

As CH_4 was constantly released from the water column into the atmosphere, there was a need for CH_4 inputs into the water column in order to sustain CH_4 supersaturation or explain the increase of CH_4 concentrations during the stratification periods. Furthermore, MOx constituted another sink of CH_4 in the water column that efficiently oxidized a major part of CH_4 migrating upward from the anoxic

[11] Please note that parts of this section are taken from Einzmann et al. (2022).

hypolimnion. However, MOx was likely inhibited by fully oxygenated conditions and/or by influence of light and which therefore enabled accumulation of CH_4 in the epilimnion (section 4.2.1 for a more detailed discussion about MOx; Murase and Sugimoto, 2005; Oswald et al., 2015; Rudd et al., 1976).

At Lake Willersinnweiher, several CH_4 sources must be considered which might contribute to CH_4 supersaturation in the epilimnion including littoral transport, dissolution of gas bubbles from ebullition, groundwater, and internal OMP.

Littoral input of CH_4 can be an important process in small lakes with organic rich sediments. Methane from anoxic methanogenesis can be distributed in the whole epilimnion e.g., by wind activity or wave induced release from sediments, as fluxes from littoral sediments are not decoupled from surface water by stratification (Hofmann et al., 2010; Loken et al., 2019; Tang et al., 2014). The littoral areas at Lake Willersinnweiher most probably contributed to surface CH_4 supersaturation by physical transport, as at the littoral site CH_4 concentrations at the water surface were usually higher compared to the deeper sites during nearly all investigated months (Figure 16). Furthermore, dissolution of uprising gas bubbles into the water column might comprise another important source of CH_4 contributing to the epilimnic CH_4 concentrations, especially in littoral areas, where ebullition fluxes were usually higher compared to deeper sites (McGinnis et al., 2006). Please note, that within the scope of this study data about bubble size and velocity of the uprising bubbles could not be obtained and, therefore, only the impact of bubble dissolution was assumed to account for 10 % of ebullitive fluxes. Even though ebullition was found to show high spatial and temporal variations in previous studies (section 4.4 for a more detailed discussion about ebullition; e.g., West et al., 2016; Thottathil and Prairie, 2021), bubble dissolution might be an important CH_4 source in the upper water column at Lake Willersinnweiher based on the observed CH_4 flux rates via ebullition. Assuming the above-mentioned assumptions bubble dissolution fluxes were in the range of 0.01 to 0.88 mmol m^{-2} d^{-1} for littoral areas, implying the potential to significantly contribute to surface CH_4 concentrations, especially during the stratification periods, where distinctively higher ebullition rates were observed compared to the mixing period (Figure 25).

In the following the spatial distribution of CH_4 in a depth of 1 m in Lake Willersinnweiher was analysed in several months during the stratification and the mixing period (Figure 15). Besides the differences in CH_4 concentrations between the stationary littoral, slope and pelagic sites (Figure 16), analysing the spatial distribution of CH_4 in the surface water of the whole lake has the potential to give further information about the transport of CH_4 from the shallower to the deeper areas of the lake. Methane concentrations in the surface water of Lake Willersinnweiher showed large concentration differences between the south-western and north-eastern basin in most observed months (up to 1 µmol l^{-1}). At the south-western basin, CH_4 concentrations were usually smaller compared to the north-eastern basin. In most months a relatively strong gradient in CH_4 concentrations of the surface water from the south-western to the north-eastern basin was present, while in May and June 2021 (Figure 15M, P) spatial CH_4 differences seemed to origin rather from local CH_4 sources. Surprisingly,

CH_4 concentrations in the shallower areas of the lake and closer to the shore were not significantly higher compared to those in the pelagic areas of the lake. Thus, contradicting the results of the stationary sites, which clearly showed higher CH_4 concentrations at the littoral site throughout the year (Figure 15 and Figure 16). However, in all analysed spatial distribution profiles of CH_4 a tendency towards a few rather punctual spots characterised by enhanced CH_4 concentrations in shallow the areas of the northern shore of the lake, as well as in the narrower elongated most north-eastern part of the lake were observed. Thus, suggesting that the input of CH_4 from littoral areas of the lake are also subject to spatial and temporal variations.

While spatial differences in the CH_4 concentrations were lowest during the mixing period in March 2021 ($\approx$ 0.01 µmol l^{-1}), highest spatial differences were detected in June 2021 where differences accounted for up to 1 µmol l^{-1}. The exact reasons for these spatial disparities of CH_4 concentrations are currently not clear, however the following hypotheses might play a role in this observation.

The higher difference of surface CH_4 concentrations during the stratification period compared to the mixing period in March 2021 were likely caused by higher activity of methanogenesis due to higher temperatures (Duc et al., 2010; Kelly and Chynoweth, 1981) and thereby higher CH_4 fluxes from the littoral areas of the lake. Furthermore, higher dissolution rates of ebullitive CH_4 during the stratification period compared to the mixing period could have contributed to higher spatial disparities of surface CH_4. Ebullition in particular, was found to strongly vary both temporally and spatially and might have therefore contributed to observed spatial differences in dissolved CH_4. However, the epilimnion showed isotopic values enriched in ^{13}C and ^{2}H compared to the gas bubbles ($\delta^{13}C$-CH_4 of -56 ‰ and $\delta^{2}H$-CH_4 of -270 ‰ for lake surface water and $\delta^{13}C$-CH_4 of -73 ± 1.0 ‰ and $\delta^{2}H$-CH_4 of -318 ± 1 ‰ for ebullitive CH_4). Therefore, ebullition was likely not the main source of surface water CH_4 supersaturation in the pelagic area of the lake.

Moreover, the wind speed and wind direction might play an important factor in the distribution of CH_4 at Lake Willersinnweiher. Higher wind speeds cause higher diffusion fluxes of CH_4 from the water column to the atmosphere by generating turbulences in the surface water (Read et al., 2012). Therefore, higher diffusion fluxes led to lower CH_4 concentrations in the surface water of the lake that were prone to higher wind speeds compared to areas that are more wind-protected. Beyond this, the direction of the wind might also alter surface CH_4 concentrations solely by controlling the physical transport of water masses to certain areas of the lake (Murase et al., 2005; Peeters et al., 2019). Interestingly, wind directions at Lake Willersinnweiher originated usually from south or south-west (Figure 15), thus providing another potential reason for the observed enrichment in CH_4 concentrations in the north-eastern basin compared to the south-western basin. When the wind direction originated from the east and the north in June and July 2021, respectively, CH_4 was more evenly distributed compared to the other months when the wind originated from south or south-west. Furthermore, the shape of the lake with its narrower north-eastern part might also be responsible for higher CH_4 concentrations in this part due to restricted mixing with the rest of Lake Willersinnweihers

water body and characterised by a higher ratio of sediment area to water volume compared to the rest of the lake. In conclusion, littoral input of CH_4 to the epilimnion at Lake Willersinnweiher was indicated by higher CH_4 concentrations measured at the stationary littoral site compared to the pelagic site. Nevertheless, the exact reasons for the observed differences in the spatial CH_4 distribution are not clear as of yet. However, the spatial distribution of CH_4 concentrations compiled in the surface water during several months implied that the predominant factor in the distribution of CH_4 in the epilimnion might have been the wind direction and subsidiary factors comprised the distance to the shore and water depth.

Another source of CH_4 at Lake Willersinnweiher was inflowing groundwater with CH_4 concentrations ranging between 0.95 to 2.06 µmol l^{-1}. Moreover, inflowing groundwater was characterised by unusually and rarely observed positive $\delta^{13}C$-CH_4 and $\delta^{2}H$-CH_4 values (-36.8 and -4.01 ‰ and +83 to +185 ‰, respectively). Compared to previously discussed CH_4 sources input of CH_4 from groundwater was not subject to a strong seasonality and therefore constantly transported CH_4 into the water column of Lake Willersinnweiher. In previous studies groundwater inflow rates at Lake Willersinnweiher were found to range between 530 to 970 m^3 d^{-1} (Kluge et al., 2007; Wollschläger et al., 2007). Kluge et al. (2007) reported that up to 60 % of groundwater infiltrates into the epilimnion of Lake Willersinnweiher, and therefore CH_4-rich groundwater contributes both to the CH_4 concentration in the epilimnion and influenced the $\delta^{13}C$-CH_4 and $\delta^{2}H$-CH_4 values in the water column.

Oxic methane production was another potential contributor to CH_4 supersaturation in lakes that has more recently been the subject of thorough debate (section 4.2.2). At Lake Willersinnweiher, the occurrence of OMP has been indicated by concurrent CH_4 and Chl-a concentration peaks in the upper metalimnion during most months of the stratified period. Thus, linking OMP with phytoplankton communities and/or primary production as also reported by numerous previous studies (e.g., Figure 9A, B and Figure 11D; Grossart et al., 2011; Bogard et al., 2014; Hartmann et al., 2020). Furthermore, phytoplankton species known to form blooms in oligotrophic lake Stechlin were all found to produce CH_4 (Hartmann 2020) and combineed with the recent discovery of a universal CH_4 formation mechanism in all organisms by Ernst et al. (2022), this supports the notion that OMP is most probably a process ubiquitous among phytoplankton communities. Therefore, OMP might have also played an important role at Lake Willersinnweiher, as already suggested by Hartmann (2018). Moreover, applying a mass balance approach suggested the occurrence of OMP with rates of up to 130 nmol l^{-1} d^{-1} during the beginning and the end of stratification period. Furthermore, stable isotope labelling experiments conducted in this study further demonstrated the occurrence of OMP at Lake Willersinnweiher. The potential precursor compounds MPn, MA, MET were identified to be converted into CH_4, highlighting the potential for OMP in the water column of the lake. However, environmental factors influencing OMP are still widely unknown. Hence, OMP in lakes might feature strong temporal and spatial variations that demand further research, especially considering the linkage between OMP with phytoplankton and the occurrence seasonal algae blooms.

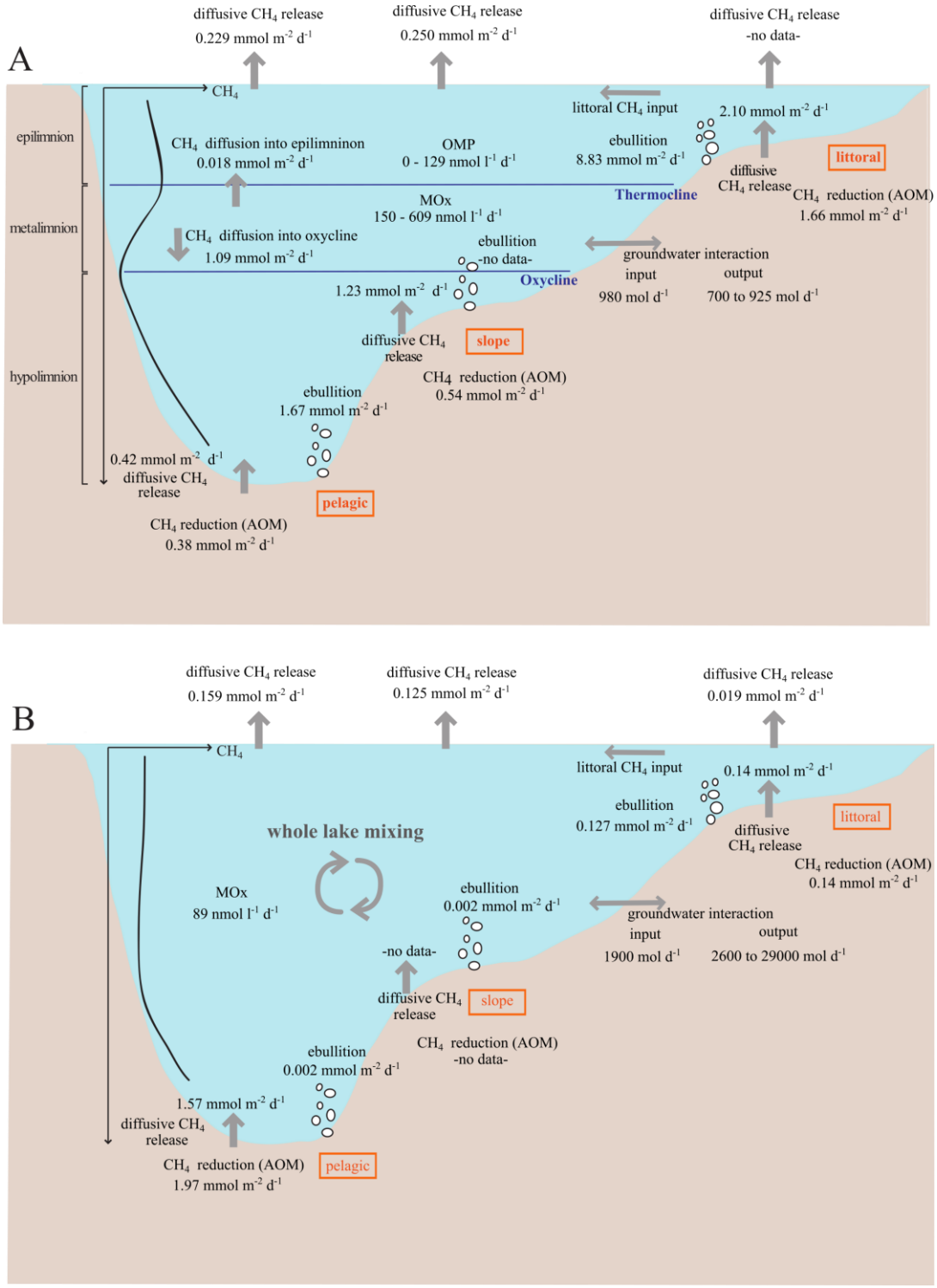

Figure 27. Methane cycle of Lake Willersinnweiher, showing fluxes of CH_4 (where available) at the pelagic, slope and littoral sites as well as transport mechanisms (grey arrows) during (A) stratification period (July 2020) and (B) mixing period (March 2021; ebullition data is taken from November 2020). Data for OMP is taken from the stratification periods between August 2019 and October 2020.

4.4 Seasonal methane emissions and its isotopic composition[12]

The known pathways of CH_4 emissions by lakes include plant-mediated transport of CH_4 from the sediment into atmosphere, diffusion from CH_4 at the water-atmosphere boundary due to CH_4 oversaturation in the surface water and uprising gas bubbles released from the sediment (ebullition) (e.g., Bastviken et al., 2004). In the scope of this study, emissions of CH_4 from plant-mediated transport were not obtained; however, their contribution to overall emissions is most likely of minor significance due to negligible plant coverage at Lake Willersinnweiher.

Diffusion of CH_4 at the water-atmosphere boundary is mostly dependent on CH_4 oversaturation in the epilimnion and near surface turbulence due to wind stress (e.g., Jähne and Haußecker, 1998; Klaus and Vachon, 2020). Since CH_4 was supersaturated throughout the whole year at Lake Willersinnweiher (section 4.3), CH_4 was released into the atmosphere during the whole observation period from August 2019 to September 2021. Diffusion rates ranged from 0.019 to 0.904 mmol m^{-2} d^{-1} at all three investigates sites (Figure 24), which is in good agreement with previously diffusion rates reported for lakes ranging from 0.002 to 2.7 mmol m^{-2} d^{-1} (Bastviken et al., 2008; Donis et al., 2017; Hartmann, 2018; Hartmann et al., 2020; Roland et al., 2017).

During most months, higher diffusive CH_4 flux rates prevailed at the littoral site compared to the pelagic and slope sites (Figure 24). However, CH_4 diffusion flux rates were very variable between the three observed sites, and no clear correlation between measured flux rates and either CH_4 concentration (R^2 = 0.41) or wind-speed (R^2 = 0.01) were detected (Figure 28). This implied that other factors were involved in driving diffusive CH_4 emissions. One factor could be the variability of wind stress throughout the lake, e.g., by sheltering effects of trees or buildings (Markfort et al., 2010; Prairie and del Giorgio, 2013; Wang et al., 2021), which could reduce wind related surface turbulences and thus lead to smaller diffusive CH_4 emissions. Another factor might constitute surface heat fluxes, as warming lakes decrease wind-driven turbulence, while cooling lakes increase turbulences due to convective movement of water masses, and thus influence diffusive CH_4 emissions (Klaus and Vachon, 2020; MacIntyre et al., 2010).

Methane concentrations in the water column and diffusive CH_4 fluxes were further linked, as higher release rates of CH_4 from water-atmosphere interface led to depleted CH_4 concentrations in the surface waters, which in turn fuelled CH_4 fluxes from the thermocline into the surface water layer (Kirillin et al., 2008, 2009). This process was also observed at Lake Willersinnweiher, where CH_4 fluxes from the metalimnion to the epilimnion accounted for up to 20 µmol m^{-2} d^{-1} and increased with elevated diffusive fluxes towards the end of stratification period in autumn (Figure 14D). Hereby, the CH_4 pool in the epilimnion is supplemented with CH_4 from the metalimnion, which was usually characterised by higher CH_4 concentrations and higher $\delta^{13}C$-CH_4 and $\delta^{2}H$-CH_4 compared to the epilimnion. Thus,

[12] Please note that parts of this section are taken from Einzmann et al. (2022).

upward fluxes from metalimnic CH_4 also contributed to CH_4 enriched in ^{13}C and ^{2}H in the epilimnion of Lake Willersinnweiher.

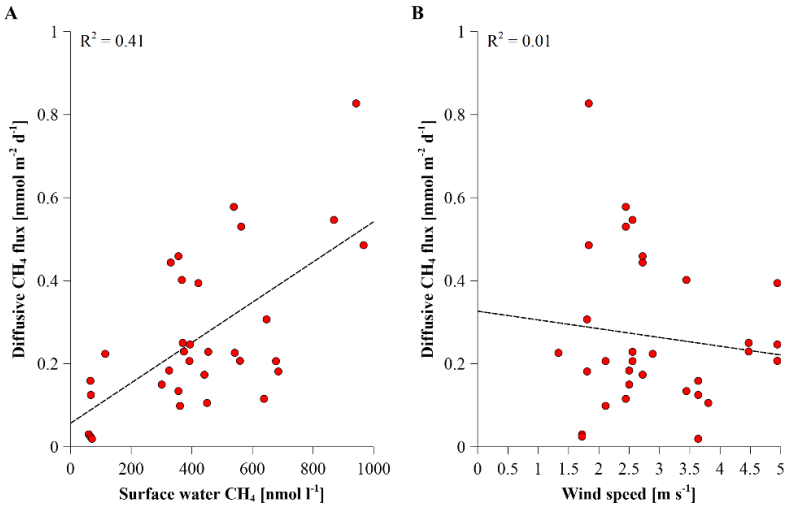

Figure 28. Relationship between diffusive CH_4 fluxes at the water-air interface and (A) the surface water CH_4 concentrations and (B) the wind speed. Data for the wind speed was obtained from a nearby weather station.

Stable carbon and hydrogen isotope values of CH_4 emitted to the atmosphere via diffusion displayed a broad range between -36 ‰ to -59 ‰ and +1 ‰ to -310 ‰, respectively throughout the year. During the stratification period, $\delta^{13}C$-CH_4 and $\delta^{2}H$-CH_4 values were more negative ranging from -59 ± 1 ‰ to -51 ± 1 ‰ and -310 ± 8 ‰ to -195 ± 22 ‰, compared to the mixing period, where $\delta^{13}C$-CH_4 and $\delta^{2}H$-CH_4 values ranged between -42 ± 1 ‰ to -36 ± 8 ‰ and 1 ± 34 to +26 ‰, respectively (Table 4). These stable isotope values closely reflected the stable isotope composition of dissolved epilimnic CH_4, which was also more enriched in both ^{13}C and ^{2}H during the mixing period compared to the stratification period.

Besides diffusion, ebullition constituted an important pathway of CH_4 release from Lake Willersinnweiher to the atmosphere. Ebullition is particularly prominent in the shallower littoral areas of aquatic systems, since uprising gas bubbles from the sediment are quickly transported to the atmosphere and circumvent CH_4 oxidation in the water column (e.g., McGinnis et al., 2006). Spatial and temporal variations were found for ebullitive flux rates as well as the CH_4 concentrations of the uprising gas bubbles and their isotopic CH_4 composition at Lake Willersinnweiher. Ebullitive flux rates of CH_4 were up to 70 times higher during the stratification period (up to 8.83 mmol m^{-2} d^{-1}) compared to the mixing period (up to 0.13 mmol m^{-2} d^{-1}) and consequently at the higher end of fluxes reported for lakes and wetlands in previous studies ranging from ≈ 1 to 12 mmol m^{-2} d^{-1} (Casper et al., 2000, 2005; DelSontro et al., 2016; Jeffrey et al., 2019; Thottathil and Prairie, 2021; Wik et al., 2020). Higher ebullitive CH_4 fluxes were observed at the littoral site compared to the pelagic and slope sites throughout the observation period from November 2020 to September 2021. Higher ebullition fluxes at littoral areas were likely caused by a lower distance to the atmosphere leading to less hydrostatic

pressure and less dissolution of gas bubbles in the water column. Moreover, higher microbial activity and methanogenesis in the sediment due to higher temperatures at the shallower littoral site compared to the deeper sites likely contributed to higher ebullition fluxes as suggested by e.g., Thottathil and Prairie (2021) and Aben et al. (2017).

Apart from ebullitive flux rates, CH_4 concentrations as well as $\delta^{13}C\text{-}CH_4$ and $\delta^{2}H\text{-}CH_4$ values released via ebullition also displayed temporal and spatial disparities at Lake Willersinnweiher. At the slope site, CH_4 released via ebullition was characterised by higher concentrations and more negative $\delta^{13}C\text{-}CH_4$ values (66.3 ± 1.2 % and -73.7 ± 1.0 ‰, respectively) when compared to the littoral site (62.1 ± 7.4 % and -50.0 ± 11.6 ‰, respectively) in November 2020. The CH_4 concentrations within uprising gas bubbles and their isotopic composition were well within the range of previously reported values for lakes and wetlands ranging from 40 to 80 %, -78 to -51 ‰ and -376 to -220 ‰, respectively (Bouchard et al., 2015; Jeffrey et al., 2019; Martens et al., 1992; Thottathil and Prairie, 2021; Wik et al., 2020). The differences in observed CH_4 concentrations and isotopic composition of uprising gas bubbles were most likely originating from CH_4 formation taking place mainly via the hydrogenotrophic pathways at the slope and the acetoclastic pathways at littoral site (section 4.1.1). Similarly, Thottathil and Prairie (2021) attributed differences in $\delta^{13}C\text{-}CH_4$ values of CH_4 emitted via ebullition to a predominantly occurring type of methanogenesis in the sediment.

In contrast to $\delta^{13}C\text{-}CH_4$ values, $\delta^{2}H\text{-}CH_4$ values of uprising gas bubbles did only show small differences between the two investigated sites. Differences between the $\delta^{2}H\text{-}CH_4$ values of ebullitive CH_4 were assigned to different water $\delta^{2}H$ values (e.g., evaporation in shallow lakes), which is a source of H_2 for methanogens (Waldron et al., 1998; Nakagawa et al., 2002; Sugimoto and Wada, 1995). As Lake Willersinnweiher is a distinctively deeper lake (average depth of 8 m), evaporation likely played only a minor role and therefore hardly affected $\delta^{2}H\text{-}CH_4$ values. On the other hand, SO_4^{2-}-dependent AOM in the sediments of Lake Willersinnweiher might have played an important role in influencing the stable isotope values of CH_4 released via ebullition. However, the influence of AOM on the stable isotope composition of gas bubbles is hard to estimate as AOM most probably took place heterogeneously throughout the sediment. In November, when there was likely less organic matter input than in September. This observation was also implied by lower ebullitive CH_4 concentrations in November compared to September (Table 5). Pockets of CH_4 within the sediment might have been subject to heterogeneously occurring AOM, which in turn could have contributed to the relatively high variability of measured $\delta^{13}C\text{-}CH_4$ values.

At Lake Willersinnweiher, estimated total CH_4 daily flux rates by ebullition were found to be up to 10 times higher compared to diffusive CH_4 fluxes during stratification periods, while during mixing period diffusive fluxes were superior to ebullitive fluxes. Thus, the contribution of CH_4 flux types from the water column to the atmosphere showed a strong seasonal variability as is shown in Figure 29. Daily CH_4 fluxes were therefore estimated to account for up to ≈ 700 mol d^{-1} during stratification period, compared to only about 70 mol d^{-1} during mixing period. Diffusive CH_4 fluxes were the main

driver of total CH_4 release from Lake Willersinnweiher during the mixing period and lower ebullitive flux rates compared to the stratification period were most likely caused by lower sediment temperatures in winter compared to summer, thus leading to lower methanogenic activity there (Duc et al., 2010; Kelly and Chynoweth, 1981).

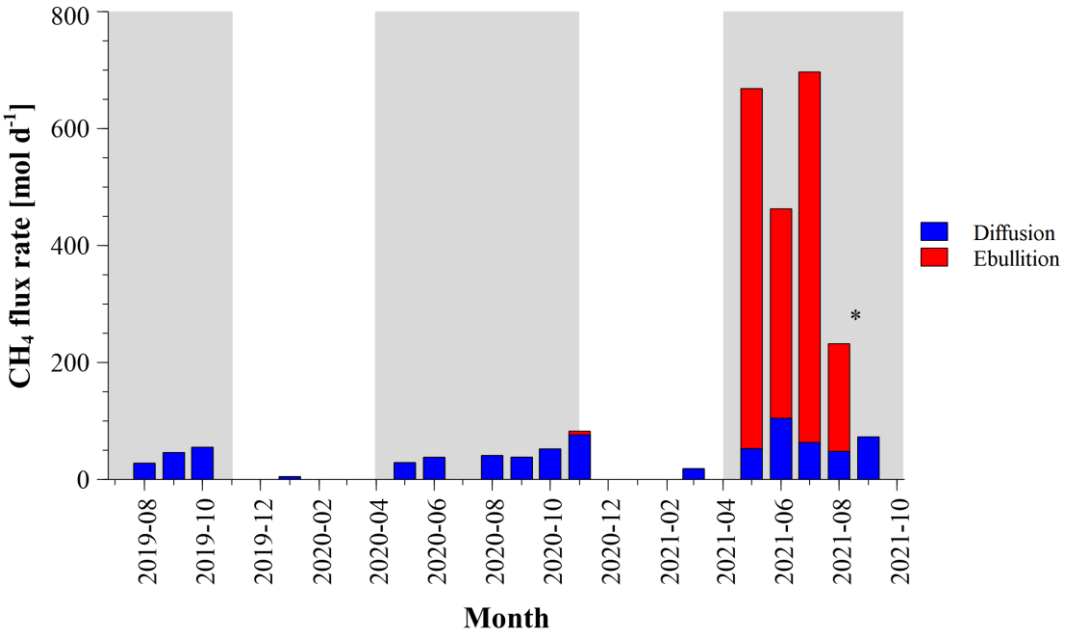

Figure 29. Calculated daily diffusive and ebullitive CH_4 flux rates for Lake Willersinnweiher from August 2019 to September 2020. Data for ebullition starts from November 2020. The asterisk (*) indicates that ebullitive CH_4 flux rates from September 2021 only show flux rates from the pelagic site. Grey background colours indicate the stratification period and white background colours represent the mixing period.

4.5 Dual stable isotope characterisation of methane in Lake Willersinnweiher[13]

In order to gain additional information about CH_4 sources and sinks at Lake Willersinnweiher, $\delta^{13}C\text{-}CH_4$ and $\delta^{2}H\text{-}CH_4$ values were determined for the water column, groundwater and the sediment between May 2020 and September 2021. Stable carbon and hydrogen isotope values of CH_4 in the water column and groundwater showed a good correlation (Figure 30A, R^2 = 0.89) indicating occurring MOx, with associated enrichment in $^{13}C\text{-}CH_4$ and $^{2}H\text{-}CH_4$ in the water column as discussed in section 4.2.1. The correlation between $\delta^{13}C\text{-}CH_4$ and $\delta^{2}H\text{-}CH_4$ values further implies that stable carbon and hydrogen isotope fractionation factors remained similar throughout the sampling period (from May 2020 to September 2021). Moreover, they indicated that inflowing groundwater at GW West in and outflowing groundwater at GW West out were subject to intense oxidation based on its unusually positive stable isotope composition (section 4.2.3).

[13] Please note that parts of this section are taken from Einzmann et al. (2022).

In the water column the stable isotope composition of CH_4 in the metalimnion stretched along the gradient typical for MOx, which is characterised by an enrichment in ^{13}C-CH_4 and ^{2}H-CH_4 (Figure 30A). Epilimnic CH_4 during the stratification period, however clustered in the lower part of Figure 30A, thus indicating that $\delta^{13}C$-CH_4 and $\delta^{2}H$-CH_4 values were the result of a mixture of multiple CH_4 sources. During the mixing period, epilimnic CH_4 plots in the middle part of the Figure 30A (orange dots in black circle), therefore implying that MOx played a greater role during this period and/or that other CH_4 sources were larger contributors to epilimnic CH_4 supersaturation compared to the stratification period.

Methane in the hypolimnic water layer was characterised by the most negative $\delta^{13}C$-CH_4 and $\delta^{2}H$-CH_4 values (Figure 30A). Interestingly, CH_4 in the pore water of the sediment at the pelagic and slope sites showed similar $\delta^{13}C$-CH_4 and $\delta^{2}H$-CH_4 values compared to the hypolimnion (Figure 30B). However, the stable isotope composition of sedimentary CH_4 also displayed a bigger range compared to hypolimnic CH_4 with a shift towards less negative $\delta^{13}C$-CH_4 and $\delta^{2}H$-CH_4 values indicating the presence of AOM (as discussed in section 4.1.2; Figure 30B). At the littoral site, pore water CH_4 was characterised by increasing $\delta^{13}C$-CH_4 and $\delta^{2}H$-CH_4 values compared to the other two sediment sites, which was most likely attributed to acetoclastic methanogenesis superordinating hydrogenotrophic methanogenesis at this site as discussed in section 4.1.1.

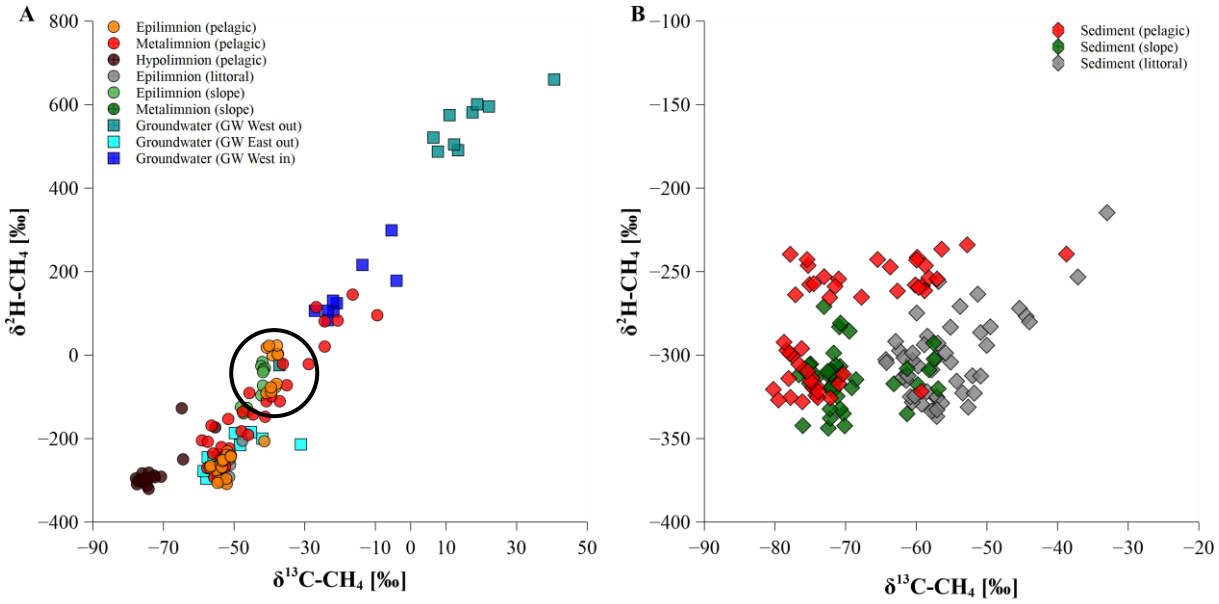

Figure 30. (A) Relationship between $\delta^{13}C$-CH_4 and $\delta^{2}H$-CH_4 of dissolved CH_4 in all samples from the water column (circles) and groundwater (squares) from May 2020 to September 2021. Epilimnic $\delta^{13}C$-CH_4 and $\delta^{2}H$-CH_4 values during the mixing period are indicated by a black circle. (B) Relationship between $\delta^{13}C$-CH_4 and $\delta^{2}H$-CH_4 values of dissolved CH_4 in the pore water of the pelagic (red), slope (green) and littoral (grey) sediment from May 2020 to March 2021.

Measuring the stable isotope composition of CH_4 is a useful tool to gain information about CH_4 sources and sinks in lakes, however processes such as CH_4 oxidation led to an enrichment of ^{13}C-CH_4 and ^{2}H-CH_4 in the CH_4 pool. In order to overcome changes in the isotopic composition of CH_4 due to CH_4 oxidation, Tsunogai et al. (2020) introduced the novel isotope indicator Δ(2,13). The Δ(2,13) indicator was applied in this study to identify the original ^{13}C- and ^{2}H isotopic composition of CH_4 in the water column, groundwater and sediment of Lake Willersinnweiher by correcting for isotope fractionation caused by CH_4 oxidation. The correction of CH_4 isotope values during CH_4 oxidation was applied by calculating Λ (Eq. (7)), which is defined by dividing the isotope fractionation of hydrogen by the isotope fractionation of carbon. Thus, the obtained Λ value of 9.3 ± 0.3 (Figure 18B) showed that CH_4 oxidation on average led to a 9-fold enrichment of ^{2}H-CH_4 compared to ^{13}C-CH_4. The determined Λ value was also in agreement with similar Λ values reported by Feisthauer et al, (2011) and Tsunogai et al. (2020), which were in the range of 12 ± 4.6 and 10.9 ± 0.2, respectively.

At Lake Willersinnweiher Δ(2,13) values were determined three times during the stratification period (early stratification: May 2020, mid stratification: July 2020, and late stratification: October 2020) and once during the mixing period (March 2021) (Figure 23). In Figure 31 an overview of all investigated CH_4 sources and emissions as well as their Δ(2,13), $\delta^{13}C$-CH_4 and $\delta^{2}H$-CH_4 values during the stratification (July 2020) and mixing period (March 2021) are illustrated.

The pelagic and slope sites were characterised by similar Δ(2,13) values across the epilimnion, metalimnion and sediment throughout the whole observation period. At the pelagic site, Δ(2,13) values of the hypolimnion and sediment overlapped during the stratification period, implying that CH_4 in the hypolimnion of the lake originated mainly from release of CH_4 from the sediment. During stratification period, the Δ(2,13) values of the epilimnion and metalimnion at the pelagic and slope sites showed distinctly lower values compared to hypolimnic and sedimentary values at these sites. Thus, vertical input of CH_4 rich bottom waters most likely did not constitute an important contribution for CH_4 supersaturation in the epilimnion and metalimnion. This is in good agreement with observations that a major proportion of CH_4 from the hypolimnion was consumed at the oxycline due to MOx (section 4.2.1).

However, during early stratification period Δ(2,13) values of the metalimnion at the pelagic and slope sites (342 ± 12 ‰ and 311 ± 47 ‰, respectively) were much higher than epilimnic values (203 ± 3 ‰). This might have been caused by unstable stratification conditions leading to the mixture of CH_4 from different sources such as release from the sediment, lateral input from sedimentary CH_4, groundwater input and/or CH_4 production in the metalimnion. At the slope site, metalimnic Δ(2,13) values overlapped with the ones from the sediment and groundwater (293 ± 49 ‰ and 307 ± 5 ‰, respectively), thus indicating that CH_4 mainly derived from one or both of these CH_4 sources.

Contrastingly, during mid stratification period Δ(2,13) values in the epilimnion (266 ± 4 ‰) and the metalimnion (276 ± 25 ‰) were very similar implying that CH_4 originated from the same source(s). At the littoral site Δ(2,13) values of the epilimnion and sediment were in the same range (183 ± 12 ‰ and 219 ± 38 ‰), indicating that CH_4 at the littoral site predominantly originated from sedimentary release of CH_4.

Interestingly, Δ(2,13) values at the littoral site were up to 50 ‰ smaller compared to the ones of the pelagic and slope sites in all investigated months. Thus, supporting the notion that even though littoral input of CH_4 most likely played an important role in sustaining the CH_4 supersaturation in the epilimnion of the entire lake, other sources, such as groundwater input or OMP also contributed in order to explain these differences in Δ(2,13) values. In contrast to this observation at Lake Willersinnweiher Tsunogai et al. (2020) reported similar Δ(2,13) values for the epilimnion of the pelagic and littoral areas of lake Biwa and thus concluded that sedimentary CH_4 input is responsible for a major part of CH_4 in the pelagic areas.

With progression of the stratification period an increase of epilimnic Δ(2,13) values at all three sites was observed, inferring that the contribution of different CH_4 sources to CH_4 in the surface water column changed with time. One reason for this observation might have been higher sedimentary CH_4 production and input from littoral sediments due to higher temperatures and microbial activity during the stratification period, as Δ(2,13) values of littoral sediments and subsequently the surface water at the littoral site also showed an increase from May to October 2020. However, the increase in epilimnic Δ(2,13) values was higher compared to the sediment, which implicated the need for (an) additional source(s).

A potential source could constitute OMP, which has been shown to occur in the oxic water column of Lake Willersinnweiher based on a mass balance approach and stable isotope labelling experiments (section 4.2.2). In previous studies higher rates of OMP have been linked to higher primary production, as well as higher temperature and light conditions (Klintzsch et al., 2020; McLeod et al., 2021). However, at this point no data about $\delta^{13}C$-CH_4, $\delta^{2}H$-CH_4 and Δ(2,13) values of CH_4 produced via OMP are available, thus making clear evaluations about its importance to epilimnic CH_4 supersaturation based on Δ(2,13) values difficult. However, evidence for the occurrence of OMP at Lake Willersinnweiher based on the mass balance approach, stable isotope labelling experiment and CH_4 peaks in the upper metalimnion that coincided with peaks in Chl-a concentrations, implied that OMP might have played an important role during stratification period at Lake Willersinnweiher.

Another potential source constituted input of CH_4-rich groundwater (307 ± 5 to 325 ± 5 ‰ between May 2020 and March 2021). It was characterised by higher Δ(2,13) values than epilimnic CH_4 (251 ± 35 ‰), but smaller values compared to hypolimnic and sedimentary CH_4 (427 ± 28 ‰ and 385 ± 39 ‰). Mixing of lake water and groundwater might led to more positive isotope values in the lake water column; however, based on the Δ(2,13) values for inflowing groundwater CH_4 and surface

lake water, groundwater CH_4 was most likely not a main contributor of CH_4 in the epilimnion of Lake Willersinnweiher during the stratification period.

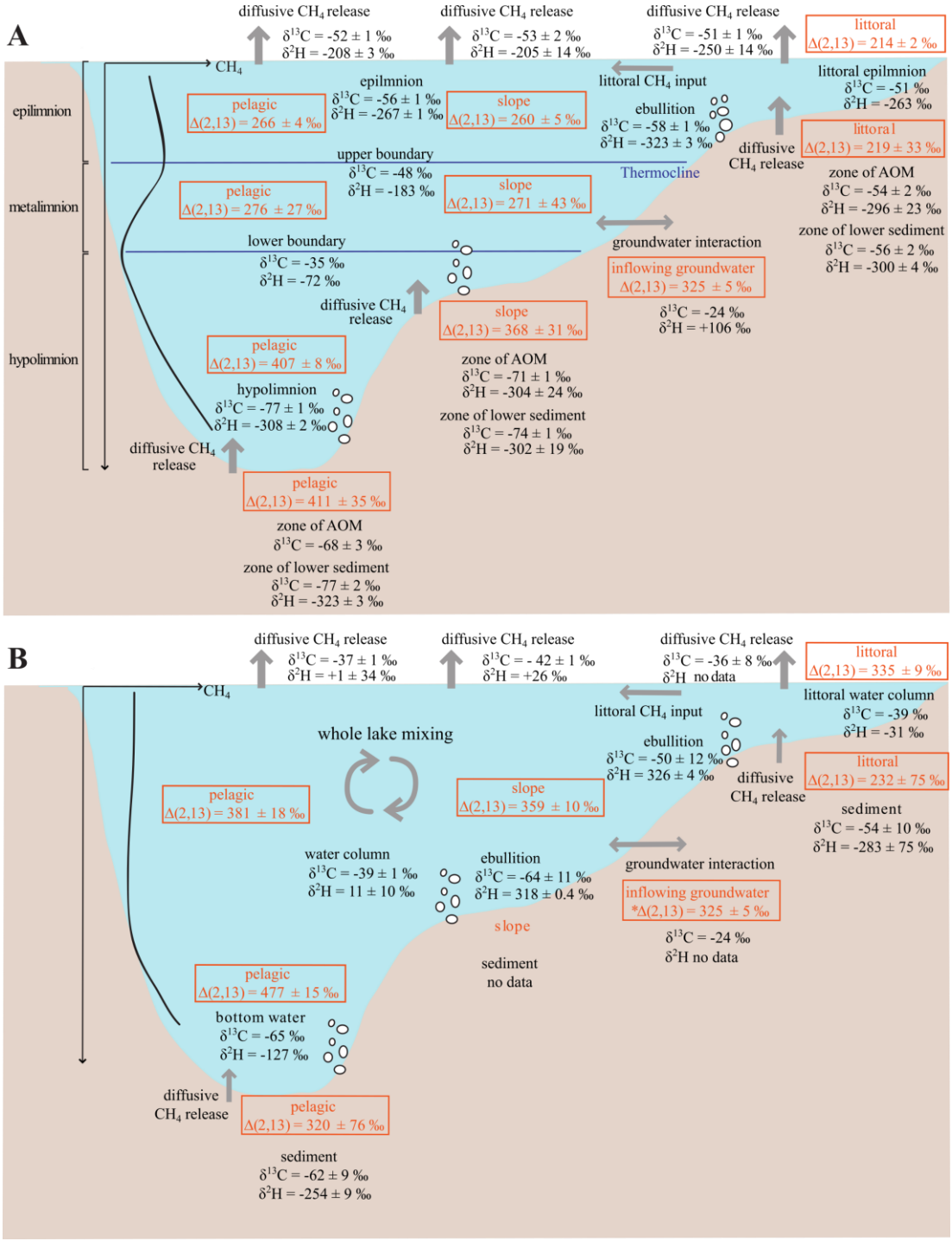

Figure 31. Proposed CH_4 cycling at Lake Willersinnweiher (A) during stratification period (July 2020) and (B) during mixing period (March 2021). Methane sources and sinks are illustrated with respective $\delta^{13}C$-CH_4 and δ^2H-CH_4 values (where available). Transport mechanisms are indicated by grey arrows and $\Delta(2,13)$ values of different water layers by orange colour. Data for diffusive CH_4 release at the water-air interface during stratification period refers to data from July 2021 and ebullition data is taken from September 2021. Ebullition data for the mixing period refers to data collected from November 2020, while $\Delta(2,13)$ values for inflowing groundwater are taken from October 2020 (modified after Einzmann et al., 2022).

In contrast to the stratification period, Δ(2,13) values inferred that during mixing period input of CH_4 from groundwater and the littoral areas were likely the main sources for sustaining CH_4 supersaturation in Lake Willersinnweiher (Figure 31B). This observation is based on epilimnic Δ(2,13) values overlapping with the ones of groundwater and the sediment at the pelagic site. Furthermore, at the littoral site very similar epilimnic and groundwater values prevailed, while sedimentary Δ(2,13) values were smaller than the epilimnic ones but characterised by a high SD (Figure 23A, C). The high SD of sedimentary Δ(2,13) values (320 ± 76 ‰ for pelagic and 232 ± 75 ‰ for littoral sediment) were a result of the high variability in $\delta^{13}C\text{-}CH_4$ values during the mixing period, which implied a complex interplay between methanogenesis and oxidation and associated isotope fractionation. Due to complete mixing of the water column, the transport of littoral CH_4 into the pelagic areas of the lake was likely. This was also expressed by similar and overlapping Δ(2,13) values of epilimnic CH_4 between all three sites (381 ± 18 ‰ for pelagic, 359 ± 10 ‰ for slope and 335 ± 9 ‰ for littoral). Nevertheless, additional data for Δ(2,13) values during the mixing period is eligible in order to disentangle the CH_4 cycle at Lake Willersinnweiher during this period.

5 Summary

In this study, the complex CH_4 cycle of a seasonally stratified freshwater lake was investigated during a period of two and a half years. Sources and sinks of CH_4 were determined using conventional analytical methods but were additionally complemented by dual isotope analysis of CH_4 and the application of the novel stable isotope indicator $\Delta(2,13)$.

Methane production in the sediment and its release represented an important source of CH_4 in the water column of Lake Willersinnweiher. The analysis of CH_4 concentrations and its $\delta^{13}C$-CH_4 and $\delta^{2}H$-CH_4 values revealed that the sediment of all three investigated sites (pelagic, slope, littoral) contributed significantly to the CH_4 cycle of Lake Willersinnweiher. Stable carbon and hydrogen isotope values of CH_4 suggested that anaerobic methanogenesis occurred mainly via the hydrogenotrophic pathway at the pelagic and slope areas of the lake, while the acetoclastic pathway was dominant at the shallow littoral site. Due to the rather unique characteristic of high SO_4^{2-} concentrations in the water column and sediment of Lake Willersinnweiher, methanogenesis was likely restricted to the lower part of the sediment, where SO_4^{2-} concentrations were low and methanogenic archaea were not outcompeted for substrates by SRB. However, higher release rates of CH_4 at the water-sediment interface were recorded with succession of the stratification period, thus showing a clear influence of increased temperatures on bioactivity and turnover of organic matter in the sediment. Therefore, in the future sedimentary CH_4 might play an even more important role in the scope of climate change and coinciding temperature increases, which would lead to strong increases in methanogenesis and thus potentially whole lake CH_4 emissions.

However, high SO_4^{2-} concentrations in the upper part of the sediment did not only inhibit methanogenesis but also led to the reduction of CH_4 concentrations due to the occurrence of SO_4^{2-}-dependent AOM and SMTZs. Sulphate-methane transition zones are usually found in marine environments and have only rarely been described for freshwater systems. Zones in the sediment that were characterised by simultaneously decreasing CH_4 and SO_4^{2-} concentrations, while S^{2-} and DIC concentrations increased, were observed all year round at all investigated sites and attributed to occurring SO_4^{2-}-dependent AOM and SMTZ. Furthermore, the analysis of $\delta^{13}C$-DIC, $\delta^{13}C$-CH_4 and $\delta^{2}H$-CH_4 values supported the occurrence of SO_4^{2-}-dependent AOM. This combined dataset of concentration measurements and stable isotope analysis provides compelling evidence that SO_4^{2-}-dependent AOM is a ubiquitous process in the upper sediment of Lake Willersinnweiher and thereby significantly reduces diffusive release of CH_4 at the sediment-water interface.

Methane that migrated upwards from the CH_4-rich anoxic bottom water was efficiently consumed by MOx at the chemocline. A strong enrichment in ^{13}C-CH_4 and ^{2}H-CH_4 in the water column indicated occurring MOx. In the scope of this study the first MOx rates for Lake Willersinnweiher were

determined using stable isotope labelling incubation experiments. The determined rates revealed that MOx increased during stratification periods and thereby effectively compensated higher sedimentary flux rates of CH_4 and furthermore prevented sedimentary CH_4 of the deeper sites from reaching the epilimnion. Moreover, MOx rates examined during the mixing period illuminated that MOx was also present throughout winter and therefore contributed to increasing $\delta^{13}C\text{-}CH_4$ and $\delta^{2}H\text{-}CH_4$ values observed during that period. Therefore, MOx was found to reduce CH_4 concentrations in the water column of Lake Willersinnweiher all year round, however further investigations are needed to better understand the occurrence and magnitude of MOx, seasonally as well as spatially.

Even though AOM and MOx reduced a large part of CH_4 fluxes in the sediment and water column, the epilimnion of Lake Willersinnweiher was still permanently supersaturated in CH_4. However, during the stratification periods in summer, CH_4 supersaturation was significantly higher compared to the mixing period during winter. Similarly, the investigation of the spatial distribution of CH_4 revealed higher variations during the stratification period. This observation might on the one hand originate from higher CH_4 production in the sediment due to higher temperatures and concomitant increase in microbial activity. On the other hand, the predominant wind direction from south-west to north-east might explain higher CH_4 concentration in the surface water of the north-eastern basin of Lake Willersinnweiher. A combination of the two parameters might therefore be the reason why for only small or no correlations between CH_4 concentrations and distance to shore as well as water depth was found. However, even though first transects of CH_4 were measured in the scope of this study, future investigations should further address the magnitude of littoral input of CH_4 as well as the importance of wind-induced transport. For this aim, modelling and a more detailed dataset concerning wind speed and wind direction are needed to better assess this issue, especially as changes in temperature and wind characteristics might highly influence future CH_4 distribution in the epilimnion and more importantly the CH_4 emissions to the atmosphere.

Another contributor to CH_4 supersaturation in the epilimnion of Lake Willersinnweiher was found in OMP. It was only in recent years that OMP via phytoplankton has been subject to intense debate and investigations but so far constitutes an underrepresented role in discussions about limnic CH_4 cycles. Local CH_4 peaks, enriched in $^{13}C\text{-}CH_4$ and $^{2}H\text{-}CH_4$ and coinciding with Chl-a peaks in the upper metalimnion indicated the presence of OMP associated with phytoplankton. Furthermore, a mass balance approach conducted in the scope of this study suggested that especially at the beginning and end of stratification period OMP occurred in Lake Willersinnweiher. Moreover, stable isotope labelling experiments revealed three potential precursor compounds (MPn, MA and MET) of OMP at Lake Willersinnweiher.

Moreover, inflowing groundwater was found to be a contributor to CH_4 supersaturation at Lake Willersinnweiher all year round, as it was characterised by high CH_4 concentrations and a strong enrichment in $^{13}C\text{-}CH_4$ and $^{2}H\text{-}CH_4$.

The two main processes of CH_4 emissions from Lake Willersinnweiher were diffusion at the water-atmosphere interface and ebullition. Since the epilimnion was supersaturated throughout the year, Lake Willersinnweiher constantly emitted CH_4 to the atmosphere. Diffusion rates of CH_4 showed strong seasonal variations and were substantially higher during the stratification periods compared to the mixing periods. The main reason for this observation likely constituted the higher CH_4 concentrations in the epilimnion during stratification period. Using the Keeling plot method, the $\delta^{13}C$-CH_4 and $\delta^{2}H$-CH_4 values of diffusive CH_4 were determined and characterised by strong seasonal variations. It was found that the stable isotope composition of diffusive CH_4 emissions was substantially enriched in ^{13}C-CH_4 and ^{2}H-CH_4 during the mixing periods compared to the stratification periods. When estimated for the whole lake area, ebullitive CH_4 flux rates were much higher than diffusive CH_4 rates during stratification period and accounted for up to 90 % of total CH_4 emissions from Lake Willersinnweiher. However, during the mixing period ebullition was responsible for only $\approx$ 10 % of emissions and diffusion was the major pathways of CH_4 emissions from Lake Willersinnweiher. Gas bubbles that were released from the sediment consisted mainly of CH_4 (60 to 80 %), and their $\delta^{13}C$-CH_4 and $\delta^{2}H$-CH_4 values closely reflected the isotopic signature of sedimentary CH_4. In the scope of temperature increases due to climate change and expected eutrophication of aquatic environments, CH_4 emissions are expected to increase even further. Especially ebullition which is fuelled by methanogenesis in the sediment and largely escapes CH_4 oxidation processes in the water column due to rapid ascension through the water column might lead to larger CH_4 emissions compared to today. Hence a thorough understanding of the parameters controlling CH_4 emissions is crucial to estimate their impact in the future. Moreover, a comprehensive understanding of seasonal differences between $\delta^{13}C$-CH_4 and $\delta^{2}H$-CH_4 values is desirable as atmospheric $\delta^{13}C$-CH_4 and $\delta^{2}H$-CH_4 values are a common tool to assign CH_4 emission to their potential sources.

Finally, the novel isotope indicator $\Delta(2,13)$, which corrects for stable isotope fractionation due to CH_4 oxidation, was applied. Hence, the application of $\Delta(2,13)$ values allowed for further interpretation of the contribution of different sources to CH_4 supersaturation, beyond the use of CH_4 flux measurements. Epilimnic $\Delta(2,13)$ values of the pelagic site indicated that during the stratification period neither input of CH_4 from littoral sediments nor input of CH_4 from groundwater, which was characterised by high CH_4 concentrations as well as unusually positive $\delta^{13}C$-CH_4 and $\delta^{2}H$-CH_4 values, constituted the main CH_4 source. Instead OMP, which was shown to occur at Lake Willersinnweiher through a combination of a mass balance approach and stable isotope labelling experiments and furthermore indicated by local CH_4 peaks enriched in ^{13}C-CH_4 and ^{2}H-CH_4 in the upper metalimnion might have strongly contributed to CH_4 supersaturation. However, further research about the stable isotope source signatures of OMP is needed in order to better resolve its role and impact in CH_4 cycles of aquatic systems based on stable isotope and $\Delta(2,13)$ values. Contrary to the stratification period, $\Delta(2,13)$ values during the mixing period implied that CH_4 supersaturation originated mainly from groundwater and littoral inputs of CH_4. Groundwater as a major source of CH_4 combined with MOx

detected during the mixing period might therefore be responsible for the more positive $\delta^{13}C\text{-}CH_4$ and $\delta^{2}H\text{-}CH_4$ values in the water column of Lake Willersinnweiher compared to the stratification period. Hence, the $\Delta(2,13)$ indicator delivered new insights into the sources contributing to CH_4 supersaturation at Lake Willersinnweiher and moreover highlights its potential to disentangle the complex interaction of these different sources.

This study provides a comprehensive multi-year dataset of sources and sinks of CH_4 combining concentrations as well as dual stable isotope analysis with the application of novel stable isotope techniques. Besides determining traditional sources and sinks of CH_4, such as the release of anaerobically produced CH_4 at the sediment-water interface and the MOx in the water column of Lake Willersinnweiher, a multi-isotope approach was used to identify the presence of SO_4^{2-}-dependent AOM and SMTZs in the sediment. Therefore, showing that a large part of produced CH_4 was removed in the sediment before being released to the water column. Furthermore, this study demonstrated the occurrence of OMP in the oxygenated water column of Lake Willersinnweiher and identified three potential precursor compounds thus supporting this notion that OMP might be an inherent component of the CH_4 cycle of aquatic systems. Finally, the application of the $\Delta(2,13)$ indicator highlighted that a multiparameter approach combining concentrations and isotope analysis as well as isotope techniques comprises a very promising approach for constraining the CH_4 cycle of Lake Willersinnweiher, but also for other aquatic systems.

6 Related scientific work

Peer-reviewed journal articles

Einzmann, T.*, **Schroll, M.***, Kleint, J. F., Greule, M. and Keppler, F.: Application of concentration and 2-dimensional stable isotope measurements of methane to constrain sources and sinks in a seasonally stratified freshwater lake, Frontiers in Environmental Science-Biogeochemistry, 2022. [Manuscript submitted for publication]

* These authors contributed equally to this work and share first authorship.

Kleint, J. F., Wellach, Y., **Schroll, M.**, Keppler, F. and Isenbeck-Schröter, M.: The impact of seasonal sulfate–methane transition zones on methane cycling in a sulfate-enriched freshwater environment, Limnology and Oceanography, 66(6), 2290–2308, doi:10.1002/lno.11754, 2021.

Additional contributions (not directly related to this thesis):

Schroll, M., Lenhart, K., Greiner, S., Keppler, F.: Making plant methane formation visible – insights from application of ^{13}C-labelled dimethyl sulfoxide, Plant-Environment Interactions, 2022. [Manuscript submitted for publication]

Schroll, M., Keppler, F., Greule, M., Eckhardt, C., Zorn, H. and Lenhart, K.: The stable carbon isotope signature of methane produced by saprotrophic fungi, Biogeosciences, 17(14), 3891–3901, doi:10.5194/bg-17-3891-2020, 2020.

Conference proceedings

Einzmann, T., **Schroll, M**., Kleint, J. F., Klintzsch, T., Greule, M., Keppler, F.: Application of 2-dimensional stable isotope measurements of methane to constrain sources and sinks in a seasonally stratified freshwater lake, orally presented at: Jahrestagung der Arbeitsgemeinschaft Stabile Isotope e.V. (ASI), online conference, 26 – 29 September 2021.

Einzmann, T., **Schroll, M.**, Kleint, J. F., Klintzsch, T., Keppler, F.: Application of 2-dimensional stable isotope measurements of methane to constrain sources and sinks in a seasonally stratified freshwater lake, orally presented at: Association for the Sciences of Limnology and Oceanography (ASLO) 2021 Aquatic Sciences Meeting, online conference, 22 – 27 June 2021.

Schroll, M., Lenhart, K., Greiner, S., Keppler, F.: Making plant methane formation visible – insights from application of ^{13}C-labelled dimethyl sulfoxide, orally presented at: Jahrestagung der Arbeitsgemeinschaft Stabile Isotope e.V. (ASI), online conference, 26 – 29 September 2021.

Schroll, M., Keppler, F., Greule, M., Eckhardt, C., Zorn, H. and Lenhart, K.: The stable carbon isotope signature of methane produced by two saprotrophic fungi, orally presented at Jahrestagung der Arbeitsgemeinschaft Stabile Isotope e.V. (ASI), Dresden, 30 September – 03 October 2019.

Sampling campaigns

2019 to 2021 Lake Willersinnweiher, Ludwigshafen am Rhein, Germany

19 sampling campaigns lasting between 2 to 4 days between May 2019 and September 2021. Measurement of CH_4 concentration as well as δ^{13}C-CH_4 and δ^{2}H-CH_4 values and other parameters in the water column, sediment, groundwater, diffusion at the water-air interface and ebullition at Lake Willersinnweiher. A detailed of overview of the measured parameters at each sampling campaign is shown in Table A 1.

7 References

Aben, R. C. H., Barros, N., van Donk, E., Frenken, T., Hilt, S., Kazanjian, G., Lamers, L. P. M., Peeters, E. T. H. M., Roelofs, J. G. M., de Senerpont Domis, L. N., Stephan, S., Velthuis, M., Van de Waal, D. B., Wik, M., Thornton, B. F., Wilkinson, J., DelSontro, T. and Kosten, S.: Cross continental increase in methane ebullition under climate change, Nature Communications, 8(1), 1682, doi:10.1038/s41467-017-01535-y, 2017.

Allan, W., Struthers, H. and Lowe, D. C.: Methane carbon isotope effects caused by atomic chlorine in the marine boundary layer: Global model results compared with southern hemisphere measurements, Journal of Geophysical Research, 112, doi:10.1029/2006JD007369, 2007.

Alperin, M. J. and Reeburgh, W. S.: Inhibition experiments on anaerobic methane oxidation, Applied and Environmental Microbiology, 50(4), 940–945, doi:10.1128/aem.50.4.940-945.1985, 1985.

Althoff, F., Benzing, K., Comba, P., McRoberts, C., Boyd, D. R., Greiner, S. and Keppler, F.: Abiotic methanogenesis from organosulphur compounds under ambient conditions, Nature Communications, 5(1), 4205, doi:10.1038/ncomms5205, 2014.

de Angelis, M. A. and Lee, C.: Methane production during zooplankton grazing on marine phytoplankton, Limnology and Oceanography, 39(6), 1298–1308, doi:10.4319/lo.1994.39.6.1298, 1994.

Barker, J. F. and Fritz, P.: Carbon isotope fractionation during microbial methane oxidation, Nature, 293(5830), 289–291, doi:10.1038/293289a0, 1981.

Bastviken, D., Ejlertsson, J. and Tranvik, L.: Measurement of methane oxidation in lakes: A comparison of methods, Environmental Science & Technology, 36(15), 3354–3361, doi:10.1021/es010311p, 2002.

Bastviken, D., Cole, J., Pace, M. and Tranvik, L.: Methane emissions from lakes: Dependence of lake characteristics, two regional assessments, and a global estimate, Global Biogeochemical Cycles, 18(4), 1–12, doi:10.1029/2004GB002238, 2004.

Bastviken, D., Cole, J. J., Pace, M. L. and Van de Bogert, M. C.: Fates of methane from different lake habitats: Connecting whole-lake budgets and CH_4 emissions, Journal of Geophysical Research: Biogeosciences, 113, doi:10.1029/2007JG000608, 2008.

Bastviken, D., Tranvik, L. J., Downing, J. A., Crill, P. M. and Enrich-Prast, A.: Freshwater methane emissions offset the continental carbon sink, Science, 331(6013), 50–50, doi:10.1126/science.1196808, 2011.

Beal, E. J., House, C. H. and Orphan, V. J.: Manganese- and iron-dependent marine methane oxidation, Science, 325(5937), 184–187, doi:10.1126/science.1169984, 2009.

Beaulieu, J. J., DelSontro, T. and Downing, J. A.: Eutrophication will increase methane emissions from lakes and impoundments during the 21st century, Nature Communications, 10(1), 1375, doi:10.1038/s41467-019-09100-5, 2019.

Benzing, K., Comba, P., Martin, B., Pokrandt, B. and Keppler, F.: Nonheme iron-oxo-catalyzed methane formation from methyl thioethers: Scope, mechanism, and relevance for natural systems, Chemistry – A European Journal, 23(43), 10465–10472, doi:10.1002/chem.201701986, 2017.

Bižić-Ionescu, M., Ionescu, D., Günthel, M., Tang, K. W. and Grossart, H.-P.: Oxic methane cycling: New evidence for methane formation in oxic lake water, in: Biogenesis of Hydrocarbons, edited by: Stams, A., Sousa, D., Springer International Publishing, Basel, 1-22, 2018.

Bižić, M., Klintzsch, T., Ionescu, D., Hindiyeh, M. Y., Günthel, M., Muro-Pastor, A. M., Eckert, W., Urich, T., Keppler, F. and Grossart, H.-P.: Aquatic and terrestrial cyanobacteria produce methane, Science Advances, 6(3), eaax5343, doi:10.1126/sciadv.aax5343, 2020a.

Bižić, M., Grossart, H. and Ionescu, D.: Methane Paradox, In eLS, John Wiley & Sons, Ltd (Ed.), 10.1002/9780470015902.a0028892, 2020b.

Blees, J., Niemann, H., Erne, M., Zopfi, J., Schubert, C. J. and Lehmann, M. F.: Spatial variations in surface water methane super-saturation and emission in Lake Lugano, southern Switzerland, Aquatic Sciences, 77(4), 535–545, doi:10.1007/s00027-015-0401-z, 2015.

Boetius, A., Ravenschlag, K., Schubert, C. J., Rickert, D., Widdel, F., Gieseke, A., Amann, R., Jørgensen, B. B., Witte, U. and Pfannkuche, O.: A marine microbial consortium apparently mediating anaerobic oxidation of methane, Nature, 407(6804), 623–626, doi:10.1038/35036572, 2000.

Bogard, M. J., del Giorgio, P. A., Boutet, L., Chaves, M. C. G., Prairie, Y. T., Merante, A. and Derry, A. M.: Oxic water column methanogenesis as a major component of aquatic CH_4 fluxes, Nature Communications, 5(1), 5350, doi:10.1038/ncomms6350, 2014.

Boros, M. and Keppler, F.: Gasotransmitters, edited by R. Wang, Royal Society of Chemistry, London., 192–234, doi:10.1039/9781788013000, 2018.

Bouchard, F., Laurion, I., Prėskienis, V., Fortier, D., Xu, X. and Whiticar, M. J.: Modern to millennium-old greenhouse gases emitted from ponds and lakes of the Eastern Canadian Arctic (Bylot Island, Nunavut), Biogeosciences, 12(23), 7279–7298, doi:10.5194/bg-12-7279-2015, 2015.

Boudreau, B. P.: Diagenetic Models and Their Implementation: modelling transport and reactions in aquatic sediments, Springer, Berlin, Heidelberg, 1997.

Bridgham, S. D., Cadillo-Quiroz, H., Keller, J. K. and Zhuang, Q.: Methane emissions from wetlands: biogeochemical, microbial, and modeling perspectives from local to global scales, Global Change Biology, 19(5), 1325–1346, doi:10.1111/gcb.12131, 2013.

Cadieux, S. B., White, J. R., Sauer, P. E., Peng, Y., Goldman, A. E. and Pratt, L. M.: Large fractionations of C and H isotopes related to methane oxidation in Arctic lakes, Geochimica et Cosmochimica Acta, 187, 141–155, doi:10.1016/j.gca.2016.05.004, 2016.

Cai, L., Zhao, Y., Gong, S., Dong, L. and Wu, C.: Use of a Novel sol–gel dibenzo-18-crown-6 solid-phase microextraction fiber and a new derivatizing reagent for determination of aliphatic amines in lake water and human urine, Chromatographia, 58(9), 615–621, doi:10.1365/S10337-003-0082-Y, 2003.

Carini, S., Bano, N., LeCleir, G. and Joye, S. B.: Aerobic methane oxidation and methanotroph community composition during seasonal stratification in Mono Lake, California (USA), Environmental Microbiology, 7(8), 1127–1138, doi:10.1111/j.1462-2920.2005.00786.x, 2005.

Casper, P., Maberly, S. C., Hall, G. H. and Finlay, B. J.: Fluxes of methane and carbon dioxide from a small productive lake to the atmosphere, Biogeochemistry, 49(1), 1–19, doi:10.1023/A:1006269900174, 2000.

Casper, P., Adams, D. D., Furtado, A. L. S., Chan, O. C., Gonsiorczyk, T. and Koschel, R.: Greenhouse gas cycling in aquatic ecosystems — methane in temperate lakes across an environmental gradient in northeast Germany, Internationale Vereinigung für theoretische und angewandte Limnologie: Verhandlungen, 29(2), 564–566, doi:10.1080/03680770.2005.11902739, 2005.

Chuang, P.-C., Yang, T. F., Wallmann, K., Matsumoto, R., Hu, C.-Y., Chen, H.-W., Lin, S., Sun, C.-H., Li, H.-C., Wang, Y. and Dale, A. W.: Carbon isotope exchange during anaerobic oxidation of methane (AOM) in sediments of the northeastern South China Sea, Geochimica et Cosmochimica Acta, 246, 138–155, doi:10.1016/j.gca.2018.11.003, 2019.

Cicerone, R. J. and Shetter, J. D.: Sources of atmospheric methane: Measurements in rice paddies and a discussion, Journal of Geophysical Research, 86(C8), 7203, doi:10.1029/JC086iC08p07203, 1981.

Cole, J. J., Bade, D. L., Bastviken, D., Pace, M. L. and Van de Bogert, M.: Multiple approaches to estimating air-water gas exchange in small lakes, Limnology and Oceanography: Methods, 8(6), 285–293, doi:10.4319/lom.2010.8.285, 2010.

Coleman, D. D., Risatti, J. B. and Schoell, M.: Fractionation of carbon and hydrogen isotopes by methane-oxidizing bacteria, Geochimica et Cosmochimica Acta, 45(7), 1033–1037, doi:10.1016/0016-7037(81)90129-0, 1981.

Conrad, R.: Quantification of methanogenic pathways using stable carbon isotopic signatures: a review and a proposal, Organic Geochemistry, 36(5), 739–752, doi:10.1016/j.orggeochem.2004.09.006, 2005.

Conrad, R.: The global methane cycle: recent advances in understanding the microbial processes involved, Environmental Microbiology Reports, 1(5), 285–292, doi:10.1111/j.1758-2229.2009.00038.x, 2009.

Coplen, T. B.: Guidelines and recommended terms for expression of stable-isotope-ratio and gas-ratio measurement results, Rapid Communications in Mass Spectrometry, 25(17), 2538–2560, doi:10.1002/rcm.5129, 2011.

Crowe, S. A., Katsev, S., Leslie, K., Sturm, A., Magen, C., Nomosatryo, S., Pack, M. A., Kessler, J. D., Reeburgh, W. S., Roberts, J. A., Gonzaléz, L., Douglas Haffner, G., Mucci, A., Sundby, B. and Fowle, D. A.: The methane cycle in ferruginous Lake Matano, Geobiology, 9(1), 61–78, doi:10.1111/j.1472-4669.2010.00257.x, 2011.

Crutzen, P.: A discussion of the chemistry of some minor constituents in the stratosphere and troposphere, Pure and Applied Geophysics, 106–108(1), 1385–1399, doi:10.1007/BF00881092, 1973.

Curry, C. L.: Modeling the soil consumption of atmospheric methane at the global scale, Global Biogeochemical Cycles, 21(4), doi:10.1029/2006GB002818, 2007.

Damm, E., Helmke, E., Thoms, S., Schauer, U., Nöthig, E., Bakker, K. and Kiene, R. P.: Methane production in aerobic oligotrophic surface water in the central Arctic Ocean, Biogeosciences, 7(3), 1099–1108, doi:10.5194/bg-7-1099-2010, 2010.

Damm, E., Rudels, B., Schauer, U., Mau, S. and Dieckmann, G.: Methane excess in Arctic surface water- triggered by sea ice formation and melting, Scientific Reports, 5(1), 16179, doi:10.1038/srep16179, 2015.

Dedysh, S. N. and Dunfield, P. F.: Facultative and obligate methanotrophs, Methods in Enzymology, 495, 31–44, 10.1016/B978-0-12-386905-0.00003-6, 2011.

DelSontro, T., Boutet, L., St-Pierre, A., del Giorgio, P. A. and Prairie, Y. T.: Methane ebullition and diffusion from northern ponds and lakes regulated by the interaction between temperature and system productivity, Limnology and Oceanography, 61(S1), S62–S77, doi:10.1002/lno.10335, 2016.

DelSontro, T., del Giorgio, P. A. and Prairie, Y. T.: No longer a paradox: The interaction between physical transport and biological processes explains the spatial distribution of surface water methane within and across lakes, Ecosystems, 21(6), 1073–1087, doi:10.1007/s10021-017-0205-1, 2018.

Deppenmeier, U., Müller, V. and Gottschalk, G.: Pathways of energy conservation in methanogenic archaea, Archives of Microbiology, 165(3), 149–163, doi:10.1007/BF01692856, 1996.

Deutzmann, J. S., Stief, P., Brandes, J. and Schink, B.: Anaerobic methane oxidation coupled to denitrification is the dominant methane sink in a deep lake, Proceedings of the National Academy of Sciences, 111(51), 18273–18278, doi:10.1073/pnas.1411617111, 2014.

Dlugokencky, E. J., Nisbet, E. G., Fisher, R. and Lowry, D.: Global atmospheric methane: Budget, changes and dangers, Philosophical Transactions of the Royal Society A: Mathematical, Physical and Engineering Sciences, 369(1943), 2058–2072, doi:10.1098/rsta.2010.0341, 2011.

Doda, T., Ramón, C. L., Ulloa, H. N., Wüest, A. and Bouffard, D.: Seasonality of density currents induced by differential cooling, Hydrology and Earth System Sciences, 26(2), 331–353, doi:10.5194/hess-26-331-2022, 2022.

Donis, D., Flury, S., Stöckli, A., Spangenberg, J. E., Vachon, D. and McGinnis, D. F.: Full-scale evaluation of methane production under oxic conditions in a mesotrophic lake, Nature Communications, 8(1), 1661, doi:10.1038/s41467-017-01648-4, 2017.

Duc, N. T., Crill, P. and Bastviken, D.: Implications of temperature and sediment characteristics on methane formation and oxidation in lake sediments, Biogeochemistry, 100(1–3), 185–196, doi:10.1007/s10533-010-9415-8, 2010.

Dutaur, L. and Verchot, L. V.: A global inventory of the soil CH_4 sink, Global Biogeochemical Cycles, 21(4), doi:10.1029/2006GB002734, 2007.

Dyhrman, S. T., Benitez-Nelson, C. R., Orchard, E. D., Haley, S. T. and Pellechia, P. J.: A microbial source of phosphonates in oligotrophic marine systems, Nature Geoscience, 2(10), 696–699, doi:10.1038/ngeo639, 2009.

Ehhalt, D. H.: The atmospheric cycle of methane, Tellus, 26(1–2), 58–70, doi:10.3402/tellusa.v26i1-2.9737, 1974.

Einzmann, T., Schroll, M., Kleint, J. F., Greule, M. and Keppler, F.: Application of concentration and 2-dimensional stable isotope measurements of methane to constrain sources and sinks in a seasonally stratified freshwater lake, Frontiers in Environmental Science-Biogeochemisty, 2022. [Manuscript submitted for publication]

Encinas Fernández, J., Peeters, F. and Hofmann, H.: On the methane paradox: Transport from shallow water zones rather than in situ methanogenesis is the major source of CH_4 in the open surface water of lakes, Journal of Geophysical Research: Biogeosciences, 121(10), 2717–2726, doi:10.1002/2016JG003586, 2016.

Ernst, L., Steinfeld, B., Barayeu, U., Klintzsch, T., Kurth, M., Grimm, D., Dick, T. P., Rebelein, J. G., Bischofs, I. B. and Keppler, F.: Methane formation driven by reactive oxygen species across all living organisms, Nature, 603(7901), 482–487, doi:10.1038/s41586-022-04511-9, 2022.

Etiope, G. and Sherwood Lollar, B.: Abiotic methane on earth, Reviews of Geophysics, 51(2), 276–299, doi:10.1002/rog.20011, 2013.

Etminan, M., Myhre, G., Highwood, E. J. and Shine, K. P.: Radiative forcing of carbon dioxide, methane, and nitrous oxide: A significant revision of the methane radiative forcing, Geophysical Research Letters, 43(24), 12,614-12,623, doi:10.1002/2016GL071930, 2016.

Ettwig, K. F., Shima, S., van de Pas-Schoonen, K. T., Kahnt, J., Medema, M. H., op den Camp, H. J. M., Jetten, M. S. M. and Strous, M.: Denitrifying bacteria anaerobically oxidize methane in the absence of Archaea, Environmental Microbiology, 10(11), 3164–3173, doi:10.1111/j.1462-2920.2008.01724.x, 2008.

Feisthauer, S., Vogt, C., Modrzynski, J., Szlenkier, M., Krüger, M., Siegert, M. and Richnow, H.-H.: Different types of methane monooxygenases produce similar carbon and hydrogen isotope fractionation patterns during methane oxidation, Geochimica et Cosmochimica Acta, 75(5), 1173–1184, doi:10.1016/j.gca.2010.12.006, 2011.

Froelich, P. N., Klinkhammer, G. P., Bender, M. L., Luedtke, N. A., Heath, G. R., Cullen, D., Dauphin, P., Hammond, D., Hartman, B. and Maynard, V.: Early oxidation of organic matter in pelagic sediments of the eastern equatorial Atlantic: suboxic diagenesis, Geochimica et Cosmochimica Acta, 43(7), 1075–1090, doi:10.1016/0016-7037(79)90095-4, 1979.

Gage, D. A., Rhodes, D., Nolte, K. D., Hicks, W. A., Leustek, T., Cooper, A. J. L. and Hanson, A. D.: A new route for synthesis of dimethylsulphoniopropionate in marine algae, Nature, 387(6636), 891–894, doi:10.1038/43160, 1997.

Ghyczy, M., Torday, C., Kaszaki, J., Szabó, A., Czóbel, M. and Boros, M.: Hypoxia-induced generation of methane in mitochondria and eukaryotic cells - An alternative approach to methanogenesis, Cellular Physiology and Biochemistry, 21(1–3), 251–258, doi:10.1159/000113766, 2008.

Gibb, S. W., Mantoura, R. F. C., Liss, P. S. and Barlow, R. G.: Distributions and biogeochemistries of methylamines and ammonium in the Arabian Sea, Deep Sea Research Part II: Topical Studies in Oceanography, 46(3–4), 593–615, doi:10.1016/S0967-0645(98)00119-2, 1999.

Grossart, H.-P., Frindte, K., Dziallas, C., Eckert, W. and Tang, K. W.: Microbial methane production in oxygenated water column of an oligotrophic lake, Proceedings of the National Academy of Sciences, 108(49), 19657–19661, doi:10.1073/pnas.1110716108, 2011.

Gruca-Rokosz, R., Szal, D., Bartoszek, L. and Pękala, A.: Isotopic evidence for vertical diversification of methane production pathways in freshwater sediments of Nielisz reservoir (Poland), CATENA, 195, doi:10.1016/j.catena.2020.104803, 2020.

Günthel, M., Donis, D., Kirillin, G., Ionescu, D., Bižić, M., McGinnis, D. F., Grossart, H.-P. and Tang, K. W.: Contribution of oxic methane production to surface methane emission in lakes and its global importance, Nature Communications, 10(1), doi:10.1038/s41467-019-13320-0, 2019.

Günthel, M., Klawonn, I., Woodhouse, J., Bižić, M., Ionescu, D., Ganzert, L., Kümmel, S., Nijenhuis, I., Zoccarato, L., Grossart, H. and Tang, K. W.: Photosynthesis-driven methane production in oxic lake water as an important contributor to methane emission, Limnology and Oceanography, 65(12), 2853–2865, doi:10.1002/lno.11557, 2020.

Hartmann, J.: Methane dynamics in lakes, Ph.D. thesis, Heidelberg University, doi: 10.11588/heidok.00026307, 2018.

Hartmann, J. F., Günthel, M., Klintzsch, T., Kirillin, G., Grossart, H.-P., Keppler, F. and Isenbeck-Schröter, M.: High spatiotemporal dynamics of methane production and emission in oxic surface water, Environmental Science & Technology, 54(3), 1451–1463, doi:10.1021/acs.est.9b03182, 2020.

Hayes, J. M.: Fractionation of carbon and hydrogen isotopes in biosynthetic processes, Reviews in Mineralogy and Geochemistry, 43(1), 225–277, doi:10.2138/gsrmg.43.1.225, 2001.

He, Z., Zhang, Q., Feng, Y., Luo, H., Pan, X. and Gadd, G. M.: Microbiological and environmental significance of metal-dependent anaerobic oxidation of methane, Science of The Total Environment, 610–611, 759–768, doi:10.1016/j.scitotenv.2017.08.140, 2018.

Herrmann, V. and Jüttner, F.: Excretion products of algae, Analytical Biochemistry, 78(2), 365–373, doi:10.1016/0003-2697(77)90098-7, 1977.

Hofmann, H., Federwisch, L. and Peeters, F.: Wave-induced release of methane: Littoral zones as source of methane in lakes, Limnology and Oceanography, 55(5), 1990–2000, doi:10.4319/lo.2010.55.5.1990, 2010.

Holler, T., Wegener, G., Knittel, K., Boetius, A., Brunner, B., Kuypers, M. M. M. and Widdel, F.: Substantial $^{13}C/^{12}C$ and D/H fractionation during anaerobic oxidation of methane by marine consortia enriched in vitro, Environmental Microbiology Reports, 1(5), 370–376, doi:10.1111/j.1758-2229.2009.00074.x, 2009.

Holler, T., Wegener, G., Niemann, H., Deusner, C., Ferdelman, T. G., Boetius, A., Brunner, B. and Widdel, F.: Carbon and sulfur back flux during anaerobic microbial oxidation of methane and coupled sulfate reduction, Proceedings of the National Academy of Sciences, 108(52), 1484–1490, doi:10.1073/pnas.1106032108, 2011.

Holmer, M. and Storkholm, P.: Sulphate reduction and sulphur cycling in lake sediments: a review, Freshwater Biology, 46(4), 431–451, doi:10.1046/j.1365-2427.2001.00687.x, 2001.

Holmkvist, L., Ferdelman, T. G. and Jørgensen, B. B.: A cryptic sulfur cycle driven by iron in the methane zone of marine sediment (Aarhus Bay, Denmark), Geochimica et Cosmochimica Acta, 75(12), 3581–3599, doi:10.1016/j.gca.2011.03.033, 2011.

Huttunen, J., Lappalainen, K., Saarijärvi, E., Väisänen, T. and Martikainen, P.: A novel sediment gas sampler and a subsurface gas collector used for measurement of the ebullition of methane and carbon dioxide from a eutrophied lake, The Science of The Total Environment, 266(1–3), 153–158, doi:10.1016/S0048-9697(00)00749-X, 2001.

IPCC: Climate change 2013 the physical science basis: Working Group I contribution to the fifth assessment report of the intergovernmental panel on climate change, edited by: Stocker, T. F., Qin, D., Plattner, G. K., Tignor, M., Allen, S. K., Boschung, J., Nauels, A., Xia, Y., Bex, V. and Midgley, P. M., Cambridge University Press, Cambridge, New York, doi: 10.1017/CBO9781107415324, 2013.

Isenbeck-Schröter, M., Aeschbach, W., Al Najem, S., Freundt, F. and Schmidt, G.: TRACE—TiefenReservoir-Analyse und Charakterisierung von der Erdoberfläche: Geochemisch-isotopisches Multimethoden-Konzept zur Charakterisierung tiefer Aquifere im Gebiet des Oberrheingrabens, Abschlussbericht TRACE Teil B. Tech. Informationsbibliothek Hann, 95, 1–90, doi:10.2314/GBV:871282461, 2016.

Jähne, B. and Haußecker, H.: Air-water gas exchange, Annual Review of Fluid Mechanics, 30(1), 443–468, doi:10.1146/annurev.fluid.30.1.443, 1998.

Jeffrey, L. C., Maher, D. T., Johnston, S. G., Kelaher, B. P., Steven, A. and Tait, D. R.: Wetland methane emissions dominated by plant-mediated fluxes: Contrasting emissions pathways and seasons within a shallow freshwater subtropical wetland, Limnology and Oceanography, 64(5), 1895–1912, doi:10.1002/lno.11158, 2019.

Joyce, J. and Jewell, P. W.: Physical Controls on methane ebullition from reservoirs and lakes, Environmental and Engineering Geoscience, 9(2), 167–178, doi:10.2113/9.2.167, 2003.

Ju, K.-S., Gao, J., Doroghazi, J. R., Wang, K.-K. A., Thibodeaux, C. J., Li, S., Metzger, E., Fudala, J., Su, J., Zhang, J. K., Lee, J., Cioni, J. P., Evans, B. S., Hirota, R., Labeda, D. P., van der Donk, W. A. and Metcalf, W. W.: Discovery of phosphonic acid natural products by mining the genomes of 10,000 actinomycetes, Proceedings of the National Academy of Sciences, 112(39),

12175–12180, doi:10.1073/pnas.1500873112, 2015.

Kamat, S. S., Williams, H. J., Dangott, L. J., Chakrabarti, M. and Raushel, F. M.: The catalytic mechanism for aerobic formation of methane by bacteria, Nature, 497(7447), 132–136, doi:10.1038/nature12061, 2013.

Kapitanov, V. A., Tyryshkin, I. S., Krivolutskii, N. P., Ponomarev, Y. N., De Batist, M. and Gnatovsky, R. Y.: Spatial distribution of methane over Lake Baikal surface, Spectrochimica Acta Part A: Molecular and Biomolecular Spectroscopy, 66(4–5), 788–795, doi:10.1016/j.saa.2006.10.036, 2007.

Karl, D. M. and Tilbrook, B. D.: Production and transport of methane in oceanic particulate organic matter, Nature, 368(6473), 732–734, doi:10.1038/368732a0, 1994.

Karl, D. M., Beversdorf, L., Björkman, K. M., Church, M. J., Martinez, A. and Delong, E. F.: Aerobic production of methane in the sea, Nature Geoscience, 1(7), 473–478, doi:10.1038/ngeo234, 2008.

Keeling, C. D.: The concentration and isotopic abundances of atmospheric carbon dioxide in rural areas, Geochimica et Cosmochimica Acta, 13(4), 322–334, doi:10.1016/0016-7037(58)90033-4, 1958.

Kelly, C. A. and Chynoweth, D. P.: The contributions of temperature and of the input of organic matter in controlling rates of sediment methanogenesis, Limnology and Oceanography, 26(5), 891–897, doi:10.4319/lo.1981.26.5.0891, 1981.

Keppler, F., Hamilton, J. T. G. G., Braß, M. and Röckmann, T.: Methane emissions from terrestrial plants under aerobic conditions, Nature, 439(7073), 187–191, doi:10.1038/nature04420, 2006.

Khatun, S., Iwata, T., Kojima, H., Fukui, M., Aoki, T., Mochizuki, S., Naito, A., Kobayashi, A. and Uzawa, R.: Aerobic methane production by planktonic microbes in lakes, Science of the Total Environment, 696, 133916, doi:10.1016/j.scitotenv.2019.133916, 2019.

Khatun, S., Iwata, T., Kojima, H., Ikarashi, Y., Yamanami, K., Imazawa, D., Kenta, T., Shinohara, R. and Saito, H.: Linking stoichiometric organic carbon–nitrogen relationships to planktonic cyanobacteria and subsurface methane maximum in deep freshwater lakes, Water (Switzerland), 12(2), 402, doi:10.3390/w12020402, 2020.

King, G. M.: Ecological aspects of methane oxidation, a key determinant of global methane dynamics, in Advances in Microbial Ecology, Advances in Microbial Ecology, edited by: Marshall, K. C., Springer, Boston, 431–468, doi: 10.1007/978-1-4684-7609-5_9, 1992.

Kirillin, G., Engelhardt, C. and Golosov, S.: A mesoscale vortex in a small stratified lake, Environmental fluid mechanics, 8(4), 349–366, doi:10.1029/2009GL040064, 2008.

Kirillin, G., Engelhardt, C. and Golosov, S.: Transient convection in upper lake sediments produced by internal seiching, Geophysical Research Letters, 36(18), doi:10.1007/s10652-008-9101-8, 2009.

Kirschke, S., Bousquet, P., Ciais, P., Saunois, M., Canadell, J. G., Dlugokencky, E. J., Bergamaschi, P., Bergmann, D., Blake, D. R., Bruhwiler, L., Cameron-Smith, P., Castaldi, S., Chevallier, F., Feng, L., Fraser, A., Heimann, M., Hodson, E. L., Houweling, S., Josse, B., Fraser, P. J., Krummel, P. B., Lamarque, J. F., Langenfelds, R. L., Le Quéré, C., Naik, V., O'doherty, S., Palmer, P. I., Pison, I., Plummer, D., Poulter, B., Prinn, R. G., Rigby, M., Ringeval, B., Santini, M., Schmidt, M., Shindell, D. T., Simpson, I. J., Spahni, R., Steele, L. P., Strode, S. A., Sudo, K., Szopa, S., Van Der Werf, G. R., Voulgarakis, A., Van Weele, M., Weiss, R. F., Williams, J. E. and Zeng, G.: Three decades of global methane sources and sinks, Nature Geoscience, 6(10), 813–823, doi:10.1038/ngeo1955, 2013.

Klaus, M. and Vachon, D.: Challenges of predicting gas transfer velocity from wind measurements over global lakes, Aquatic Sciences, 82(3), 1–17, doi:10.1007/s00027-020-00729-9, 2020.

Kleint, J. F., Wellach, Y., Schroll, M., Keppler, F. and Isenbeck-Schröter, M.: The impact of seasonal sulfate–methane transition zones on methane cycling in a sulfate-enriched freshwater environment, Limnology and Oceanography, 1–19, doi:10.1002/lno.11754, 2021.

Klintzsch, T.: Methane production by widespread marine limnic phytoplankton species, Ph.D. thesis, Heidelberg University, 2021.

Klintzsch, T., Langer, G., Nehrke, G., Wieland, A., Lenhart, K. and Keppler, F.: Methane production by three widespread marine phytoplankton species: release rates, precursor compounds, and potential relevance for the environment, Biogeosciences, 16(20), 4129–4144, doi:10.5194/bg-16-4129-2019, 2019.

Klintzsch, T., Langer, G., Wieland, A., Geisinger, H., Lenhart, K., Nehrke, G. and Keppler, F.: Effects of temperature and light on methane production of widespread marine phytoplankton, Journal of Geophysical Research: Biogeosciences, 125(9), doi: 10.1029/2020JG005793, 2020.

Kluge, T., Ilmberger, J., Von Rohden, C. and Aeschbach-Hertig, W.: Tracing and quantifying groundwater inflow into lakes using a simple method for radon-222 analysis, Hydrology and Earth System Sciences, 11(5), 1621–1631, doi:10.5194/hess-11-1621-2007, 2007.

Knittel, K. and Boetius, A.: Anaerobic oxidation of methane: progress with an unknown process, Annual review of microbiology, 63, 311–334, doi:10.1146/annurev.micro.61.080706.093130, 2009.

Kutovaya, O. A., McKay, R. M. L. and Bullerjahn, G. S.: Detection and expression of genes for phosphorus metabolism in picocyanobacteria from the Laurentian Great Lakes, Journal of Great Lakes Research, 39(4), 612–621, doi:10.1016/j.jglr.2013.09.009, 2013.

Kwan, J. and Taylor, P. A.: On gas fluxes from small lakes and ponds, Boundary-layer meteorology, 68(4), 339–356, doi:10.1007/BF00706795, 1994.

Laukenmann, S.: Transport und Austausch redoxsensitiver Elemente zwischen Freiwasser und Sediment in einem eutrophen Hartwassersee (Willersinnweiher/Ludwigshafen), unter besonderer Berücksichtigung des geochemischen Verhaltens von Uran, Ph.D. thesis, Heidelberg University, doi:10.11588/heidok.00002919, 2002.

Lenhart, K., Bunge, M., Ratering, S., Neu, T. R., Schüttmann, I., Greule, M., Kammann, C., Schnell, S., Müller, C., Zorn, H. and Keppler, F.: Evidence for methane production by saprotrophic fungi, Nature Communications, 3(1), 1–8, doi:10.1038/ncomms2049, 2012.

Lenhart, K., Althoff, F., Greule, M. and Keppler, F.: Technical note: Methionine, a precursor of methane in living plants, Biogeosciences, 12(6), 1907–1914, doi:10.5194/bg-12-1907-2015, 2015.

Lenhart, K., Klintzsch, T., Langer, G., Nehrke, G., Bunge, M., Schnell, S. and Keppler, F.: Evidence for methane production by the marine algae *Emiliania huxleyi*, Biogeosciences, 13(10), 3163–3174, doi:10.5194/bg-13-3163-2016, 2016.

León-Palmero, E., Contreras-Ruiz, A., Sierra, A., Morales-Baquero, R., Reche, I. and Reche, I.: Dissolved CH_4 coupled to photosynthetic picoeukaryotes in oxic waters and to cumulative chlorophyll a in anoxic waters of reservoirs, Biogeosciences, 17(12), 3223–3245, doi:10.5194/bg-17-3223-2020, 2020.

Lessner, D. J.: Methanogenesis biochemistry, In eLS, Chichester, John Wiley & Sons, Ltd (Ed.), doi:10.1002/9780470015902.a0000573.pub2, 2009.

Li, L., Wei, S. and Shen, W.: The role of methane in plant physiology: a review, Plant Cell Reports, 39(2), 171–179, doi:10.1007/s00299-019-02478-y, 2020.

Li, W., Dore, J. E., Steigmeyer, A. J., Cho, Y., Kim, O., Liu, Y., Morgan-Kiss, R. M., Skidmore, M. L. and Priscu, J. C.: Methane production in the oxygenated water column of a perennially ice-covered Antarctic lake, Limnology and Oceanography, 65(1), 143–156, doi:10.1002/lno.11257, 2020.

Liu, J., Chen, H., Zhu, Q., Shen, Y., Wang, X., Wang, M. and Peng, C.: A novel pathway of direct methane production and emission by eukaryotes including plants, animals and fungi: An overview, Atmospheric Environment, 115, 26–35, doi:10.1016/j.atmosenv.2015.05.019, 2015.

Liu, J., Xiao, S., Wang, C., Yang, Z., Liu, D., Guo, X., Liu, L. and Lorke, A.: Spatial and temporal variability of dissolved methane concentrations and diffusive emissions in the Three Gorges Reservoir, Water Research, 117788, doi:10.1016/j.watres.2021.117788, 2021.

Liu, L.-Y., Xie, G.-J., Ding, J., Liu, B.-F., Xing, D.-F., Ren, N.-Q. and Wang, Q.: Microbial methane emissions from the non-methanogenesis processes: A critical review, Science of The Total Environment, 806, 151362, doi:10.1016/j.scitotenv.2021.151362, 2022.

Loken, L. C., Crawford, J. T., Schramm, P. J., Stadler, P., Desai, A. R. and Stanley, E. H.: Large spatial and temporal variability of carbon dioxide and methane in a eutrophic lake, Journal of Geophysical Research: Biogeosciences, 124(7), 2248–2266, doi:10.1029/2019JG005186, 2019.

Lovley, D. R. and Klug, M. J.: Methanogenesis from methanol and methylamines and acetogenesis from hydrogen and carbon dioxide in the sediments of a eutrophic lake, Applied and Environmental Microbiology, 45(4), 1310–1315, doi:10.1128/aem.45.4.1310-1315.1983, 1983.

Luxem, K. E., Leavitt, W. D. and Zhang, X.: Large hydrogen isotope fractionation distinguishes nitrogenase-derived methane from other methane sources, Applied and Environmental Microbiology, 86(19), e00849-20, doi:10.1128/AEM.00849-20, 2020.

MacIntyre, S., Jonsson, A., Jansson, M., Aberg, J., Turney, D. E. and Miller, S. D.: Buoyancy flux, turbulence, and the gas transfer coefficient in a stratified lake, Geophysical Research Letters, 37(24), doi:10.1029/2010GL044164, 2010.

Markfort, C. D., Perez, A. L. S., Thill, J. W., Jaster, D. A., Porté-Agel, F. and Stefan, H. G.: Wind sheltering of a lake by a tree canopy or bluff topography, Water Resources Research, 46(3), 2010.

Martens, C. S. and Berner, R. A.: Methane production in the interstitial waters of sulfate-depleted marine sediments, Science, 185(4157), 1167–1169, doi:10.1126/science.185.4157.1167, 1974.

Martens, C. S., Kelley, C. A., Chanton, J. P. and Showers, W. J.: Carbon and hydrogen isotopic characterization of methane from wetlands and lakes of the Yukon-Kuskokwim Delta, Western Alaska, Journal of Geophysical Research: Atmospheres, 97, 16689–16701, doi:10.1029/91JD02885, 1992.

Mattson, M. D. and Likens, G. E.: Air pressure and methane fluxes, Nature, 347(6295), 718–719, doi:10.1038/347718b0, 1990.

McDonald, I. R., Bodrossy, L., Chen, Y. and Murrell, J. C.: Molecular ecology techniques for the study of aerobic methanotrophs, Applied and Environmental Microbiology, 74(5), 1305–1315, doi:10.1128/AEM.02233-07, 2008.

McGinnis, D. F., Greinert, J., Artemov, Y., Beaubien, S. E. and Wüest, A.: Fate of rising methane bubbles in stratified waters: How much methane reaches the atmosphere?, Journal of Geophysical Research: Oceans, 111(9), 1–15, doi:10.1029/2005JC003183, 2006.

McLeod, A. R., Brand, T., Campbell, C. N., Davidson, K. and Hatton, A. D.: Ultraviolet radiation drives emission of climate-relevant gases from marine phytoplankton, Journal of Geophysical Research: Biogeosciences, 126(9), doi:10.1029/2021JG006345, 2021.

Metcalf, W. W., Griffin, B. M., Cicchillo, R. M., Gao, J., Janga, S. C., Cooke, H. A., Circello, B. T., Evans, B. S., Martens-Habbena, W. and Stahl, D. A.: Synthesis of methylphosphonic acid by marine microbes: a source for methane in the aerobic ocean, Science, 337(6098), 1104–1107, doi:10.1126/science.1219875, 2012.

Mikaloff Fletcher, S. E., Tans, P. P., Bruhwiler, L. M., Miller, J. B. and Heimann, M.: CH_4 sources estimated from atmospheric observations of CH_4 and its $^{13}C/\ ^{12}C$ isotopic ratios: 1. Inverse modeling of source processes, Global Biogeochemical Cycles, 18(4), doi:10.1029/2004GB002223, 2004.

Mook, W. G.: Environmental isotopes in the hydrological cycle, edited by W.G. Mook, UNESCO/IAEA, IHP-V Technical Documents in Hydrology No. 39, Vol. 1, Paris, 2000.

Morana, C., Bouillon, S., Nolla-Ardèvol, V., Roland, F. A. E., Okello, W., Descy, J.-P., Nankabirwa, A., Nabafu, E., Springael, D. and Borges, A. V: Methane paradox in tropical lakes? Sedimentary fluxes rather than pelagic production in oxic conditions sustain methanotrophy and emissions to the atmosphere, Biogeosciences, 17(20), 5209–5221, doi:10.5194/bg-17-5209-2020, 2020.

Murase, J. and Sugimoto, A.: Inhibitory effect of light on methane oxidation in the pelagic water column of a mesotrophic lake (Lake Biwa, Japan), Limnology and Oceanography, 50(4), 1339–1343, doi:10.4319/lo.2005.50.4.1339, 2005.

Murase, J., Sakai, Y., Kametani, A. and Sugimoto, A.: Dynamics of methane in mesotrophic Lake Biwa, Japan, in: Forest Ecosystems and Environments, edited by: Kohyama, T., Canadell, J., Ojima, D. S., Pitelka, L.F., 143–151, Springer, Tokyo, doi:10.1007/4-431-29361-2_14, 2005.

Myhre, G., Samset, B. H., Schulz, M., Balkanski, Y., Bauer, S., Berntsen, T. K., Bian, H., Bellouin, N., Chin, M., Diehl, T., Easter, R. C., Feichter, J., Ghan, S. J., Hauglustaine, D., Iversen, T., Kinne, S., Kirkeväg, A., Lamarque, J. F., Lin, G., Liu, X., Lund, M. T., Luo, G., Ma, X., Van Noije, T., Penner, J. E., Rasch, P. J., Ruiz, A., Seland, Skeie, R. B., Stier, P., Takemura, T., Tsigaridis, K., Wang, P., Wang, Z., Xu, L., Yu, H., Yu, F., Yoon, J. H., Zhang, K., Zhang, H. and Zhou, C.: Radiative forcing of the direct aerosol effect from AeroCom Phase II simulations, Atmospheric Chemistry and Physics, 13(4), 1853–1877, doi:10.5194/acp-13-1853-2013, 2013.

Nakagawa, F., Yoshida, N., Nojiri, Y. and Makarov, V.: Production of methane from alasses in eastern Siberia: Implications from its ^{14}C and stable isotopic compositions, Global Biogeochemical Cycles, 16(3), 11–14, doi:10.1029/2000GB001384, 2002.

Natchimuthu, S., Sundgren, I., Gålfalk, M., Klemedtsson, L., Crill, P., Danielsson, Å. and Bastviken, D.: Spatio-temporal variability of lake CH_4 fluxes and its influence on annual whole lake emission estimates, Limnology and Oceanography, 61(S1), S13–S26, doi:10.1002/lno.10222, 2016.

Nisbet, E. and Weiss, R.: Top-down versus bottom-up, Science, 328(5983), 1241–1243, doi:10.1126/science.1189936, 2010.

Nisbet, E. G., Dlugokencky, E. J., Fisher, R. E., France, J. L., Lowry, D., Manning, M. R., Michel, S. E. and Warwick, N. J.: Atmospheric methane and nitrous oxide: challenges along the path to Net Zero, Philosophical Transactions of the Royal Society A: Mathematical, Physical and Engineering Sciences, 379(2210), 20200457, doi:10.1098/rsta.2020.0457, 2021.

Norði, K. and Thamdrup, B.: Nitrate-dependent anaerobic methane oxidation in a freshwater sediment, Geochimica et Cosmochimica Acta, 132, 141–150, doi:10.1016/j.gca.2014.01.032, 2014.

Norði, K. à, Thamdrup, B. and Schubert, C. J.: Anaerobic oxidation of methane in an iron-rich Danish freshwater lake sediment, Limnology and Oceanography, 58(2), 546–554, doi:10.4319/lo.2013.58.2.0546, 2013.

Orcutt, B. and Meile, C.: Constraints on mechanisms and rates of anaerobic oxidation of methane by microbial consortia: process-based modeling of ANME-2 archaea and sulfate reducing bacteria interactions, Biogeosciences, 5(6), 1587–1599, doi:10.5194/bg-5-1587-2008, 2008.

Orphan, V. J., Hinrichs, K.-U., Ussler III, W., Paull, C. K., Taylor, L. T., Sylva, S. P., Hayes, J. M. and Delong, E. F.: Comparative analysis of methane-oxidizing archaea and sulfate-reducing bacteria in anoxic marine sediments, Applied and Environmental Microbiology, 67(4), 1922–1934, doi:10.1128/AEM.67.4.1922-1934.2001, 2001.

Osadchyy, V., Nabyvanets, B., Linnik, P., Osadcha, N. and Nabyvanets, Y.: Biological processes. Effects of hydrobionts on surface water quality, in: Processes Determining Surface Water Chemistry, 165–221, Springer, Cham, doi: 10.1007/978-3-319-42159-9_4, 2016.

Ostrovsky, I., McGinnis, D. F., Lapidus, L. and Eckert, W.: Quantifying gas ebullition with echosounder: The role of methane transport by bubbles in a medium-sized lake, Limnology and Oceanography: Methods, 6(2), 105–118, doi:10.4319/lom.2008.6.105, 2008.

Oswald, K., Milucka, J., Brand, A., Littmann, S., Wehrli, B., Kuypers, M. M. M. and Schubert, C. J.: Light-dependent aerobic methane oxidation reduces methane emissions from seasonally stratified lakes, PLoS ONE, 10(7), 1–22, doi:10.1371/journal.pone.0132574, 2015.

Paul, D., Skrzypek, G. and Fórizs, I.: Normalization of measured stable isotopic compositions to isotope reference scales - A review, Rapid Communications in Mass Spectrometry, 21(18), 3006–3014, doi:10.1002/rcm.3185, 2007.

Peeters, F. and Hofmann, H.: Oxic methanogenesis is only a minor source of lake-wide diffusive CH_4 emissions from lakes, Nature Communications, 12(1), 1–5, doi:10.1038/s41467-021-21215-2, 2021.

Peeters, F., Encinas Fernandez, J. and Hofmann, H.: Sediment fluxes rather than oxic methanogenesis explain diffusive CH_4 emissions from lakes and reservoirs, Scientific Reports, 9(1), 1–10, doi:10.1038/s41598-018-36530-w, 2019.

Perez-Coronel, E., Hart, S. C. and Beman, J. M.: Methane dynamics of high-elevation lakes in the Sierra Nevada California: the role of elevation, temperature, and inorganic nutrients, Inland Waters, 11(3), 267–277, doi:10.1080/20442041.2021.1903287, 2021.

Pimenov, N. V, Kallistova, A. Y., Rusanov, I. I., Yusupov, S. K., Montonen, L., Jurgens, G., Münster, U., Nozhevnikova, A. N. and Ivanov, M. V: Methane formation and oxidation in the meromictic oligotrophic Lake Gek-Gel (Azerbaijan), Microbiology, 79(2), 247–252, doi:10.1134/S0026261710020177, 2010.

Prairie, Y. T. and del Giorgio, P. A.: A new pathway of freshwater methane emissions and the putative importance of microbubbles, Inland Waters, 3(3), 311–320, doi:10.5268/IW-3.3.542, 2013.

Raghoebarsing, A. A., Pol, A., Van de Pas-Schoonen, K. T., Smolders, A. J. P., Ettwig, K. F., Rijpstra, W. I. C., Schouten, S., Damsté, J. S. S., Op den Camp, H. J. M. and Jetten, M. S. M.: A microbial consortium couples anaerobic methane oxidation to denitrification, Nature, 440(7086), 918–921, doi:10.1038/nature04617, 2006.

Read, J. S., Hamilton, D. P., Desai, A. R., Rose, K. C., MacIntyre, S., Lenters, J. D., Smyth, R. L., Hanson, P. C., Cole, J. J. and Staehr, P. A.: Lake-size dependency of wind shear and convection as controls on gas exchange, Geophysical Research Letters, 39(9), doi:10.1029/2012GL051886, 2012.

Reeburgh, W. S.: Methane consumption in Cariaco Trench waters and sediments, Earth and Planetary Science Letters, 28(3), 337–344, doi:10.1016/0012-821X(76)90195-3, 1976.

Reeburgh, W. S.: “Soft spots” in the global methane budget, in: Microbial growth on C1 compounds, edited by: Lidstrom, M. E., Tabita, F. R., 334–342, Springer, Dordrecht, doi: 10.1007/978-94-009-0213-8_44, 1996.

Reeburgh, W. S.: Oceanic methane biogeochemistry, Chemical Reviews, 107(2), 486–513, doi:10.1021/cr050362v, 2007.

Repeta, D. J., Ferrón, S., Sosa, O. A., Johnson, C. G., Repeta, L. D., Acker, M., DeLong, E. F. and Karl, D. M.: Marine methane paradox explained by bacterial degradation of dissolved organic matter, Nature Geoscience, 9(12), 884–887, doi:10.1038/ngeo2837, 2016.

Riedinger, N., Brunner, B., Lin, Y.-S., Vossmeyer, A., Ferdelman, T. G. and Jørgensen, B. B.: Methane at the sediment–water transition in Black Sea sediments, Chemical Geology, 274(1–2), 29–37, doi:10.1016/j.chemgeo.2010.03.010, 2010.

Roland, F. A. E., Darchambeau, F., Morana, C. and Borges, A. V: Nitrous oxide and methane seasonal variability in the epilimnion of a large tropical meromictic lake (Lake Kivu, East-Africa), Aquatic Sciences, 79(2), 209–218, doi:10.1007/s00027-016-0491-2, 2017.

Rolle, I., Hobucher, H.-E., Kneifel, H., Paschold, B., Riepe, W. and Soeder, C. J.: Amines in unicellular green algae: 2. Amines in Scenedesmus acutus, Analytical Biochemistry, 77(1), 103–109, doi:10.1016/0003-2697(77)90294-9, 1977.

Rosentreter, J. A., Borges, A. V, Deemer, B. R., Holgerson, M. A., Liu, S., Song, C., Melack, J., Raymond, P. A., Duarte, C. M., Allen, G. H., Olefeldt, D., Poulter, B., Battin, T. I. and Eyre, B. D.: Half of global methane emissions come from highly variable aquatic ecosystem sources, Nature Geoscience, 14(4), 225–230, doi:10.1038/s41561-021-00715-2, 2021.

Roslev, P. and King, G. M.: Aerobic and anaerobic starvation metabolism in methanotrophic bacteria, Applied and Environmental Microbiology, 61(4), 1563–1570, doi:10.1128/aem.61.4.1563-1570.1995, 1995.

Rudd, J. W. M., Furutani, A., Flett, R. J. and Hamilton, R. D.: Factors controlling methane oxidation in shield lakes: The role of nitrogen fixation and oxygen concentration, Limnology and Oceanography, 21(3), 357–364, doi:10.4319/lo.1976.21.3.0357, 1976.

Sander, R.: Compilation of Henry's law constants (version 4.0) for water as solvent, Atmospheric Chemistry and Physics, 15(8), 4399–4981, doi:10.5194/acp-15-4399-2015, 2015.

Sandler, B.: Die Wirkung von Sanierungs- und Restaurierungsmaßnahmen auf die Nährstoffströme und die biotische Dynamik eines anthropogenen Gewässers am Beispiel des Willersinnweihers/Ludwigshafen, Ph.D. thesis, Heidelberg University, 2000.

Saunois, M., Bousquet, P., Poulter, B., Peregon, A., Ciais, P., Canadell, J. G., Dlugokencky, E. J., Etiope, G., Bastviken, D., Houweling, S., Janssens-Maenhout, G., Tubiello, F. N., Castaldi, S., Jackson, R. B., Alexe, M., Arora, V. K., Beerling, D. J., Bergamaschi, P., Blake, D. R., Brailsford, G., Brovkin, V., Bruhwiler, L., Crevoisier, C., Crill, P., Covey, K., Curry, C., Frankenberg, C., Gedney, N., Höglund-Isaksson, L., Ishizawa, M., Ito, A., Joos, F., Kim, H. S., Kleinen, T., Krummel, P., Lamarque, J. F., Langenfelds, R., Locatelli, R., Machida, T., Maksyutov, S., McDonald, K. C., Marshall, J., Melton, J. R., Morino, I., Naik, V., O'Doherty, S., Parmentier, F. J. W., Patra, P. K., Peng, C., Peng, S., Peters, G. P., Pison, I., Prigent, C., Prinn, R., Ramonet, M., Riley, W. J., Saito, M., Santini, M., Schroeder, R., Simpson, I. J., Spahni, R., Steele, P., Takizawa, A., Thornton, B. F., Tian, H., Tohjima, Y., Viovy, N., Voulgarakis, A., Van Weele, M., Van Der Werf, G. R., Weiss, R., Wiedinmyer, C., Wilton, D.

J., Wiltshire, A., Worthy, D., Wunch, D., Xu, X., Yoshida, Y., Zhang, B., Zhang, Z. and Zhu, Q.: The global methane budget 2000-2012, Earth System Science Data, 8(2), 697–751, doi:10.5194/essd-8-697-2016, 2016.

Saunois, M., R. Stavert, A., Poulter, B., Bousquet, P., G. Canadell, J., B. Jackson, R., A. Raymond, P., J. Dlugokencky, E., Houweling, S., K. Patra, P., Ciais, P., K. Arora, V., Bastviken, D., Bergamaschi, P., R. Blake, D., Brailsford, G., Bruhwiler, L., M. Carlson, K., Carrol, M., Castaldi, S., Chandra, N., Crevoisier, C., M. Crill, P., Covey, K., L. Curry, C., Etiope, G., Frankenberg, C., Gedney, N., I. Hegglin, M., Höglund-Isaksson, L., Hugelius, G., Ishizawa, M., Ito, A., Janssens-Maenhout, G., M. Jensen, K., Joos, F., Kleinen, T., B. Krummel, P., L. Langenfelds, R., G. Laruelle, G., Liu, L., MacHida, T., Maksyutov, S., C. McDonald, K., McNorton, J., A. Miller, P., R. Melton, J., Morino, I., Müller, J., Murguia-Flores, F., Naik, V., Niwa, Y., Noce, S., O'Doherty, S., J. Parker, R., Peng, C., Peng, S., P. Peters, G., Prigent, C., Prinn, R., Ramonet, M., Regnier, P., J. Riley, W., A. Rosentreter, J., Segers, A., J. Simpson, I., Shi, H., J. Smith, S., Paul Steele, L., F. Thornton, B., Tian, H., Tohjima, Y., N. Tubiello, F., Tsuruta, A., Viovy, N., Voulgarakis, A., S. Weber, T., Van Weele, M., R. Van Der Werf, G., F. Weiss, R., Worthy, D., Wunch, D., Yin, Y., Yoshida, Y., Zhang, W., Zhang, Z., Zhao, Y., Zheng, B., Zhu, Q. Q., Zhu, Q. Q. and Zhuang, Q.: The global methane budget 2000-2017, Earth System Science Data, 12(3), 1561–1623, doi:10.5194/essd-12-1561-2020, 2020.

Schenk, J., Sawakuchi, H. O., Sieczko, A. K., Pajala, G., Rudberg, D., Hagberg, E., Fors, K., Laudon, H., Karlsson, J. and Bastviken, D.: Methane in lakes: Variability in stable carbon isotopic composition and the potential importance of groundwater input, Frontiers in Earth Science, 1012, doi:10.3389/feart.2021.722215, 2021.

Schloemer, S., Elbracht, J., Blumenberg, M. and Illing, C. J.: Distribution and origin of dissolved methane, ethane and propane in shallow groundwater of Lower Saxony, Germany, Applied Geochemistry, 67, 118–132, doi:10.1016/j.apgeochem.2016.02.005, 2016.

Schmale, O., Wäge, J., Mohrholz, V., Wasmund, N., Gräwe, U., Rehder, G., Labrenz, M. and Loick-Wilde, N.: The contribution of zooplankton to methane supersaturation in the oxygenated upper waters of the central Baltic Sea, Limnology and Oceanography, 63(1), 412–430, doi:10.1002/lno.10640, 2018.

Schmid, J.: Calcitfällung und Phosphor-Kopräzipitation im Phosphorhaushalt eines eutrophen Hartwassersees mit anoxischem Hypolimnion (Willersinnweiher, Ludwigshafen am Rhein), Ph.D. thesis, Heidelberg University, doi:10.11588/heidok.00002118, 2002.

Schröder, H.: Saisonale Redoxfronten im Kopplungsbereich zwischen Schwefel- Eisen- und Mangankreislauf im System Seewasser – Sediment – Grundwasser des Willersinnweihers, Ph.D. thesis, Heidelberg University, doi:10.11588/heidok.00004894, 2004.

Schroll, M., Keppler, F., Greule, M., Eckhardt, C., Zorn, H. and Lenhart, K.: The stable carbon isotope signature of methane produced by saprotrophic fungi, Biogeosciences, 17(14), 3891–3901, doi:10.5194/bg-17-3891-2020, 2020.

Schubert, C. J., Lucas, F. S., Durisch-Kaiser, E., Stierli, R., Diem, T., Scheidegger, O., Vazquez, F. and Müller, B.: Oxidation and emission of methane in a monomictic lake (Rotsee, Switzerland), Aquatic Sciences, 72(4), 455–466, doi:10.1007/s00027-010-0148-5, 2010.

Schubert, C. J., Vazquez, F., Lösekann-Behrens, T., Knittel, K., Tonolla, M. and Boetius, A.: Evidence for anaerobic oxidation of methane in sediments of a freshwater system (Lago di Cadagno), FEMS Microbiology Ecology, 76(1), 26–38, doi:10.1111/j.1574-6941.2010.01036.x, 2011.

Scranton, M. I. and Brewer, P. G.: Occurrence of methane in the near-surface waters of the western subtropical North-Atlantic, Deep Sea Research, 24(2), 127–138, doi:10.1016/0146-6291(77)90548-3, 1977.

Sebacher, D. I., Harriss, R. C. and Bartlett, K. B.: Methane emissions to the atmosphere through aquatic plants, Journal of Environment Quality, 14(1), 40–46, doi: 10.2134/jeq1985.00472425001400010008x, 1985.

Sepulveda-Jauregui, A., Hoyos-Santillan, J., Martinez-Cruz, K., Anthony, K. M. W., Casper, P., Belmonte-Izquierdo, Y. and Thalasso, F.: Eutrophication exacerbates the impact of climate warming on lake methane emission, Science of the Total Environment, 636, 411–419, doi:10.1016/j.scitotenv.2018.04.283, 2018.

Sosa, O. A., Casey, J. R. and Karl, D. M.: Methylphosphonate oxidation in Prochlorococcus strain MIT9301 supports phosphate acquisition, formate excretion, and carbon assimilation into purines, Applied and Environmental Microbiology, 85(13), e00289-19, doi:10.1128/AEM.00289-19, 2019.

Stawiarski, B., Otto, S., Thiel, V., Gräwe, U., Loick-Wilde, N., Wittenborn, A. K., Schloemer, S., Wäge, J., Rehder, G. and Labrenz, M.: Controls on zooplankton methane production in the central Baltic Sea, Biogeosciences, 16(1), 1–16, doi:10.5194/bg-16-1-2019, 2019.

Steinke, M., Hodapp, B., Subhan, R., Bell, T. G. and Martin-Creuzburg, D.: Flux of the biogenic volatiles isoprene and dimethyl sulfide from an oligotrophic lake, Scientific reports, 8(1), 1–10, doi:10.1038/s41598-017-18923-5, 2018.

Su, G., Zopfi, J., Yao, H., Steinle, L., Niemann, H. and Lehmann, M. F.: Manganese/iron-supported sulfate-dependent anaerobic oxidation of methane by archaea in lake sediments, Limnology and Oceanography, 65(4), 863–875, doi:10.1002/lno.11354, 2020.

Sugimoto, A. and Wada, E.: Hydrogen isotopic composition of bacterial methane: CO_2/H_2 reduction and acetate fermentation, Geochimica et Cosmochimica Acta, 59(7), 1329–1337, doi:10.1016/0016-7037(95)00047-4, 1995.

Summers, P. S., Nolte, K. D., Cooper, A. J. L., Borgeas, H., Leustek, T., Rhodes, D. and Hanson, A. D.: Identification and stereospecificity of the first three enzymes of 3-dimethylsulfoniopropionate biosynthesis in a chlorophyte alga, Plant Physiology, 116(1), 369–378, doi:10.1104/pp.116.1.369, 1998.

Sun, J., Mausz, M. A., Chen, Y. and Giovannoni, S. J.: Microbial trimethylamine metabolism in marine environments, Environmental Microbiology, 21(2), 513–520, doi:10.1111/1462-2920.14461, 2019.

Tang, K. W., McGinnis, D. F., Frindte, K., Brüchert, V. and Grossart, H.-P.: Paradox reconsidered: Methane oversaturation in well-oxygenated lake waters, Limnology and Oceanography, 59(1), 275–284, doi:10.4319/lo.2014.59.1.0275, 2014.

Tang, K. W., McGinnis, D. F., Ionescu, D. and Grossart, H.-P. P.: Methane production in oxic lake waters potentially increases aquatic methane flux to air, Environmental Science and Technology Letters, 3(6), 227–233, doi:10.1021/acs.estlett.6b00150, 2016.

Templeton, A. S., Chu, K.-H., Alvarez-Cohen, L. and Conrad, M. E.: Variable carbon isotope fractionation expressed by aerobic CH_4-oxidizing bacteria, Geochimica et Cosmochimica Acta, 70(7), 1739–1752, doi:10.1016/j.gca.2005.12.002, 2006.

Thauer, R. K., Kaster, A.-K., Seedorf, H., Buckel, W. and Hedderich, R.: Methanogenic archaea: ecologically relevant differences in energy conservation, Nature Reviews Microbiology, 6(8), 579–591, doi:10.1038/nrmicro1931, 2008.

Thottathil, S. D. and Prairie, Y. T.: Coupling of stable carbon isotopic signature of methane and ebullitive fluxes in northern temperate lakes, Science of the Total Environment, 777, 146117, doi:10.1016/j.scitotenv.2021.146117, 2021.

Thottathil, S. D., Reis, P. C. J. and Prairie, Y. T.: Methane oxidation kinetics in northern freshwater lakes, Biogeochemistry, 143(1), 105–116, doi:10.1007/s10533-019-00552-x, 2019.

Timmers, P. H. A., Suarez-Zuluaga, D. A., van Rossem, M., Diender, M., Stams, A. J. M. and Plugge, C. M.: Anaerobic oxidation of methane associated with sulfate reduction in a natural freshwater gas source, The ISME journal, 10(6), 1400–1412, doi:10.1038/ismej.2015.213, 2016.

Trotsenko, Y. A. and Khmelenina, V. N.: Biology of extremophilic and extremotolerant methanotrophs, Archives of Microbiology, 177(2), 123–131, doi:10.1007/s00203-001-0368-0, 2002.

Tsunogai, U., Miyoshi, Y., Matsushita, T., Komatsu, D. D., Ito, M., Sukigara, C., Nakagawa, F. and Maruo, M.: Dual stable isotope characterization of excess methane in oxic waters of a mesotrophic lake, Limnology and Oceanography, 65(12), 2937–2952, doi:10.1002/lno.11566, 2020.

Utsumi, M., Nojiri, Y., Nakamura, T., Takeshi, N., Otsuki, A. and Seki, H.: Oxidation of dissolved methane in a eutrophic, shallow lake: Lake Kasumigaura, Japan, Limnology and oceanography, 43(3), 471–480, doi:10.4319/lo.1998.43.3.0471, 1998.

Valentine, D. L.: Biogeochemistry and microbial ecology of methane oxidation in anoxic environments: a review, Antonie Van Leeuwenhoek, 81(1), 271–282, doi:10.1023/A:1020587206351, 2002.

del Valle, D. and Karl, D.: Aerobic production of methane from dissolved water-column methylphosphonate and sinking particles in the North Pacific Subtropical Gyre, Aquatic Microbial Ecology, 73(2), 93–105, doi:10.3354/ame01714, 2014.

Varadharajan, C. and Hemond, H. F.: Time-series analysis of high-resolution ebullition fluxes from a stratified, freshwater lake, Journal of Geophysical Research: Biogeosciences, 117(G2), doi:10.1029/2011JG001866, 2012.

Waldron, S., Watson-Craik, I. A., Hall, A. J. and Fallick, A. E.: The carbon and hydrogen stable isotope composition of bacteriogenic methane: a laboratory study using a landfill inoculum, Geomicrobiology Journal, 15(3), 157–169, doi:10.1080/01490459809378073, 1998.

Wang, B., Hou, L., Liu, W. and Wang, Z.: Non-microbial methane emissions from soils, Atmospheric Environment, 80, 290–298, doi:10.1016/j.atmosenv.2013.08.010, 2013.

Wang, N., Huang, D., Li, C., Deng, Y., Li, W., Yao, Y. and Liao, W.: Regulatory roles of methane in plants, Scientia Horticulturae, 272, 109492, doi:10.1016/j.scienta.2020.109492, 2020.

Wang, Q., Dore, J. E. and McDermott, T. R.: Methylphosphonate metabolism by *Pseudomonas sp*. populations contributes to the methane oversaturation paradox in an oxic freshwater lake, Environmental Microbiology, 19(6), 2366–2378, doi:10.1111/1462-2920.13747, 2017.

Wang, Q., Alowaifeer, A., Kerner, P., Balasubramanian, N., Patterson, A., Christian, W., Tarver, A., Dore, J. E., Hatzenpichler, R., Bothner, B. and McDermott, T. R.: Aerobic bacterial methane synthesis, Proceedings of the National Academy of Sciences of the United States of America, 118(27), doi:10.1073/pnas.2019229118, 2021.

Wasserstein, R. L., Schirm, A. L. and Lazar, N. A.: Moving to a World Beyond “p < 0.05,” American Statistician, 73, 1–19, doi:10.1080/00031305.2019.1583913, 2019.

Weber, H. S., Habicht, K. S. and Thamdrup, B.: Anaerobic methanotrophic archaea of the ANME-2d cluster are active in a low-sulfate, iron-rich freshwater sediment, Frontiers in Microbiology, 8, 619, doi:10.3389/fmicb.2017.00619, 2017.

Wegener, G., Shovitri, M., Knittel, K., Niemann, H., Hovland, M. and Boetius, A.: Biogeochemical processes and microbial diversity of the Gullfaks and Tommeliten methane seeps (Northern North Sea), Biogeosciences, 5(4), 1127–1144, doi:10.5194/bg-5-1127-2008, 2008.

Wegener, G., Gropp, J., Taubner, H., Halevy, I. and Elvert, M.: Sulfate-dependent reversibility of intracellular reactions explains the opposing isotope effects in the anaerobic oxidation of methane, Science Advances, 7(19), eabe4939, doi:10.1126/sciadv.abe4939, 2021.

West, W. E., Creamer, K. P. and Jones, S. E.: Productivity and depth regulate lake contributions to atmospheric methane, Limnology and Oceanography, 61(S1), S51–S61, doi:10.1002/lno.10247, 2016.

White, A. K. and Metcalf, W. W.: Microbial metabolism of reduced phosphorus compounds, Annual Review of Microbiolgy, 61, 379–400, doi: 10.1146/annurev.micro.61.080706.093357, 2007.

Whiticar, M. J.: Carbon and hydrogen isotope systematics of bacterial formation and oxidation of methane, Chemical Geology, 161(1), 291–314, doi:10.1016/S0009-2541(99)00092-3, 1999.

Whiticar, M. J.: The biogeochemical methane cycle, in: Hydrocarbons, oils and lipids: Diversity, origin, chemistry and fate, Handbook of Hydrocarbon and Lipid Microbiology, edited by: Wilkes, H., 669–746, Springer, Cham, doi: 10.1007/978-3-319-90569-3_5, 2020.

Whiticar, M. J., Faber, E. and Schoell, M.: Biogenic methane formation in marine and freshwater environments: CO_2 reduction vs. acetate fermentation—isotope evidence, Geochimica et Cosmochimica Acta, 50(5), 693–709, 1986.

Whiting, G. J. and Chanton, J. P.: Primary production control of methane emission from wetlands, Nature, 364(6440), 794–795, doi:10.1038/364794a0, 1993.

Wiesenburg, D. A. and Guinasso, N. L.: Equilibrium solubilities of methane, carbon monoxide, and hydrogen in water and sea water, Journal of Chemical and Engineering Data, 24(4), 356–360, doi: 10.1021/je60083a006, 1979.

Wik, M., Crill, P. M., Varner, R. K. and Bastviken, D.: Multiyear measurements of ebullitive methane flux from three subarctic lakes, Journal of Geophysical Research: Biogeosciences, 118(3), 1307–1321, doi:10.1002/jgrg.20103, 2013.

Wik, M., Varner, R. K., Anthony, K. W., MacIntyre, S. and Bastviken, D.: Climate-sensitive northern lakes and ponds are critical components of methane release, Nature Geoscience, 9(2), 99–105, doi:10.1038/ngeo2578, 2016.

Wik, M., Thornton, B. F., Varner, R. K., McCalley, C. and Crill, P. M.: Stable methane isotopologues from northern lakes suggest that ebullition is dominated by sub-lake scale processes, Journal of Geophysical Research: Biogeosciences, 125(10), doi:10.1029/2019JG005601, 2020.

Wilson, J. T., Vandegrift, S. A., Kampbell, D. H., Wilson, J. T. and Vandegrift, S. A.: Dissolved oxygen and methane in water by a gc headspace equilibration technique, International Journal of Environmental Analytical Chemistry, 36(4), 249–257, doi:10.1080/03067318908026878, 1989.

Wollschläger, U., Ilmberger, J., Isenbeck-Schröter, M., Kreuzer, A. M., Von Rohden, C., Roth, K. and Schäfer, W.: Coupling of groundwater and surface water at Lake Willersinnweiher: Groundwater modeling and tracer studies, Aquatic Sciences, 69(1), 138–152, doi:10.1007/s00027-006-0825-6, 2007.

Xiao, S., Liu, L., Wang, W., Lorke, A., Woodhouse, J. and Grossart, H.-P.: A Fast-Response Automated Gas Equilibrator (FaRAGE) for continuous in situ measurement of CH_4 and CO_2 dissolved in water, Hydrology and Earth System Sciences, 24(7), 3871–3880, doi:10.5194/hess-24-3871-2020, 2020.

Yamamoto, S., Alcauskas, J. B. and Crozier, T. E.: Solubility of methane in distilled water and seawater, Journal of Chemical and Engineering Data, 21(1), 78–80, doi:10.1021/je60068a029, 1976.

Yao, M., Henny, C. and Maresca, J. A.: Freshwater bacteria release methane as a by-product of phosphorus acquisition, Applied and Environmental Microbiology, 82(23), 6994–7003, doi:10.1128/AEM.02399-16, 2016.

Yoshinaga, M. Y., Holler, T., Goldhammer, T., Wegener, G., Pohlman, J. W., Brunner, B., Kuypers, M. M. M., Hinrichs, K.-U. and Elvert, M.: Carbon isotope equilibration during sulphate-limited anaerobic oxidation of methane, Nature Geoscience, 7(3), 190–194, doi:10.1038/ngeo2069, 2014.

Zheng, Y., Harris, D. F., Yu, Z., Fu, Y., Poudel, S., Ledbetter, R. N., Fixen, K. R., Yang, Z.-Y., Boyd, E. S. and Lidstrom, M. E.: A pathway for biological methane production using bacterial iron-only nitrogenase, Nature Microbiology, 3(3), 281–286, doi:10.1038/s41564-017-0091-5, 2018.

8 Appendix

Table A 1. Overview of measured parameters and performed experiments in the water column, groundwater, and sediments. The abbreviations “pel”, “slo”, “lit” and “GW” stand for pelagic, slope, littoral, and groundwater, respectively.

Field	Water column and groundwater					Sediment					Spatial CH_4 distribution	Diffusion	Ebullition	MOx	Precursor
campaigns	Sites	CH_4	$\delta^{13}C$-CH_4	$\delta^{2}H$-CH_4	Ions	Sites	CH_4	$\delta^{13}C$-CH_4	$\delta^{2}H$-CH_4	Ions	in surface water	rates	rates	rates	incubations
May 2019	pel, lit	✓	✓	-	✓	pel, lit	✓	✓	-	✓	-	-	-	-	-
June 2019	pel, slo, lit	✓	✓	-	✓	slo	✓	✓	-	✓	-	-	-	-	-
July 2019	pel, slo, lit	✓	✓	-	✓	pel, slo	✓	✓	-	✓	-	-	-	-	-
August 2019	pel, slo, lit	✓	✓	-	✓	slo, lit	✓	✓	-	✓	-	✓	-	-	-
September 2019	pel, slo, lit	✓	✓	-	✓	pel	✓	✓	-	✓	-	✓	-	-	-
October 2019	pel	✓	✓	-	✓	slo, lit	✓	✓	✓	✓	-	✓	-	-	-
January 2020	pel, lit	✓	✓	-	✓	pel, lit	✓	✓	✓	✓	-	✓	-	-	-
May 2020	pel, slo, lit	✓	✓	✓	✓	pel, slo, lit	✓	✓	✓	✓	-	✓	-	-	-
June 2020	pel	✓	✓	✓	✓	-	-	-	-	-	-	✓	-	-	-
July 2020	pel, slo, lit	✓	✓	✓	✓	pel, slo, lit	✓	✓	✓	✓	✓	✓	-	✓	-
September 2020	pel	✓	✓	✓	✓	-	-	-	-	-	✓	✓	-	✓	✓
October 2020	pel, slo, lit	✓	✓	✓	✓	pel, slo, lit	✓	✓	✓	✓	✓	✓	-	✓	-
November 2020	-	-	-	-	-	-	-	-	-	-	-	✓	✓	-	-
March 2021	pel, slo, lit	✓	✓	✓	✓	pel, slo, lit	✓	✓	✓	✓	✓	✓	-	✓	-
May 2021	pel, slo, lit	✓	✓	✓	✓	-	-	-	-	-	✓	✓	✓	-	-
June 2021	pel, slo, lit	✓	✓	✓	✓	-	-	-	-	-	✓	✓	✓	-	-
July 2021	pel, slo, lit	✓	✓	✓	✓	-	-	-	-	-	✓	✓	✓	✓	-
August 2021	pel, slo, lit, no GW	✓	✓	✓	✓	-	-	-	-	-	-	✓	✓	-	-
September 2021	pel, slo, lit	✓	✓	✓	✓	-	-	-	-	-	-	✓	-	✓	✓

Table A 2. Calibration data for the FaRAGE and CRDS conducted with water temperatures of 6 °C and 19 °C. Methane mixing ratios from the CRDS represent the difference between the measured CH_4 mixing ratio using the FaRAGE unit and background air. Samples of the CH_4 mixing ratios measured with the GC-FID were generated from water samples using the headspace technique in triplicate (section 2.2.3).

6 °C		19°C	
CH_4 (CRDS) [ppmv]	**CH_4 (GC-FID) [ppmv] ± SD**	**CH_4 (CRDS) [ppmv]**	**CH_4 (GC-FID) [ppmv] ± SD**
0.005	9.4 ± 0.7	0.006	11.1 ± 0.7
0.254	48.3 ± 1.1	0.270	45.9 ± 0.2
0.531	92.8 ± 2.9	1.492	232.4 ± 8.4
0.803	143.8 ± 5.2	2.499	395.2 ± 9.1
1.279	232.8 ± 7.5	3.622	571.3 ± 17.7

Table A 3. Volume, sediment area, and planar area of Lake Willersinnweiher derived from the bathymetric map and subdivided into intervals of one meter.

Lake Depth [m]	**Volume [m³]**	**Sediment Area [m²]**	**Planar Area [m²]**
0-1	163659	12845	12761
1-2	149177	13814	13597
2-3	136790	11416	11111
3-4	126777	9457	9138
4-5	118046	8791	8471
5-6	109429	9249	8932
6-7	99488	11687	11368
7-8	88141	10381	10034
8-9	79024	8996	8623
9-10	70691	8612	8237
10-11	62234	9347	8978
11-12	53444	8488	8171
12-13	46225	6585	6290
13-14	39657	7693	7431
14-15	29941	12832	12571
15-16	17656	10878	10672
16-17	7067	9447	9282
17-18	1627	2663	2586
18-19	300	479	461
19-20	86	126	119
20-21	3	26	26
total	1399463	173813	168858

Tables A4 and A5 are accessible online from heiDATA, an institutional repository for data of Heidelberg University (https://doi.org/10.11588/data/MU3CON, Schroll, 2022)

Table A 4. Dissolved CH_4 concentrations, $\delta^{13}C$-CH_4, $\delta^{2}H$-CH_4 values and dissolved ions in the pore water of the sediment at the pelagic, slope and littoral sites of Lake Willersinnweiher for field campaigns between May 2019 and March 2021.

Table A 5. In-situ parameters, CH_4 concentrations, $\delta^{13}C$-CH_4, $\delta^{2}H$-CH_4 values and dissolved ions in the water column of the pelagic, slope and littoral sites at Lake Willersinnweiher for field campaigns between May 2019 and September 2021.

Table A 6. Potential MOx rates at Lake Willersinnweiher for July, September, October 2020 and March, July and September 2021. Potential MOx rates are presented as the results of the linear regression analysis and its standard error.

Month	**depth [m]**	**MOx rate [nmol l^{-1} d^{-1}]**
July 2020	8	49 ± 5
September 2020	7	109 ± 7
October 2020	7	251 ± 13
March 2021	7	89 ± 13
July 2021	1	-
	5	150 ± 78
	6	258 ± 33
	9	609 ± 137
September 2021	1	43 ± 5
	6	174 ± 73
	7	950 ± 149
	8	133 ± 6

GESAMTFAKULTÄT FÜR MATHEMATIK, INGENIEUR- UND NATURWISSENSCHAFTEN

COMBINED FACULTY OF MATHEMATICS, ENGINEERING AND NATURAL SCIENCES

RUPRECHT-KARLS-
UNIVERSITÄT
HEIDELBERG

Eidesstattliche Versicherung gemäß § 8 der Promotionsordnung für die Gesamtfakultät für Mathematik, Ingenieur- und Naturwissenschaften der Universität Heidelberg /
Sworn Affidavit according to § 8 of the doctoral degree regulations of the Combined Faculty of Mathematics, Engineering and Natural Sciences at Heidelberg University

1. Bei der eingereichten Dissertation zu dem Thema / The thesis I have submitted entitled

   ……

   ……

   handelt es sich um meine eigenständig erbrachte Leistung / is my own work.

2. Ich habe nur die angegebenen Quellen und Hilfsmittel benutzt und mich keiner unzulässigen Hilfe Dritter bedient. Insbesondere habe ich wörtlich oder sinngemäß aus anderen Werken übernommene Inhalte als solche kenntlich gemacht. / I have only used the sources indicated and have not made unauthorised use of services of a third party. Where the work of others has been quoted or reproduced, the source is always given.

3. Die Arbeit oder Teile davon habe ich wie folgt/bislang nicht[1)] an einer Hochschule des In- oder Auslands als Bestandteil einer Prüfungs- oder Qualifikationsleistung vorgelegt. / I have not yet/have already[1)] presented this thesis or parts thereof to a university as part of an examination or degree.

   Titel der Arbeit / Title of the thesis: ……

   Hochschule und Jahr / University and year: ……

   Art der Prüfungs- oder Qualifikationsleistung / Type of examination or degree: ……

4. Die Richtigkeit der vorstehenden Erklärungen bestätige ich. / I confirm that the declarations made above are correct.

5. Die Bedeutung der eidesstattlichen Versicherung und die strafrechtlichen Folgen einer unrichtigen oder unvollständigen eidesstattlichen Versicherung sind mir bekannt. / I am aware of the importance of a sworn affidavit and the criminal prosecution in case of a false or incomplete affidavit.

Ich versichere an Eides statt, dass ich nach bestem Wissen die reine Wahrheit erklärt und nichts verschwiegen habe. / I affirm that the above is the absolute truth to the best of my knowledge and that I have not concealed anything.

…….. ……..

Ort und Datum / Place and date — Unterschrift / Signature

[1)] Nicht Zutreffendes streichen. Bei Bejahung sind anzugeben: der Titel der andernorts vorgelegten Arbeit, die Hochschule, das Jahr der Vorlage und die Art der Prüfungs- oder Qualifikationsleistung. / Please cross out what is not applicable. If applicable, please provide: the title of the thesis that was presented elsewhere, the name of the university, the year of presentation and the type of examination or degree.

The German text is legally binding.